

# CONTENTS

RESEARCH ON DESIGN OF CHINESE TEACHING AND LEARNING IN VIRTUAL COMMUNITY.....	PAN SHUNZHAO; PEIFANG LI 135
THE STUDY ON SIMULATION EXPERIMENT OF CARBONATE DISSOLUTION PROCESS UNDER VARIOUS BURIAL CONDITION.....	WANG DIJU 139
A NOVEL DESIGN OF DIGITAL AC VOLTMETER.....	BUXIN ZHOU; CHENGWEI CAI 142
RESEARCH ON A CONTROL CIRCUIT OF SINGLE-PHASE SINE FULL-BRIDGE INVERTER.....	YANNAN YU; XUEJUN WEI; WENYUAN WANG; YIZHAO ZHANG 144
OPTIMAL DESIGN AND STUDY FOR PIPELINE DIAMETER OF DISTRICT HEATING SYSTEM.....	XIANLIANG YANG; CUICUI HUANG 148
THE DEVELOPMENT AND IMPLEMENTATION OF LATHE SIMULATOR.....	HONGGE FU; XIAO GUANG WANG 153
ARCHITECTURAL CAD COURSE CONSTRUCTION IN HIGHER VOCATIONAL TEACHING.....	CHEN YU; GAO HAIYING 156
ADAPTIVE SYNCHRONIZATION FOR FRACTIONAL-ORDER CHAOTIC SYSTEMS BASED ON OBSERVER.....	ZHANG ZHAOHAN; ZHANG YUEPING; ZHENG WANG 159
SEPARATE-FREQUENCY INVERSION OF THE ORGANIC CARBON CONTENT IN SOURCE ROCK.....	WEI YANG; MINGYI HU 163
THE DESIGN AND DEVELOPMENT OF BASKETBALL CAI COURESWARE.....	WEI CHUNKUI 169
RELIABILITY ANALYSIS FOR THE METAL STRUCTURE OF BRIDGE CRANE.....	YAN XU WEI; ZHENG MAO YANG; YU GUI LI; FEI LONG NIE 171
HYBRID ANT COLONY ALGORITHM FOR THE TRAVELING SALESMAN PROBLEM.....	CHUANDONG QIN; HUIXIA ZHAO 176
AN EMPIRICAL STUDY ON FACTORS AFFECTING LBS USERS' ADOPTION.....	ZHAO YU AN; LU CHUAN LIU 179
FLOW FIELD SIMULATION AND STRUCTURAL OPTIMIZATION OF AIR BAFFLE IN THE PASSIVE CONTAINMENT COOLING SYSTEM.....	CHUNLAI TIAN; SHAN ZHOU; LIYONG HAN 183
MILDEW PREDICTION MODEL FOR WAREHOUSING TOBACCO BASED ON QGA-BP.....	ZHANG LIHUA; LE GUOQING; DAI XICHANG 187
RECIPROCAL EFFECTS OF OCCUPATIONAL CONDITIONS AND PSYCHOLOGICAL FUNCTIONING: A CASE STUDY.....	QINGBO SONG 191
RESEARCH ON CURRICULUM TOPIC MAP BASED DOMAIN KNOWLEDGE MANAGEMENT.....	ZHANG JIN; WANG TIANYI 194

# Research on Design of Chinese Teaching and Learning in Virtual Community

Pan Shunzhao<sup>1</sup>; Peifang Li<sup>2</sup>

1. Institute of Marxism Southwest University, Chongqing, China

2. Southwest University Yucai College, Chongqing, China

**Abstract**—The interaction design of web-based Chinese teaching as a foreign language shall follow the general rules of second language teaching besides the general web-based teaching design process to reflect the features of the Chinese language and the teaching characteristics of Chinese as a foreign language. This article, based upon the existing researches on interactive design for web-based Chinese teaching as a foreign language, further discusses the interactive design process and the influencing factors and summarizes the interactive design principle for web-based Chinese teaching as a foreign language.

**Index Terms**—Network; Web-based Chinese Teaching as a Foreign Language; Interactive Design; Process

## I. INTRODUCTION

Interactive design is the core of teaching design in web-based Chinese teaching as a foreign language, which plays a critical role in deciding the teaching effect [1-4]. Since interactive design is a systematic project with various influencing factors, systematic method shall be followed. Zhou Rong proposes the interactive design frame of web-based teaching [5-8] on the basis of both domestic and foreign researches. Xu Juan furthermore raises the interactive design process [9-10] of web-based Chinese teaching as a foreign language. This process includes the following:

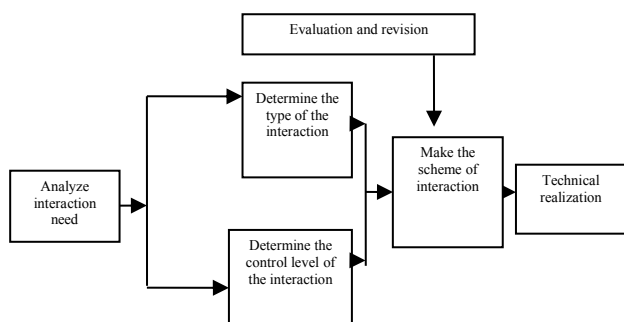


Figure 1. Interactive Design Process of Web-Based Chinese Teaching as a Foreign Language

## II. ANALYSIS OF INTERACTIVE NEED

It includes target analysis and object analysis.

### A. Target Analysis

Target analysis is to analyze the target domain that interactive teaching shall reach and the proportion of each target. Bloom’s teaching target theory classifies teaching targets into cognitive domain, affective domain and psychomotor domain as per categories of behavior, and further categorizes the targets in each domain with

the purpose to realize the final target in each domain. The cognitive domain includes: knowledge, comprehension, application, analysis, synthesis and evaluation.

The contents of Chinese teaching as a foreign language include language elements (pronunciation, vocabulary, grammar, and character), verbal skills (listening, speaking, reading, and writing), verbal communication skills and relative cultural knowledge (Liu Xun, 2000). Based upon Bloom’s taxonomy, Jiang Liping (2006) raises that the targets of the cognitive domain of Chinese teaching as a foreign language include language knowledge, pragmatic rules, cultural and historic knowledge etc. The targets in psychomotor domain include verbal skills and verbal communication skills. And the targets in affective domain include Chinese human geography, folkways and customs, and cultural knowledge.

With reference to the above teaching target classification and contents of each teaching target domain, the article divides the interactive targets of Chinese teaching as a foreign language into cognitive domain, psychomotor domain and affective domain.

Target analysis is to analyze the targets that teaching interaction shall achieve and the proportion of each target. For example, it is to help the learner to learn one or several language elements, to give training of the verbal skills (listening, speaking, reading, and writing), to cultivate enthusiasm for the Chinese culture, or to include all these targets.

### B. Object Analysis

Object analysis is mainly the analysis of the learner, including analysis of the learner’s nationality, age, Chinese language level, learning style and motive etc. These are the influencing factors in interaction.

The analysis of target and object is the first step of the interactive design of web-based Chinese teaching as a foreign language and is the basis for the following tasks.

## III. DETERMINATION OF THE TYPE OF INTERACTION

The interaction between the students and the learning resources is the process of the learner to obtain knowledge and skills using the learning resources. The interaction of web-based Chinese teaching as a foreign language can be classified into the following:

Operative interaction: the interaction is for the learner to choose learning contents or to control learning progress etc. For example, at the beginning of learning, the learner chooses certain part as the learning content,

and during the course of learning, the learner plays the audio and video content and browse the content by choosing pages. During the course of operative interaction, the learner mainly receives information with simple human-machine setting function. The influence of the interaction on cognition is mainly instruction and assistance.

Reflective interaction: the learner needs to go through a thinking process for expressing his opinions, or he needs to check the learning contents, e.g. exercises, notes, evaluation etc. By reflective interaction, the learner completes the reprocess of the learning contents, sending information while receiving information with a simple course of information process.

Constructive interaction: the interaction is for the learner to complete the process of the learning resources, or to complete the cognition of the object, e.g. inquiry, sequencing, downloading, new link setting up etc. During this course, the learner completes the cognition of the object in various ways. A complicated cognition and process course is incorporated in this interaction.

Immersive interaction: this interaction is for the learner to achieve knowledge transfer in an analogue learning environment, e.g. role play, communicative activity imitation etc. The learner immerses himself into the specific environment and the cognitive course is completed in the specific environment.

From the above, we can see that the supporting level to the cognitive course becomes higher and higher from operative interaction to immersive interaction, and the information process required during the interactions become more and more complicated.

#### IV. DETERMINATION OF CONTROL LEVEL

##### A. Interaction Control Level

The control level of interaction embodies the teaching ideas. It can be classified into 3 types: control by the teacher, control by the learner with guidance, and self control by the learner. In web-based teaching and learning, the learner studies by himself using net coursewares without a specific teacher to control the interactive activities of the learner. The control of the teacher to the learner's interactive activities thus refers to the access control to the coursewares and settings. The control level refers to the content, quantity and time of the interaction. Control by the teacher means that the teacher controls all or nearly all the access permissions. The learner cannot change or reselect the teaching steps, teaching time and interaction contents that are already set up. Control by the learner with guidance is that the teacher gives some access permits to the learner and provides some schemes for the learner to choose as per his specific conditions. Self control by the learner is that the learner controls the quantity, time and content of interaction all by himself and the teacher cannot interfere or change the learner's choice.

Reflective interaction is usually skill or related exercises. If the course regulates that the learner must complete an exercise or reach certain rate of correctness for proceeding to the next part, it is reflective interaction under the control of the teacher. If the learner can choose whether to do this exercise or not as per his own

conditions, it is the control of the learner usually with the guidance of the teacher. That is, certain reference schemes are given, and it is up to the learner to decide which one to use.

In constructive interaction, the learner studies in the way of uploading, downloading, inquiry, and new link setting up etc. It demands higher information process level of the learner during the interaction. For example, at higher learning stage when studying social hot topics, the learner summarizes and arranges the learning contents through information processing, and exhibits and shares the learning outcomes by setting up new links. When the control level of the teacher is high, the teacher can limit the modes of learning outcome sharing, for example, exhibition only in text; the teacher can also give some exhibition ways for the learner to choose, and the teacher's control level is lowered and the learner's control level is increased. When the control level of the learner is furthermore increase, the learner can choose the exhibition mode of the learning outcomes by himself.

##### B. Determination of the Interaction Control Level

To determine the control level of interaction, first the learner's Chinese language level needs to be considered. Generally, the teacher's control level comes from high to low, while the control level of the learner comes from low to high. At the beginning stage, the learner has just started learning a new language and he needs a lot of instructions and help from the teacher, which requires higher control level of the teacher. Meanwhile, the teaching contents at the beginning stage are mainly language knowledge and language skills. Exercises need to be done with teacher's instructions to obtain language knowledge and skills. At this stage, there are not many topic discussions and self controlled communication activities. Therefore, the control level of the learner is relatively low. Then at the intermediate stage, the learner has got certain language knowledge and skills, and has cultivated certain communication capability. The main teaching point at this stage is word teaching. The learner has grasped some learning tactics and his dependence on the teacher decreases. The teacher's function changes from providing help and support to creating environment and cultivating the learner's communication skills. Compared with the beginning stage, the teacher's control reduces, and the learner's control under guidance and the learner's self control increase. From the senior stage, the learning contents change to be language communication skills and high level information processing like culture, literature and history etc. Now the teacher's control is mainly in the field of learning method and tactics. Chinese language becomes the tool of learning for the learner with fewer language exercises and less interaction under the teacher's control. The learner starts learning by cooperation and discussion. And the interaction controlled by the learner increases.

#### V. MAKE THE SCHEME OF INTERACTION

The teaching contents of Chinese as a foreign language generally include pronunciation, grammar, vocabulary and text etc. The skills training of listening, speaking, reading and writing are carried out in combination with the teaching of language elements.

Therefore, the interaction design of web-based Chinese teaching as a foreign language can take reference to the teaching steps of class teaching of Chinese. Based on various learning contents, the interaction activities for web-based Chinese teaching can be designed and interaction schemes subject to specific teaching target and learners can be made as per the interaction types and levels determined upon interaction need analysis. This article analyzes and compares the influence of interaction needs on interaction schemes. As the influence of various elements in interaction need analysis on interaction design is complicated, one example is given below respectively from the aspect of pronunciation, vocabulary, grammar, character and text to show the influence of an element on interaction design scheme.

### C. Interaction Design Scheme for Vocabulary

Vocabulary is the building material of language and is the basic unit of sentence. The goal of Chinese vocabulary teaching is to make the learner grasp the pronunciation, meaning, form and basic usage of certain amount of Chinese words under the guidance of relevant Chinese vocabulary knowledge, and to cultivate the capability of understanding and expression of words in communication. The steps of class vocabulary teaching generally include: to lead the students to read, to explain, to make the students read without leading, to let the students speak and practice. With reference to the class teaching steps, the interaction design for web-based Chinese teaching as a foreign language shall also be about the pronunciation, form, meaning and usage of the vocabulary. The specific types and control levels of interaction shall be decided as per analysis of interaction need and object.

Vocabulary learning exists in all the stages of web-based Chinese learning as a foreign language. However, at different stages, the interaction design will be different. At intermediate stage, vocabulary learning is the focus, teaching targets including the language knowledge like sound, form and meaning etc. in cognitive domain, and correct usage of the words in psychomotor domain, and also the understanding of the cultural meaning of the words in affective domain. The learner needs to learn the vocabulary knowledge under the teacher's control with the teacher's explanation, and needs to have self controlled skill training with the teacher's instructions, and self studying is also required. The interaction activities for the intermediate stage can be designed like this: first demonstrate the correct pronunciation of the word, and audio playing can be adopted here. Then explain the word in the way of new word list or more visualized way like picture and animation etc. In case of difficult words, detailed explanation and exercises are also required. Besides the explanation of the usage of the word, exercises shall be given for the learner to practice. Exercises can be in many forms: sentence pattern changing, sentence making, question and answer etc. The pronunciation, form and meaning matching exercises equal to reading without leading in class teaching. With the multimedia advantages of web teaching, the matching exercises can be in more forms: word choosing, blank filling, lining, or more interesting ways like game etc. The learning of tactics can help the learner to cultivate vocabulary learning tactics. Methods include

word assembly, word grouping, and word list setting up by the student. The interaction type here is constructive interaction. The design scheme control level for the vocabulary at the intermediate stage is the control by the learner with the guidance of the teacher.

### D. Interaction Design Scheme for Grammar

Grammar teaching is the teaching of the organization pattern of the phrases and sentences of the target language, which is to guide the language skill training and to cultivate the communication capability using the target language. The principle of grammar teaching includes: to highlight the difficulty and important points of grammar by language comparison, to practice sentence patterns and also summarize the grammar points; to teach the essential and ensure plenty of practice with focus on practice. The general steps of class grammar teaching include: introduction, explanation, mechanical practice and flexible practice (Yang Huiyuan, 2007). The interaction on grammar in web-based Chinese teaching as a foreign language can be divided into these sections: grammar explanation, mechanical practice, meaningful practice and communication practice.

To different type learners, the type and control level of the interaction design on grammar can be different. The grammar explanation is to help the learner to understand grammar rules. The necessary explanation, conclusion and summary of the grammar points can be designed as operative interaction. The mechanical practice includes listening and reading, repetition, variation, extension etc. The meaningful practice includes question answer, sentence completion, text summary and retelling etc. The mechanical practice and meaningful practice can be designed as reflective interaction for the independent type learners, and for the dependent type learners who expect more social type learning, immersive interaction is more proper. Compared with mechanical practice, the learner's information processing level is higher in meaningful practice. Communication practice includes free conversation, role play, discussion and writing etc. This is the real communication or practice close to true communication for which immersive interaction is the most proper one. And the teacher's control level for the independent type learner is lower than that for the dependent type learner, and the learner's control level is higher than that of the dependent type learner.

## VI. CONCLUSION

Based upon the general interaction design process of web-based teaching and interaction design process of digital Chinese teaching as a foreign language, this article goes into further details of the interaction design process of web-based Chinese teaching as a foreign language. First, the analysis of interaction needs includes target analysis and object analysis. About target analysis, the teaching targets of web-based Chinese teaching as a foreign language in cognitive domain, psychomotor domain and affective domain are analyzed as per Bloom's teaching theory. Object analysis includes the analysis of the learner's nationality, age, Chinese language level, cognitive style and learning motive. The

second step is to determine the interaction type through target analysis. The third step is to determine the interaction control level through object analysis. And the fourth step is to raise the general interaction design scheme for various aspects (pronunciation, vocabulary, grammar, character, text) of web-based Chinese teaching as a foreign language with reference to the teaching features and class teaching steps of Chinese as a foreign language.

#### REFERENCE

- [1] Allen, B., Kligyte, G., Bogle, M., & Pursey, R. (2008). Communities in practice : a community dimension for the UNSW Learning & Teaching Exchange. Paper presented at the 25th annual ASCILITEconference.
- [2] Ardichvili, A., Maurer, M., Li, W., Wentling, T., & Stuedemann, R. (2006). Cultural influences on knowledge sharing through online communities of practice. *Journal of Knowledge Management*, 10(1), 94 -107.
- [3] Baek, E. O., & Barab, S. A. (2005). A Study of Dynamic Design Dualities in a Web-Supported Community of Practice for Teachers. *Educational Technology and Society*, 8(4), 161-177.
- [4] Bhagat, R. S., Kedia, B. L., Harveston, P. D., & Triandis, H. C. (2002). Cultural Variations in the Cross-Border Transfer of Organizational Knowledge: An Integrative Framework. *The Academy of Management Review*, 27(2), 204-221.
- [5] Oliver, M., & Carr, D. (2009). Learning in virtual worlds: Using communities of practice to explain how people learn from play. [Feature DER: 20090512]. *British Journal of Educational Technology*, 40(3), 444-457.
- [6] Rogers, J. (2000). Communities of practice: A framework for fostering coherence in virtual learning communities. *Educational Technology and Society*, 3(3), 384-392.
- [7] Thomas, A. (2005). Children online: learning in a virtual community of practice. *E - Learning*, 2(1).
- [8] Wenjing, X. (2005). Virtual space, real identity: Exploring cultural identity of Chinese Diaspora in virtual community. *Telematics and Informatics*, 22(4), 395-404.
- [9] Krumsvik, R. (2005). ICT and community of practice. *Scandinavian Journal of Educational Research*, 49(1),27-50.
- [10] McLoughlin, C. (1999). Culturally responsive technology use: developing an on-line community of learners. *British Journal of Educational Technology*, 30(3), 231-243.

# The study on Simulation Experiment of Carbonate Dissolution Process under Various Burial Condition

Wang Diju

Xinjiang exploration and Development Center,  
Henan Oilfield Branch Company of Sinopec Ltd, Korla Xinjiang, China

**Abstract**—Burial dissolution can effectively improve the reservoir properties of carbonate rocks. However, its research is hard to conduct due to complex water-rock reaction condition and various controlling factors. The simulation experiment was able to provide useful parameter for the study of dissolution. For this experiment, the samples come from Ordovician carbonates, Tazhong Area. The test fluid is the formation water from well interval of Tazhong Well-44 at depth 4857m-4888m. The flow velocity was set up to 1.5ml/min. Under the constant pressure of 40MPa, the temperature variation experiment indicated that dissolution rate is positively correlated with temperature at 25°C-75°C range and negatively correlated when temperature > 75 °C . Carbonate dissolution rate > transitional rock dissolution rate > dolomite dissolution rate. When the temperature reaches to 200 °C , the difference between the three aforesaid rates become less. Dissolution rate from various composition of carbonate shows little difference. Under the constant temperature of 70 °C , the pressure variation experiment shows that the dissolution rate is positively correlated with pressure. The rate under pressure > 30MPa is higher than that of under pressure range of 10-30MPa. Carbonate dissolution rate > transitional rock dissolution rate > dolomite dissolution rate. Dissolution rate from various composition of carbonate shows little difference .

**Index Terms**—dissolution; carbonate rocks; simulation experiment; buried diagenetic environment; Tazhong Area

## I. INTRODUCTION

The Carbonate, as a soluble rock, the dissolution at its diagenetic stage will determine the formation and preservation of its reservoir<sup>[1]</sup>. In recent years, by the in-depth study and exploration practice, it's found that the interaction between the fluid and rock at the reservoir in the deep stratum can effectively improve the reservoir permeability of the carbonate rock<sup>[2-4]</sup>. And different from the dissolution at supergene period, the condition of the water-rock reaction in deeper stratum is complex. The temperature and pressure change greatly. And the materials are also quite abundant, including acidic water, acidic gas, hot water, sulfate and microorganisms. These will make the burial dissolution study difficult. Aiming at the dissolution simulation experiments under burial condition, the predecessors did a lot of researches, but the conclusion of the researches being different<sup>[5-7]</sup>. For example, the dissolution simulation experiment for different lithology at Majiagou formation in the Erdos

basin by Yang Junjie and some others shows that under shallow burial condition, the calcite dissolves significantly faster than the dolomite, while under deep burial condition, the dolomite dissolves faster than the calcite<sup>[8-10]</sup>; but Jiang Xiaoqiong and some others think that the dissolution rate under burial condition would be limestone > transitional rock > dolomite<sup>[11-12]</sup>. In this paper, it carries dissolution experiments on carbonate rocks under different burial conditions at Ordovician in Tazhong area of the Tarim Basin to analyze the dissolution quantity and dissolution rate change, in order to provide useful parameters for the research on dissolution under burial conditions.

## II. EXPERIMENTAL SAMPLE SELECTION AND PREPARATION

### A. Sample selection

This experiment selects the carbonate rocks from different wells and different layers at Yingshan formation in the Lower Ordovician of Tazhong area, including four types: calcarenite, micritic limestone, calcareous dolomite and fine-crystal dolomite (Figure. 1), which basically cover the main rock types at Yingshan formation in this area, and also attend to the different mineral compositions, structural components, chemical compositions and reservoir distributions formed by burial dissolution. The selected samples are pretreated by crushing, sieving, ultrasonic cleaning and baking to choose the 10-25 mesh samples for this simulation experiment.

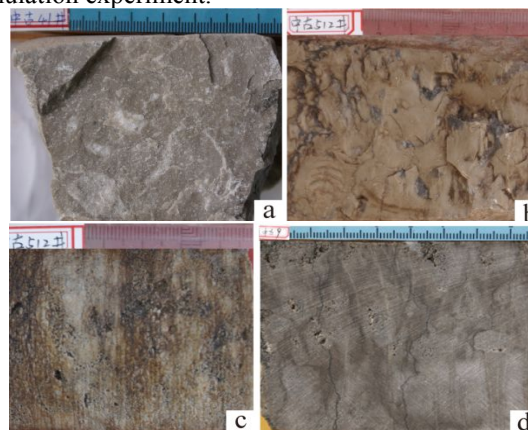


Figure 1. Rocks Types of Yingshan Formation Lower Ordovician of Tazhong Area  
a. calcarenite; b. micritic limestone; c. calcareous dolomite; d. fine-crystal dolomite

B. Sample mineral composition and order degree analysis

At the same time, by grinding, X - ray diffraction analysis and order degree analysis, it determines the

samples' mineral components, the chemical components and the order degrees of dolomite. The results are as shown in table 1.

TABLE I. MAIN MINERAL COMPONENTS AND THE DOLOMITE'S ORDER DEGREE OF EXPERIMENTAL SAMPLES

Rock types	Wells and Layers	No.	Main mineral components(%)		Dolomite's order degree
			Calcite	Dolomite	
Calcarenrite	Medieval times 41, Ying second section	a	99.1	0	
Micritic limestone	Medieval times 512, Ying second section	b	99.6	0	
Calcareous dolomite	Medieval times 512, Ying third section	c	21.3	78.0	0.65
Fine-crystal dolomite	Medieval times 9, Ying third section	d	7.5	92.1	0.72

Note: the measuring unit for the main mineral components and the dolomite's order degree is the Oil and Gas Geology Laboratory of Southwest Petroleum University

III. EXPERIMENTAL DEVICE AND PROCESS

It uses reservoir water rock reaction experiment which has been researched maturely in the world to simulate<sup>[13-15]</sup>, and the experiment is completed in the State Key Laboratory of Oil and Gas Geology and Development Engineering of Southwest Petroleum University. The experimental device is shown in Figure 2. The experiment uses the dynamic balance method, namely under the premise of using tube furnace heating to control experiment temperature, taking the way of fixing time, flow and total to control the process, by testing the solution and the ion concentration in the solution from the outlet to research the dissolution process of different samples. After the experiment completed, it calculates the "dissolution rate" by weighing on residue samples.

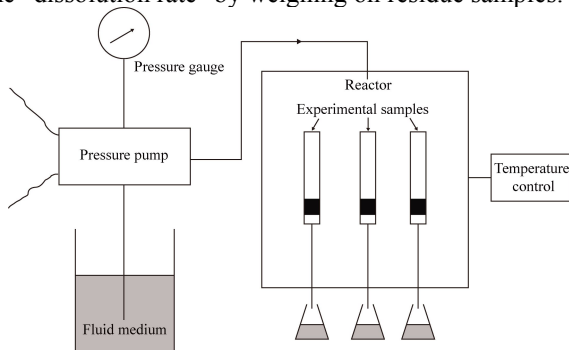


Figure 2. Schematic Diagram Showing Simulation Device of Burial Dissolution

The average values of the main components of the stratum water at the researching district are:  $K^+ + Na^+ = 18450.71 \text{ mg/L}$ ,  $Mg^{2+} = 417.04 \text{ mg/L}$ ,  $Ca^{2+} = 29062.5 \text{ mg/L}$ ,  $HCO_3^- = 683.42 \text{ mg/L}$ ,  $Cl^- = 51317.78 \text{ mg/L}$ ,  $SO_4^{2-} = 859.93 \text{ mg/L}$ . The experimental fluid medium used the stratum water selected from the 4857-4888m well section at Ritag formation Upper Ordovician in Tazhong 44 well. The components are close to the average value of stratum water, respectively:  $K^+ + Na^+ = 20407.53 \text{ mg/L}$ ,  $Mg^{2+} = 344.51 \text{ mg/L}$ ,  $Ca^{2+} = 21856.7 \text{ mg/L}$ ,  $HCO_3^- = 688.31 \text{ mg/L}$ ,  $Cl^- = 51957.64 \text{ mg/L}$ ,  $SO_4^{2-} = 788.27 \text{ mg/L}$ .

IV. EXPERIMENTAL RESULTS ANALYSIS

To analyze the dissolution of carbonate rocks of different components in different temperature and pressure conditions, the samples are placed in different

temperatures and pressures to carry out dissolution experiments. First, the pressure is set to be 40MPa and the temperature is regulated to analyze how temperature affects the dissolution rate. The temperatures are respectively 25 °C, 50 °C, 75 °C, 100 °C, 125 °C, 150 °C, 175 °C and 200 °C, while the fluid velocity keeps 1.5ml/min for 10 hours. The measured dissolution rates of different samples are shown in Figure 3.

From the analysis of the experimental results, it's known that: 1. In the case of constant pressure, the dissolution rate is obviously influenced by temperature. In 25 °C -75 °C, the dissolution rate increases with the temperature increase, showing positive correlation. When the temperature is >75 °C, the dissolution rate decreases with the temperature increase, showing negative correlation. 2. Considering the different lithology, the dissolution rate of limestone > transitional rock > dolomite, the maximum dissolution rate difference can reach 1.92 times. But at 200 °C, the three dissolution rates differ less. 3. The dissolution rates of the limestone of different structural components differ a little, and sometimes the dissolution rate of the micritic limestone may be even slightly larger than the calcarenite.

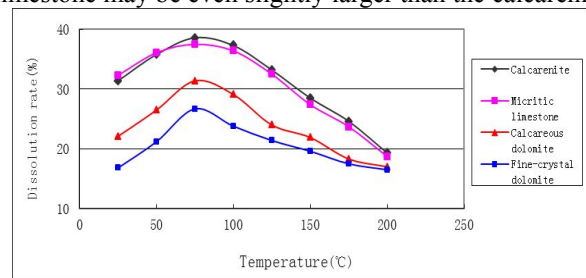


Figure 3. Dissolution Rate of Different Type Carbonate Rocks in Temperature Variation

To analyze the changes of the dissolution rate in different pressures, let the temperature be a fixed value, as 70 °C. The pressure is adjusted to analyze the influence of pressure on dissolution rate. The pressures are respectively 10MPa, 20MPa, 30MPa, 40MPa and 50MPa. At the same time, the fluid velocity keeps 1.5ml/min for 10 hours. The measured dissolution rates of different samples are shown in Figure 4.

From analyzing the experimental results: 1. At a certain temperature, the dissolution rate increases with the pressure increase, showing positive correlation. But in 10-30MPa, with the pressure increase, the dissolution rate shows no significant change. When the pressure

>30MPa, the dissolution rate significantly increases with the pressure increase. 2.For different lithology, in most cases, the dissolution rate of the limestone > transitional rock > dolomite.But the dissolution velocity is different making the dissolution rate of calcareous dolomite> limestone at 50MPa.3. Similarly, the dissolution rates of different structural components in limestone also differ small, and sometimes the dissolution rate of micritic limestone is even slightly larger than the calcarenite.

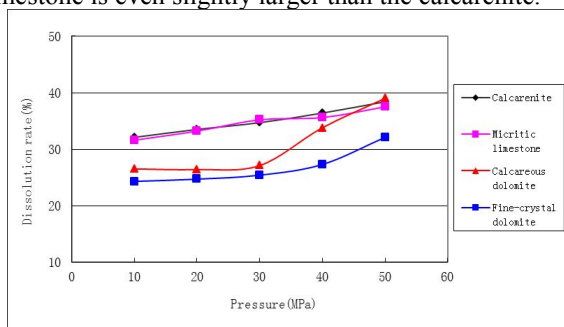


Figure 4. Dissolution Rate of Different Type Carbonate Rocks in Pressure Variation

#### V. CONCLUSION AND DISCUSSION

(1) At 40MPa, the dissolution rate change is shown as increasing with the temperature increase in 25 °C -75 °C and decreasing with the temperature increase when >75 °C; the dissolution rate of limestone > transitional rock > dolomite, but when reaching 200 °C the three dissolution rates differing a little.

(2) At 70 °C, the dissolution rate is positively associated with pressure; the dissolution rate of limestone > transitional rock > dolomite, but the dissolution velocity being different.

(3) The conclusion of this paper is different from the researchers before. The main reason lies in the different experimental conditions. For example, the dissolution rate in Yang Junjie's simulation experiment is controlled by both temperature and pressure, while here uses the way of regulating pressure at a certain temperature or regulating the temperature at a certain pressure to measure the dissolution rate which is similar to Jiang Xiaoqiong's experimental conditions and comes to similar conclusions that also proves that different experimental conditions have great effects on the experimental results. In addition, the research in this paper shows that when the temperature above 200 °C or the pressure above 50MPa, the dissolution rates differ a little, and with the further increase of temperature and pressure, it may also occur that the dissolution rate of the dolomite is greater than the limestone.

(4) In the actual exploration, the dissolution degree of dolomite is always better than limestone. There are many reasons for this result. For example, the dolomitization may cause crystal volume narrowing and surface ratio increasing, and the dolomite is brittleness and easy to cause crack. These make the porosity of the dolomite is higher than that of the limestone.

#### REFERENCES

- [1] ZHANG Yun-feng, WANG Zhen-yu, QU Hai-zhou, et al. Sedimentary microtopography in sequence stratigraphic framework of Upper Ordovician and its control over penecontemporaneous karstification, No. 1 slope break, Tazhong, Tarim block[J]. J. Cent. South Univ, 2014, 21: 1-10.
- [2] CUI Dian, XU Shumei. The developmental modes of buried modifications in Lower Paleozoic Buried Hill in Zhuanghai area of Jiyang Depression[J]. Science & Technology Review, 2010, 28(18): 26-31.
- [3] HUANG Kangjun, WANG Wei, BAO Zhengyu, et al. Dissolution and alteration of Feixianguan Formation in the Sichuan Basin by organic acid fluids under burial condition: Kinetic dissolution experiments[J]. Geochimica, 2011, 40(3): 289-300.
- [4] YANG Haijun, LI Kaikai, PAN Wenqing, et al. Burial hydrothermal dissolution fluid activity and its transforming effect on the reservoirs in Ordovician in Central Tarim[J]. Acta Petrologica Sinica, 2012, 28(3): 783-792.
- [5] XIAO Linping. Thermodynamic Model For Experimental simulation of dissolution of the carbonate rocks in the burial environments: An example from the fifth member of The Lower Devonian Majiagou Formation in the Shaanxi-Gansu-Ningxia Basin[J]. Sedimentary Facies and Palaeogeography, 1997, 17 (4): 57-68.
- [6] Alkattan M. An experimental study of calcite dissolution rates at acidic conditions and 25 °C in the presence of NaPO<sub>3</sub> and MgCl<sub>2</sub>[J]. Chem. Geol., 2002, 190: 291-302.
- [7] Holdren G R J, Speyer P M. Reaction rate surface area relationships for an alkali feldspar during the early stages of weathering, initial observations[J]. Geochimica et Cosmochimica Acta, 1985, 49 (3): 675-681.
- [8] YANG Junjie, HUANG Sijing, ZHANG Wenzheng, et al. Experimental simulation of dissolution for carbonate with different composition under the conditions from epigenesis to burial diagenesis environment[J]. Acta Sedimentologica Sinica, 1995, 13(4): 49-54.
- [9] YANG Junjie, ZHANG Wenzheng, HUANG Sijing, et al. Experimental simulation for dolomite dissolution under the conditions of burial temperature and pressure[J]. Acta Sedimentologica Sinica, 1995, 13(3): 83-88.
- [10] CUI Zhenang, BAO Zhengyu, ZHANG Tianfu, et al. Dissolve kinetics experiment of carbonate rocks in Burial Temperature and Pressure[J]. Journal of Oil and Gas Technology, 2007, 29(3): 204-207.
- [11] JIANG Xiaoqiong, WANG Shuyi, FAN Ming, et al. Study of simulation experiment for carbonate rocks dissolution in burial diagenetic environment[J]. Petroleum Geology & Experiment, 2008, 30(6): 643-646.
- [12] FAN Ming, JIANG Xiaoqiong, LIU Xinwei, et al. Dissolution of carbonate rocks in CO<sub>2</sub> Solution under the different temperatures[J]. Acta Sedimentologica Sinica, 2007, 5(6): 825-830.
- [13] Luquot L., Gouze P. Experimental determination of porosity and permeability changes induced by injection of CO<sub>2</sub> into carbonate rocks[J]. Chemical Geology, 2009, 265: 148-159.
- [14] FAN Ming, XU Liangfa, LIU Xinwei, et al. Experiment geology research of carbonate dolomitization[J]. Petroleum Geology & Experiment, 2012, 34(6): 635-640.
- [15] ZHANG Wenzheng, YANG Junjie, HUANG Yueming. Experimental simulation of deep burial dissolution process of carbonate rocks[J]. Journal of low permeability oil and gas field, 1997, (3): 34-37.

# A Novel Design of Digital AC Voltmeter

Buxin Zhou; Chengwei Cai

Department of Electronics and Communication Engineering, Suzhou Institute of Industrial Technology, Suzhou, Jiangsu Province, P.R.China, 215104

**Abstract**—This system can provide real-time measurements and indications for the AC voltage of electric circuit. It has regular measurement and display functions. It is programmable and can achieve functions such as remote data transmission and monitor the system network. The system is reliable and robust, with high precision and good electromagnetic compatibility. It can directly replace the original pointer instrument.

**Index Terms**—Voltmeter, ATmega16 Microcontroller, Current Output

## I. INTRODUCTION

Digital Voltmeter is widely used in power plant, electric switch cabinet and electrical equipment for measuring or displaying the parameters of the electric circuit, such as AC voltage, current and frequency, active power and power factor of AC single/3 phase. Compared with traditional pointer instruments, the digital ones are more accurate, convenient, flexible for installation, anti-shock, anti-EMI with parallax-free and clearer display. The requirements of the system design are listed as below,

- 1) Voltage measurement (directly) range: AC 0~600V(50/60Hz)+10%
- 2) Settable high and low voltage alarms, with alarm output double circuit relay (on-load AC 250V/3A DC 30V/5A)
- 3) Can transduce 4-20mA current (with an accuracy<0.1mA) for remote measurement of real-time voltage
- 4) Equip with RS-232 communication interface, which can exchange data with computers easily, to achieve the automation of monitor, measurement and control

## II. OVERALL SYSTEM DESIGN

The key control module of the system is an ATmega16 AVR microcontroller. The design flowchart is shown in Figure 1. Mains electricity is converted to AC low voltage signal through attenuator circuit. The microcontroller samples the peak voltage of the signal. Based on the set value, the microcontroller determines the range of the measurement, re-samples the voltage value with an output on 3 1/2 digit led display. Meanwhile, the RS-232 interface transmits the numeric value of the voltage to PC and converts the voltage signal into current signal which can be remotely transmitted as well. In addition, users can manually set the high and low voltage alarms by keyboard input, which will be used for microcontroller to determine if the alarm relay should be on or off.

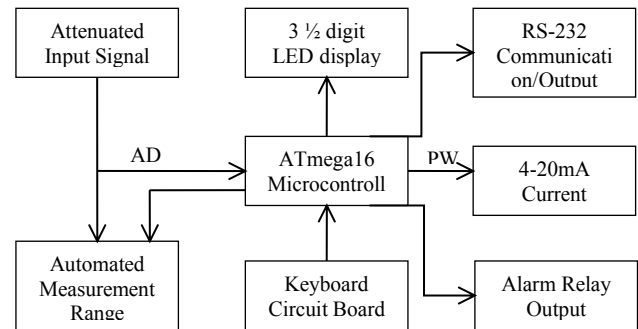


Figure 1. Design Flowchart

## III. HARDWARE DESIGN

The whole system includes input signal attenuator and automated measurement range selection circuit, keyboard display circuit and remote signal output circuit.

### A. input signal attenuator and automated measurement range selection circuit

As shown in Figure 2, the input signal attenuator and automated measurement range selection circuit is designed to decrease the voltage of the input Mains electricity. First of all, the microcontroller sets SW2 as high level and SW1 as low level, Q8 as connected and Q7 as not unconnected. The input 30-300 Vac AC signal is decreased with a ratio of 100:1 through Q8 and converted to 0.3-3 Vac signal.

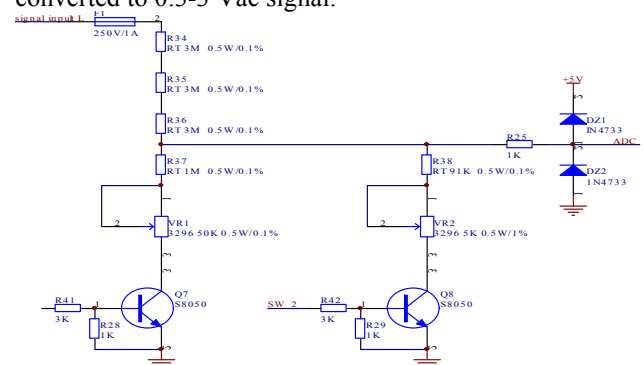


Figure 2. Input Signal Attenuator And Automated Measurement Range Selection Circuit

Then the attenuated signal is sent to ADC interface of the microcontroller for sampling. The microcontroller takes 10 filtered samples of peak value. If the input value is less or equal to 30V, the microcontroller will switch the measure range by disconnecting Q8 and connecting Q7, which results in a 10:1 attenuation of the signal instead of 100:1. The following sampling procedure is the same as previously described.

**B. display circuit**

Figure 3 shows the display circuit. The circuit applies simple software decoding displacement output. The data

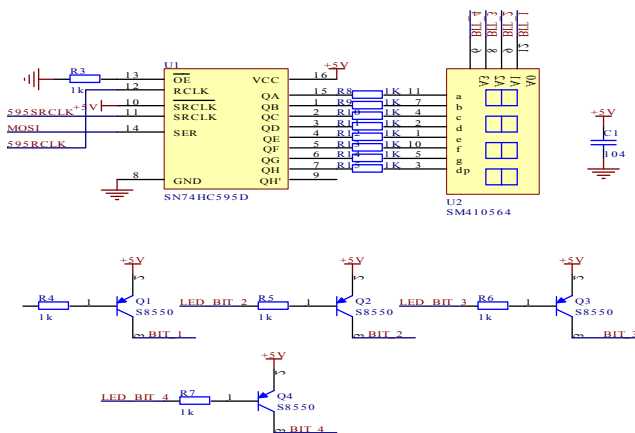


Figure 3. Display Circuit

for display is transmitted through SN74HC595D which is a serial port to parallel port chip. Then the converted parallel data is displayed on LED display, and the number of digits is controlled by Q1, Q2, Q3, Q3.

**C. output circuit for the transduction of 4-20mA current**

Remote signal output circuit includes two parts. One is the RS232 serial port circuit and another is the output circuit for the transduction of 4-20mA current. The previous one is widely used in the communications with software on the host computers. The design of it is very mature and will not be described in this article. The output circuit which is shown in figure 4 includes operational amplifier LM358, triode S8050 and other auxiliary elements. When the input voltage is between 0 to 300V, the microcontroller changes the duty cycle of PWM signal, and then obtain the corresponding analog voltage through double-pole low-pass filter. After filter, the PWM signal attenuates, therefore, an additional same phase signal is added to the operational amplifier. Finally, the signal enters the circuit that transforms signal from voltage to current. In all, the circuit converts the input voltage signal into current signal. The converted current is equal to a constant current source with adjustable output, while the output current is constant without being influenced by the change in loading. Usually, the loading is 250 Ω, if over-loading, the power for Q9 can be increased.

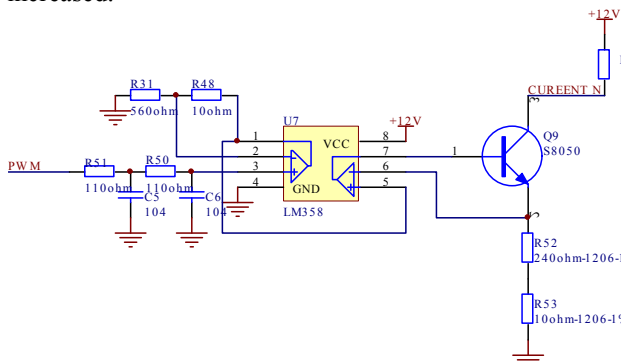


Figure 4. Output Circuit for the Transduction of 4-20ma Current

**IV. RESULT**

AC 10V, 50V, 100V, 400V and 600V voltages were tested as input. Table 1 showed the actual results and

errors. The higher the tested voltage is, the lower the error is. Other functions also worked well as expected during the test. The system met all the requirements for the design.

TABLE I RESULT AND ERRORS

Input[V]	Actual[V]	Error
10	10.91	9 %
50	51.12	2.24%
100	101.5	1.5%
400	405.3	1.33%
600	597.9	0.35%

**V. CONCLUSION**

The designed circuit for voltmeter has advantages such as fast process speed, convenient user interfaces, reliable and with low cost. Currently the product has already passed the examination and is likely to be in the market soon.

**REFERENCES**

- [1] Dj.M. Maric, P.F. Meier and S.K. Estreicher: Mater. Sci. Forum Vol. 83-87 (1992), p. 119
- [2] M.A. Green: *High Efficiency Silicon Solar Cells* (Trans Tech Publications, Switzerland 1987).
- [3] Y. Mishing, in: *Diffusion Processes in Advanced Technological Materials*, edited by D. Gupta Noyes Publications/William Andrew Publishing, Norwich, NY (2004), in press.
- [4] G. Henkelman, G.Johannesson and H. Jónsson, in: *Theoretical Methods in Condensed Phase Chemistry*, edited by S.D. Schwartz, volume 5 of Progress in Theoretical Chemistry and Physics, chapter, 10, Kluwer Academic Publishers (2000).
- [5] R.J. Ong, J.T. Dawley and P.G. Clem: submitted to Journal of Materials Research (2003)
- [6] P.G. Clem, M. Rodriguez, J.A. Voigt and C.S. Ashley, U.S. Patent 6,231,666. (2001)
- [7] Information on <http://www.weld.labs.gov.cn>

# Research on a control circuit of single-phase sine full-bridge inverter

Yannan Yu; Xuejun Wei; Wenyuan Wang; Yizhao Zhang

School of Electrical and Control Engineering, Heilongjiang University of Science and Technology, Harbin, CHINA

**Abstract**—To simplify the control method of single-phase sine wave of full bridge inverter and improve the control system anti-jamming capability, the author designed a control circuit of single-phase sine full-bridge inverter which is based on ICL8038 as the reference sine wave generator chip, SG3525 as control chip and IR2110 as drive chip. At the same time, the author designed the chips peripheral circuits, calculated the main parameters, and set up a simulation model in MATLAB Simulink environment to verify the feasibility of the design.

**Index Terms**—SG3525, Full-bridge inverter, control circuit, MATLAB Simulation

## I. INTRODUCTION

Inverter is a power converter that uses power electronic semiconductor switch combined with electronic technology to change original DC voltage into AC voltage. It is widely used in motor control, uninterruptible power supply (UPS), car inverter, grid-connected photovoltaic, and other fields[1]. Sine wave full-bridge inverter is favored in many systems and occasions with its efficiency, convenience, safety and reliability. In a variety of inverter control systems, the driving integrated circuit of SPWM control and semiconductor switch is the key of it[2].

The author designed a control circuit of single-phase sine full-bridge inverter which is based on ICL8038 as the reference sine wave generator chip, SG3525 as control chip and IR2110 as drive chip. At the same time, the author designed the chips peripheral circuits, calculate the main parameters, and set up a simulation model in MATLAB Simulink environment to verify the feasibility of the design[3],[4].

## II. THE CONTROL PRINCIPLE

Figure.1 shows the power circuit of the single-phase full-bridge inverter. When it works in sinusoidal pulse width modulation (SPWM) mode, the process is as follows: when in positive half cycle sine wave, Q<sub>2</sub> and Q<sub>3</sub> are cut-off, Q<sub>1</sub> and Q<sub>4</sub> run at a high frequency; when in the negative half cycle sine wave, Q<sub>1</sub> and Q<sub>4</sub> are cut-off, Q<sub>2</sub> and Q<sub>3</sub> run at a high frequency.

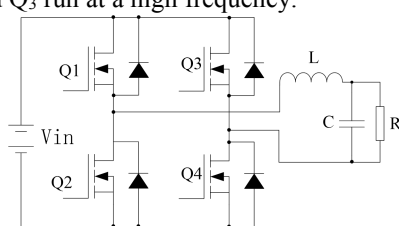


Figure 1. The Main Power Topology

Figure.2 shows the commonly used signal generation circuits of ICL8038. In the figure, R<sub>3</sub> and R<sub>4</sub> are timing resistances and all are adjustable. Adjusting R<sub>3</sub> and R<sub>4</sub> can adjust the oscillation frequency and the duty cycle of the rectangular wave. C is the timing capacitor, and its oscillation frequency is:

$$f = \frac{3}{10R_3 \cdot C} \tag{1}$$

Take  $f = 50\text{Hz}$ ,  $C = 1\mu\text{F}$

$$50 = \frac{3}{10R_3 \times 0.1 \times 10^{-6}} \tag{2}$$

$$R_3 = 6\text{k}\Omega \tag{3}$$

In order to improve the frequency precision of the wave and reduce distortion, it is designed that pin 8 connecting potentiometer. Pin 8 potential can be changed in this way, so as to achieve the purpose of adjustable frequency. Meanwhile the pin1 and pin2 connect adjustable resistance, to adjust distortion of sine wave, shown in Figure.3.

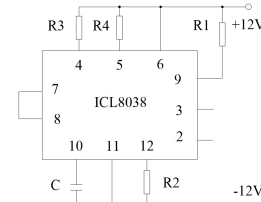


Figure 2.Signal generating circuits of ICL8038.

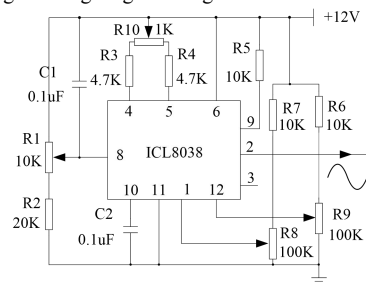


Figure 3.Peripheral circuits of ICL8038.

## III. SINUSOIDAL PULSE WIDTH MODULATION CIRCUIT

### A. SG3525 peripheral circuits

Using SG3525 as main control chip, comparing the internal triangle wave with the input reference sine wave, generates SPWM pulse. The main parameters are designed as follows:

### Determination of the oscillation frequency

Oscillation frequency of internal oscillator depends on

the size of the external timing resistor ( $R_t$ ) of pin6, and the external timing capacitor ( $C_t$ ) of pin5, and discharge resistor ( $R_d$ ) connected to between pin7 and pin 5. The equation of oscillation frequency is:

$$f = \frac{1}{C_t(0.7R_t + 3R_d)} \quad (4)$$

**Determination of the dead time**

Dead time is related to  $R_d$  and external timing resistor  $R_t$ . Literature [5] gives a relation curve between a maximum value of  $R_d$  and minimum value of  $R_t$ . In this design, full-bridge switch's frequency is 62.6 kHz, so the control chip SG3525 oscillation frequency is 125.2 kHz.

Take  $R_t = 10K\Omega$ ,  $R_d = 330\Omega$

$$125.2KHz = \frac{1}{C_t \times (0.7 \times 10K + 3 \times 330)} \quad (5)$$

$$C = 1nF \quad (6)$$

**Pin 8 is soft-start pin.**

Soft-start time is determined by the external soft-start capacitor. Take  $C = 1\mu F$ .

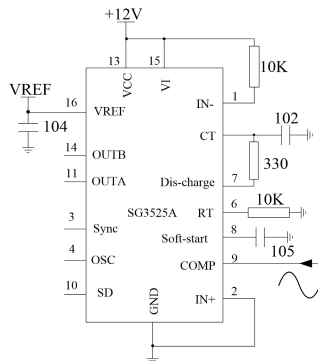


Figure 4.SG3525 external circuits.

Pin8 and pin2 are the inverting input and non-inverting input of the op amp, in this design the reference sine wave signal is directly sent to pin9, and compared with the internal triangle wave, so connect pin1 to  $V_{cc}$  by pull-up resistor, pin2 to ground[6],[7].The peripheral circuit of SG3525 controller chip is shown in Figure.4.

**B. SPWM forming circuit**

In the design the reference sine wave is sent to SG3525 pin9, compared with SG3525 internal triangle wave, to modulate the SPWM pulse, shown in Figure.5. Since SG3525 internal triangle amplitude is 0.9V-3.3V, we need to reduce the sine wave into this range. The operational amplifier OP07 chip is used to build SUB to reduce the amplitude of the sine wave in the design, as shown in Figure.6[8]-[10].

Setting the amplitude of the sine wave after being reduced is: 0.9V-3.3V.

Take  $R_{15} = R_{16}$ ,  $R_{17} = R_{18}$ . Calculating from virtual short circuit and virtual break circuit:

$$V_o = V \sin - \frac{R_{17}}{R_{15}} V_1 \quad (7)$$

$$\begin{aligned} \text{Take } R_{15} = R_{16} = 1K\Omega \\ R_{17} = R_{18} = 10K\Omega \end{aligned} \quad (8)$$

We can adjust the amplitude of the sine wave by

adjusting potentiometer  $R_{13}$  and  $R_{14}$  in practice debugging.

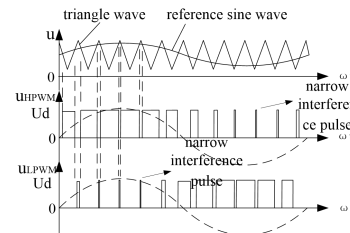


Figure 5.SPWM pulse modulation schematics.

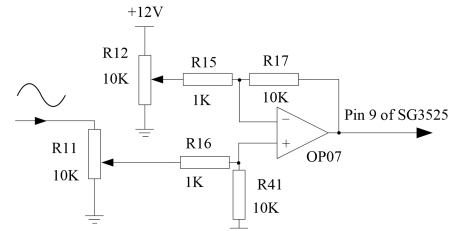


Figure 6.Sine subtraction circuits.

As shown in Figure.5, the positive half cycle ULPWM of the sine wave will generate a very narrow interference pulse, the negative half cycle UHPWM will generate an extremely narrow interference pulse. To prevent the interference pulses effects to the driving circuit, a circuit is offered in this design. Firstly, the sine wave signal is sent to a comparator and output the high and low electrical level signal. And then this high and low electrical level signal and SPWM pulse signal are sent to AND gate to remove the interference signal, as is shown in Figure.7. It is the pulse signal after removing the interference by AND gate in Figure.8 [11]-[13].

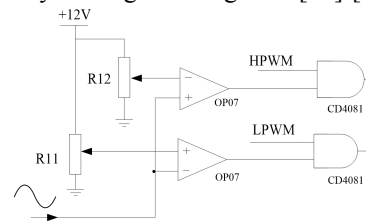


Figure 7.Circuits for removing interference signal.

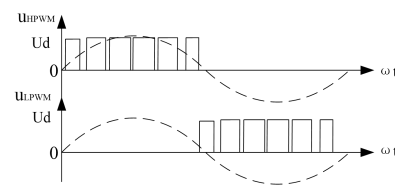


Figure 8.The pulse signal after removing the interference signal.

**IV. MOSFET DRIVE CIRCUIT**

The author uses IR2110 which is high pressure suspension type bootstrap driver chip as the driver module, the external circuit of IR2110 chip is shown in Figure.9.As is shown in the Figure.9, SPWM pulse is sent to HIN and LIN, HO and HI are the output pins of the two driver. The follows are features of the diode: a. can block high pressure of DC trunk; b. low charge loss; c. Forward Current Capability is the product of  $Q_g$  and switching frequency; d. low Sink Current Capability; e. ultra-fast switching speed.

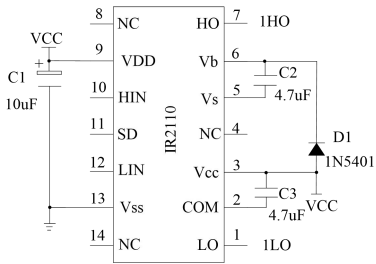


Figure 9. External circuits of IR2110.

The power supply for the internal high voltage module of the chip is from the bootstrap capacitor. To ensure sufficient power supply for the drive circuit of the high pressure module, the capacitance value is neither too small to meet the driving requirements of

wide pulse, nor too big to effect the drive signal. The capacitor should be selected from the switch operating frequency, switching speed, and other characteristics. As usual the capacitor can be decided by debugging in the design, the capacitor values  $4.7\mu F$  in this design [1].

V. THE MATLAB SIMULATION

To verify the feasibility of the scheme, the author set up simulation of single-phase SPWM full bridge inverter in MATLAB simulation environment. The system simulation model is shown in Figure.11. The simulation results show that pulse modulation stable and low interference. The inverter output waveform distortion.

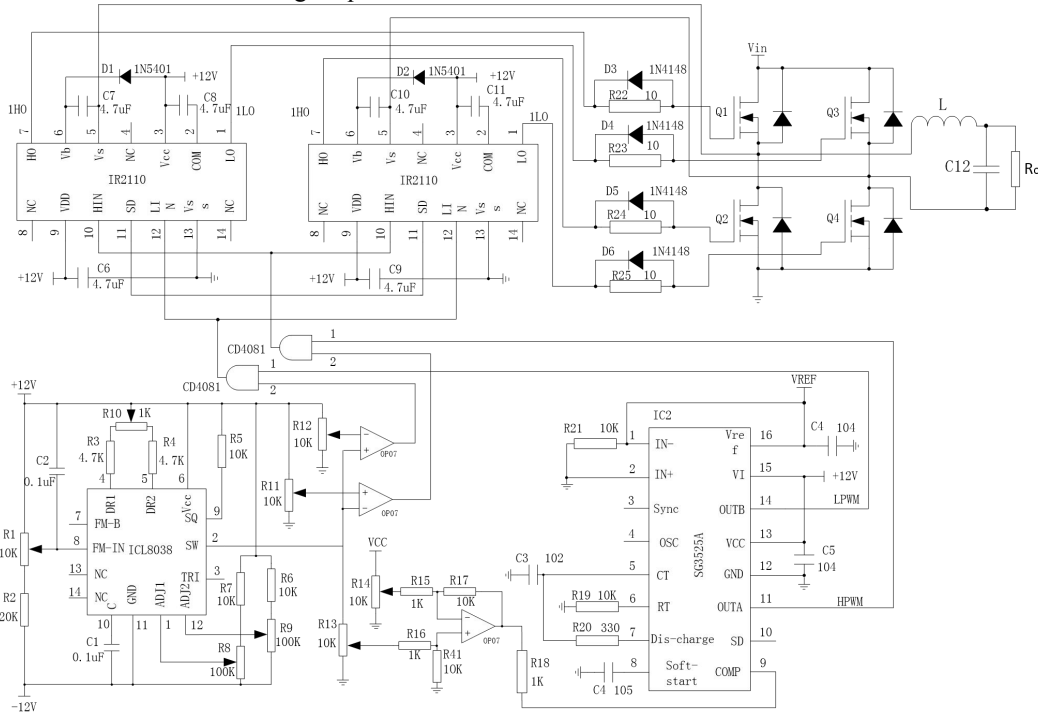


Figure 10. Control circuits of single-phase sine wave full-bridge inverter

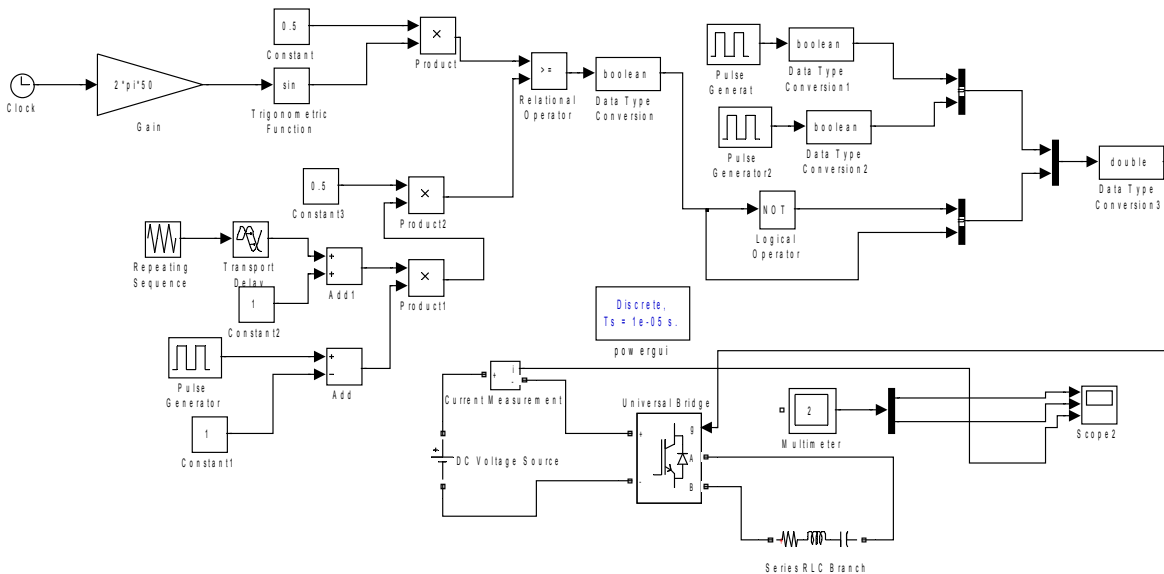


Figure 11. System simulation block diagram.

## VI. CONCLUSION

Research and design a control circuit of single-phase sine full-bridge inverter which is based on ICL8038 as the reference sine wave generator chip, SG3525 as control chip and IR2110 as drive chip. Simulation results verify the feasibility of the circuit. The circuit structure is simple, easy to implement, and can improved full bridge inverter control system anti-interference ability and reliability.

## ACKNOWLEDGMENT

This work was supported by Chinese Heilongjiang Education Department Science and Technology Research (project Number: 12531594).

## REFERENCES

- [1] Guojing, "Design of single phase grid inverter." *Journal of Harbin Institute of Technology*, 2007,25 (17).
- [2] Ribeiro H S, Borges B V. "New optimized full-bridge single-stage ac/dc converters[J]." *Industrial Electronics*, IEEE Transactions on, 2011, 58(6): 2397-2409.
- [3] Roggia L, Schuch L, Baggio J E, et al. "Integrated Full-Bridge-Forward DC-DC Converter for a Residential Microgrid Application[J]." *Power Electronics*, IEEE Transactions on, 2013, 28(4): 1728-1740.
- [4] Wang Shuiping. "MOSFET/IGBT driver integrated circuit application of [M]." Beijing: Chinese electric power press, 2010
- [5] Cho I H, Cho K M, Kim J W, et al. "A new phase-shifted full-bridge converter with maximum duty operation for server power system[J]." *Power Electronics*, IEEE Transactions on, 2011, 26(12): 3491-3500.
- [6] Lü Hong, HUANG Yushui, ZHANG Zhongchao. "Research on Control Methods of Serial Resonant Single-phase Full-Bridge Inverter." *Application of power technology*, 2002,5(5).
- [7] Salvi A, Santini S, Biel D, et al. "Model reference adaptive control of a full-bridge buck inverter with minimal controller synthesis[C]." IEEE CDC. 2013.
- [8] Fan S, Ma W, Liu G, et al. "A current output hard-switched full bridge DC/DC converter for wind energy conversion system[C]." *Renewable Power Generation Conference (RPG 2013)*, 2nd IET. IET, 2013: 1-4.
- [9] Nguyen M K, Lim Y C, Cho G B, " Switched-inductor quasi-Z-source inverter[J]." *Power Electronics*, IEEE Transactions on, 2011, 26(11): 3183-3191.
- [10] de Oliveira L R, dos Santos Barros T A, Villalva M G, et al. "Input voltage regulation of an isolated full-bridge boost converter fed by a photovoltaic device with the state-space feedback control method[C]." *Power Electronics Conference (COBEP)*, 2013 Brazilian. IEEE, 2013: 595-600.
- [11] Wai R J, Lin C Y, Huang Y C, et al. "Design of high-performance stand-alone and grid-connected inverter for distributed generation applications[J]." *Industrial Electronics*, IEEE Transactions on, 2013, 60(4): 1542-1555.
- [12] "Design of simulation of single-phase SPWM inverse power sources," *Journal of Liaoning Technical University (NATURAL SCIENCE EDITION)*, 2008,27(3).
- [13] Wu Jiayu, Lin Jincheng, Wang Wenting, Sugimoto Eihiko. "Simulation study of single-phase full bridge SPWM inverter." *Journal of system simulation*, 2008,20 (21)

**Yannan Yu** was born in Heilongjiang province, China, in 1979. She received the B.S. and M.S. degrees in electrical engineering from the Harbin Institute of Technology, Harbin, China, in 2003 and 2006, respectively, where she is currently working toward the Ph.D. degree. Since 2009, she has been a Lecturer in E.C. Dept, Heilongjiang University of Science and Technology.

She is currently working toward the Ph.D. degree in electrical engineering at Harbin Institute of Technology, and her research interests include high-power power electronics, switching power, multilevel converters and power quality mitigation.

**Xuejun Wei** was born in Jiangsu province, China, in 1990. He is currently working toward the B.S. degree.

**Wenyuan Wang** was born in Jiangsu province, China, in 1991. He is currently working toward the B.S. degree.

**Yizhao Zhang** was born in Heilongjiang province, China, in 1991. He is currently working toward the B.S. degree.

# Optimal Design And Study For Pipeline Diameter Of District Heating System

Xianliang Yang; Cuicui Huang

Energy and Power Engineering College, North China Electric Power University, Baoding, China

**Abstract**—For the central heating supply network with fixed structure, an objective function equation of a primary network in a central heating system is set up, taking the least sum of the heating system infrastructure investment costs and operation energy consumption costs in the life cycle as optimization goal, and its constraints are operational characteristics of the primary network. For a municipal water supply network, using the penalty interior point method to calculate the objective function. Finally, comparing the method with traditional design method through an example, Pointing out this method is not only can meet the design requirements, but also save the cost of investment.

**Index Terms**—heating pipe network, objective function, investment cost, penalty interior point method

## I. INTRODUCTION

The central heating system consists of three parts: heat sources, networks and consumers. As an important part of the central heating system, heat networks bear the task that delivering and assigning the heat from the heat source to each user timely, and has played the role of a bridge connecting the heat networks and consumers. The design rationality of heat-supply network is directly related to the initial investments and operation costs of the whole heat-supply system. Therefore, reasonable selection of the diameters is of great concern to the cost saving[1]. Traditional heat-supply network engineering design is according to the allowable range of the pipe flow, the economic specific frictional resistance and the velocity to determine the diameter without considering the effect of the size of the diameter on the infrastructure investment costs and operating costs, but the diameter meeting the conditions is not the only one, therefore selection of the diameters is blind very much, and then bring about wasting of the initial investments and operation costs[3-7]. In view of this, this paper puts forward the following design method.

### A. Mathematical Model

Mathematical model of global optimization in the complex heat-supply network mainly includes two aspects: one is the objective function, taking account of the capital construction investment and operation energy consumption costs, and the decision variable is the diameter; the other is the constraint condition in the network design, including the flow, pressure, velocity and diameter constraints.

### B. Establishment of The Objective Function

The cost of heat-supply network includes four parts: infrastructure investment costs, operation energy consumption costs, thermal lost costs and maintenance costs. To a certain specific central heating supply network, the thermal lost costs and maintenance costs when operating mainly depend on the size and capability of heating area, and the heating demand and capacity is certain, as a result, the above two costs can be treated as constant. Therefore, the total cost of heat-supply network depends on the infrastructure investment costs and operation energy consumption costs, they are interdependent. To a heating network with fixed layout, if choosing the smaller diameter, then infrastructure investment costs will reduce and the operation energy consumption costs will increase; otherwise the opposite. Consequently, we should fully take into account the two aspects when designing, so that making sure the total cost minimum in its life cycle.

#### Capital Construction Investment

Infrastructure investment costs include all costs of the infrastructure, such as pipe, insulation, pipe laying and construction etc. Annual infrastructure investment costs(  $C_{np}$  ) can be written into the function of pipe diameter and pipe length:

$$C_{np} = \sum_{i=1}^n f(d_i)l_i \quad (1)$$

Where:  $C_{np}$  is the infrastructure investment costs, ten thousand dollars;

$n$  is the pipe section number;

$d_i$  is the nominal bore about pipe section  $i$ , m;

$l_i$  is the length about pipe section  $i$ , m;

$f(d_i)$  is the cost per meter about pipe section  $i$ , ten thousand dollars/m.

Outdoor heat-supply pipe network adopts directly buried installation without compensation, its cost per meter of hot-water pipe and its heating scale and cost of circulating water pump with different model number and specification can be figured out according to the National Municipal Engineering Investment Estimation Index. The cost of hot-water direct buried pipeline can see table 1, the cost of circulating water pump can see table 2. The results in table 1 can be fitted into curve equations by lest square method as shown in figure 1.

As you can see from figure 1, the polynomial relationship between pipeline investment and pipe diameter is:

$$f(d_i) = 0.021 + 0.433d_i + 0.4d_i^2 \quad (2)$$

So the cost of construction can be written as:

$$C_{np} = \sum_{i=1}^n (0.021 + 0.433d_i + 0.4d_i^2)l_i \quad (3)$$

TABLE I. THE COST OF THE DIRECT BURIED PIPELINE

Nominal bore /mm	Cost/(ten thousand dollars/m)	Nominal bore/mm	Cost/(ten thousand dollars/m)
80	0.053	450	0.311
100	0.0641	500	0.348
125	0.078	600	0.421
150	0.090	700	0.512
200	0.1211	800	0.632
250	0.146	900	0.701
300	0.1861	1000	0.840
350	0.235	1200	1.137
400	0.269		

TABLE II. THE COST AND HEATING SCALE OF CIRCULATING WATER PUMP

Circulating water pump's model number and specification	Price /ten thousand dollars	Heating scale /ten thousand m2	Number of units
G=180m3/h,	2.7	5	2
G=360m3/h,	3.8	10	2
G=500m3/h,	4.5	15	2
G=700m3/h, H=42m, N=132K	8	20	2
G=420m3/h,	4.3	25	3
G=500m3/h, H=45m, N=110KW	7.5	30	3

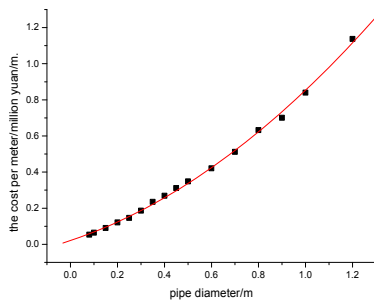


Figure 1. The curve about the cost of direct buried pipeline

In order to make the data more accurate, adding the purchasing expense about circulating water pump( $C_{nb}$ )

$$C_{nb} = \sum_{i=1}^p C_{nbi} \quad (4)$$

Where:  $C_{nb}$  is the purchasing expense about circulating water pump, ten thousand dollars;  
 P is number of units about circulating water pump, unit;  
 $C_{nbi}$  is the price about per circulating water pump, ten thousand dollars/unit.

**Operating Cost**

Annual operation energy consumption costs of the pipe network mainly refer to the operating electricity consumption, it relates to these elements: flow capacity, lift ,operating time, operating efficiency of the circulating water pump, local electricity etc. The annual operation cost ( $C_d$ ) is:

$$C_d = \frac{1}{3600} \sum_{i=1}^p P_i j_d n_{i0} \quad (5)$$

Where:  $C_d$  is the annual operation cost, ten thousand

dollars;

P is the unit number of circulating water pump, unit;

$P_i$  is the operating efficiency about the circulating water pump i, kw;

$n_{i0}$  is the annual operating time about circulating water pump i, h;

$j_d$  is the local electricity, dollar/kwh.

And because:

$$P_i = \frac{H_i G_i}{\rho \eta} \quad (6)$$

$$H_i = R(l_i + l_d) = 0.00688K^{0.25} \frac{G_i^2}{\rho d_i^{5.25}} (1 + \alpha_j) l_i \quad (7)$$

Where:  $G_i$  is the export flow about the circulating water pump i, t/h;

$H_i$  is the lift about the circulating water pump i, Pa ;

$\rho$  is the density of hot water,  $kg / m^3$  ;

$\alpha_j$  is the percentage of local resistance, %;

$K$  is the equivalent roughness on pipeline' inner wall, mm;

$\eta$  is the motor power, taking 0.6~0.8.

So:

$$C_d = 1.911 \times 10^{-6} \sum_{i=1}^n \frac{G_i^3 K^{0.25}}{\rho^2 \eta d_i^{5.25}} j_d n_{i0} (1 + \alpha_j) l_i \quad (8)$$

**C. Constraint Condition**

**Node Flow Continuity Constraint**

$$\sum_j G_{ij} + Q_i = 0 \quad i=1,2,3,\dots,N \quad (9)$$

Where: j is the associated node with node i;

$G_{ij}$  is the pipeline flow associated with node i, t/h;

$Q_i$  is the flow from node i to the out, t/h;

N is the total number of nodes.

**Pressure Constraint**

$$\sum_{l_k} \Delta H_i = 0 \quad k=1,2,3,\dots,N \quad (10)$$

Where:  $l_k$  is the pipe network loop k;

$\Delta H_i$  is the pressure drop of pipeline i about the loop.

**Users, Node Head Demand Constraint**

$$H_{i,s} \geq H_{i,ys} \quad i=1,2,\dots,U \quad (11)$$

Where:  $H_{i,s}$  is the calculation pressure about heat user i,  $mH_2O$  ;

$H_{i,ys}$  is pre-reservation pressure,  $mH_2O$  ;

U is the total number of the heat consumers.

**The Standard Diameter Constraint**

The maximum diameter is DN1400,and the minimum diameter is DN15 which is available in engineering, the minimum diameter about outdoor heat-supply network is just like DN50, the decision variable d should be chosen in the diameter range available in engineering. Therefore, the diameter range constraint is:

$$d_{\min} \leq d_i \leq d_{\max} \quad (12)$$

**The Pipe Velocity Constraint**

According to the city heat-supply network standard, the medium flow rate in the pipe network is usually not more than 3.5m/s.

$$0 \leq v_i = \frac{G_i}{0.9 \rho \pi d_i^2} \leq 3.5 \tag{13}$$

Among them, the hydraulic calculation about heat-supply network immediately satisfy the node flow continuity constraint, the pressure constraint and the users, node head demand constraint. The cost of construction is belong to the input which were finished once, and the operating costs need to be done every year, so we can consider the time value of capital using future value method, that is the less about the total cost of life cycle the more in the condition with the same income.

*D. The Establishment of The Mathematical Model*

According to the above analysis, an objective function equation can be set up, taking the least sum of the infrastructure investment costs and operation energy consumption costs in the life cycle, expressing the terminal value of the total cost in the end of the life cycle using F, that is:

$$F = (1+i)^N \sum_{i=1}^n (0.021 + 0.433d_i + 0.4d_i^2)l_i + \sum_{i=1}^p C_{nbi} + 1.911 \times 10^{-6} \left[ \frac{(1+i)^N - 1}{i} \right] \sum_{i=1}^n \frac{K^{0.25} G_i^3}{\rho^2 d_i^{5.25} \eta} (1 + \alpha_j) l_i j_d n_{io}$$

$$s.t. \begin{cases} 0 \leq v_i = \frac{G_i}{0.9 \rho \pi d_i^2} \leq 3.5 \\ 0.05 \leq d_i \leq 1.4 \end{cases} \tag{15}$$

Among them: i is the discount rate; N is the periodic numbers of life cycle, taking N as 15 in this paper.

**II. NONLINEAR PROGRAMMING METHOD**

*A. Internal Penalty Function Method*

SUMT method [13] ( Sequential Unconstrained Minimization Technique)that is sequential unconstrained minimization technique, also be called penalty function method. Its principle is structuring a new objective function that is the penalty function by using the objective function and constraint function of the problem, then transforming the constrained optimization problem into a unconstrained one of the penalty function to solve. Penalty function method is divided into the internal penalty function method and the exterior penalty function method. The internal penalty function method always starts from the feasible point on the iteration process, and searches on the interior of the feasible region. Therefore this method applies to optimization problems which have only inequality constraints. This paper will employ the internal penalty function method to solve the problem. Introducing briefly the internal penalty function method below:

This paper considers the problem: 
$$\begin{cases} \min f(X) \\ s.t. g_i(X) \geq 0 \end{cases}$$

$i=1, 2, 3, \dots, m$

Let the set  $D^0 = \{X / g_i(X) > 0, i=1,2,\dots,m\} \neq \emptyset$ ,  $D^0$  denotes the set of all strictly feasible interior point in the feasible region.

Structuring the obstacle function:

$$I(X, r) : I(X, r) = f(X) + r \sum_{i=1}^m \ln g_i(X)$$

$$\text{or } I(X, r) = f(X) + r \sum_{i=1}^m \frac{1}{g_i(X)}$$

Among them calling  $r \sum_{i=1}^m \ln g_i(X)$  or  $r \sum_{i=1}^m \frac{1}{g_i(X)}$  as the obstacle term, r as the obstacle factor. So the problem is transformed into a series of extreme value problems:

$$\min_{X \in D^0} I(X, r_k), \text{ getting } X^k(r_k)$$

*B. The Iteration Step of Internal Penalty Function Method*

- (1) Given a permissible error  $\varepsilon > 0$ , taking  $r_1 > 0$ ,  $0 < \beta < 1$ ;
- (2) Obtaining a interior point of the constraint set D,  $X^0 \in D^0$ , ordering  $k=1$ ;
- (3) Letting  $X^{k-1} \in D^0$  as initial point, solving  $\min_{X \in D^0} I(X, r_k)$ , among which setting the optimal solution of  $X \in D^0$  as  $X^k = X(r_k) \in D^0$
- (4) To test whether it meet  $\left| -r \sum_{i=1}^m \ln g_i(X^k) \right| \leq \varepsilon$  or  $\left| r_k \sum_{i=1}^m \frac{1}{g_i(X)} \right| \leq \varepsilon$ , if meet then stop the iteration,  $X^* \approx X^k$ ; otherwise  $r_{k+1} = \beta r_k$ , ordering  $k=k+1$ , returning(3).

The calculation process about internal penalty function method is showing as below:

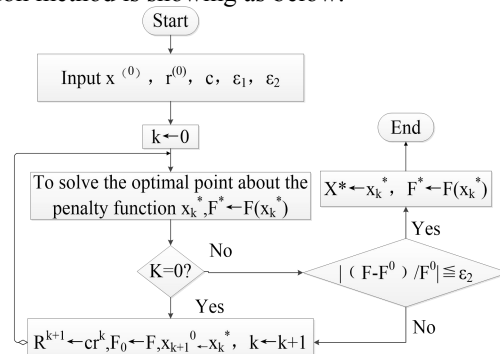


Figure2. The flow chart about internal penalty function method

**III. EXAMPLE CHECKING PRESENTS**

As figure 3-the graph layout about hot water heating network in a certain city in Hebei Province shows that it is composed mainly of one heat source and 14 heating power stations, the calculation water-supply temperature and the water-return temperature are:  $t_1 = 130 \text{ }^\circ\text{C}$ ,  $t_2 = 80 \text{ }^\circ\text{C}$ . The total heating scale of the heating power

station is 238 million m<sup>2</sup>, the designed discharges respectively are: 133.27 t/h, 141.01 t/h, 165.08 t/h, 163.36 t/h, 137.57 t/h, 142.73 t/h, 147.89 t/h, 149.61 t/h, 171.96 t/h, 154.76 t/h, 146.17 t/h, 130.69 t/h, 134.13 t/h, 128.97 t/h. In the light of flow equilibrium, we can figure out the calculated flow rate of every pipe section, as shown in table 2. The pipe network adopts non-compensating buried laying mode, the insulation materials use polyurethane foam plastic, the protection layer use polyethylene plastic. For the percentage of local resistance, the main pipe takes 0.2, the separated and branch pipe take 0.3, the comprehensive square thermal index takes 65 W/m<sup>2</sup>. Taking  $K = 0.5 \times 10^{-3} m$ ,  $n_{i0} = 120d$ ,  $i = 10\%$ ,  $N = 15a$ ,  $\eta = 0.7$ ,  $j_d = 0.8 \text{ yuan} / KWh$ ,  $\rho = 958.4 \text{ kg} / m^3$ . According to the former proceeding optimization method,

carrying out the hydraulic calculation for the actual pipe network to determine the diameter, the calculation results are shown in table 3, the comparisons about all costs are shown in table 4.

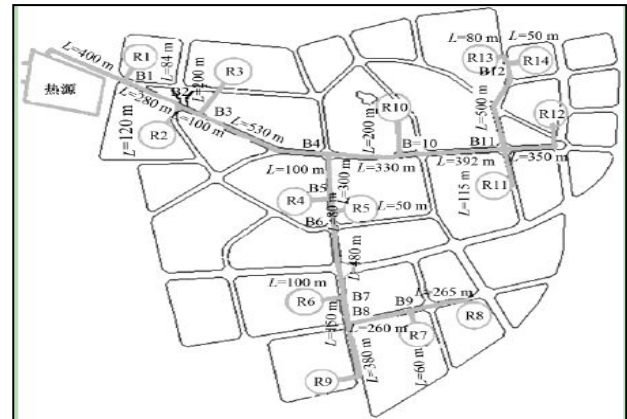


Figure3. The graph layout about hot water heating network in a certain city in Hebei Province

TABLE III. COMPARISON OF THE DESIGN RESULTS ABOUT THE PIPELINE NETWORK PARAMETERS

Pipe section	The flow in pipe section / (t/h)	The length about pipe section /m	The total length after conversion /m	New design			Original design		
				Resistance /MPa	Pipe diameter /mm	Velocity in pipe section / (m/s)	Resistance /MPa	Pipe diameter /mm	Velocity in pipe section / (m/s)
Heat source-B1	2047.19	400	480	0.021	650	1.79	0.027	600	1.96
B1-B2	1913.92	280	336	0.013	650	1.67	0.017	600	1.83
B2-B3	1772.91	100	120	0.004	650	1.55	0.005	600	1.7
B3-B4	1607.83	530	636	0.067	500	2.37	0.057	500	2.21
B4-B10	694.71	330	396	0.020	350	2.09	0.023	400	1.54
B10-B11	539.95	392	470.4	0.030	300	2.22	0.032	350	1.52
B11-B12	263.09	500	600	0.065	250	1.55	0.021	300	1.02
B12-R13	134.13	80	96	0.008	150	2.20	0.007	200	1.16
B4-B5	913.12	100	130	0.007	400	2.11	0.006	450	1.53
B5-B6	749.76	300	390	0.028	350	2.26	0.026	400	1.65
B6-B7	612.19	480	624	0.059	300	2.51	0.054	350	1.73
B7-B8	469.46	160	208	0.027	300	1.93	0.011	350	1.33
B8-B9	297.5	260	338	0.047	250	1.76	0.015	300	1.15
B9-R8	149.61	265	344.5	0.045	150	2.46	0.033	200	1.29
B1-R1	133.27	84	109.2	0.010	200	1.23	0.008	200	1.15
B2-R2	141.01	120	156	0.016	200	1.30	0.013	200	1.22
B3-R3	165.08	200	260	0.036	200	1.52	0.010	250	0.92
B5-R4	163.36	80	104	0.008	200	1.51	0.004	250	0.99
B6-R5	137.57	50	65	0.009	150	2.26	0.005	200	1.19
B7-R6	142.73	100	130	0.060	150	2.34	0.011	200	1.23
B9-R7	147.89	60	78	0.039	150	2.43	0.007	200	1.27
B8-R9	171.96	380	494	0.073	200	1.59	0.020	250	0.96
B10-R10	154.76	200	260	0.009	150	2.54	0.008	250	0.86
B11-R11	146.17	115	149.5	0.065	150	2.40	0.014	200	1.26
B11-R12	130.69	350	455	0.046	150	2.14	0.033	200	1.13
B12-R14	128.97	50	65	0.009	150	2.12	0.005	200	1.11

Marking: the original design result is based on the hydraulic calculation table about the thermal pipe network from The Design Manual for Thermal Pipeline

to calculate.

IV. CONCLUSIONS

A. For the central heating supply network with fixed structure, setting up an objective function equation with the least sum of the infrastructure investment costs and operation energy consumption costs, and applying it to the network design, finally proving that it can save investment cost.

B. Applying the internal penalty function method to solve the objective function equation, and analyzing the problem through an example. Compared this method with the original design, the total cost can be saved by more than 4%.

C. The optimization design method can not only provide theoretical basis for the engineering design personnel, but also can provide technical assurance for the efficient and energy saving operation about the system. It is of great both theoretical and practical significance.

TABLE IV. THE COMPARISON OF COSTS

	New design	Original design	saving
The Infrastructure Investment Costs /ten thousand dollars	5219.12	5694.82	475.7
The Operation Energy Consumption Costs ten thousand dollars	1177.56	978.06	-190.5
The Purchasing Expense About Circulating Water Pump /ten thousand dollars	21.5	12.9	-8.6
The Total Cost /ten thousand dollars	6418.18	6685.78	267.6

## REFERENCES

- [1] Deying Li. *Heating engineering* [M]. Beijing: Chinese Building Industry Press. 2004.
- [2] Jinxiang Liu. The analysis and calculation of economic friction factor about hot-water heating network [J]. *Journal of Nanjing Architectural and Civil Engineering Institute*, 1998(4): 38-43.
- [3] Yin Juan. Optimization of the central heating pipe network in the city [D]. Tianjin: Hebei Industrial University, 2005: 3.
- [4] Xinagli Li, Zhongyu Sun, Pinghua Zhou. Hydraulic calculation and analysis of hot water pipe network with multiple heat source [J] *HV & AC*. 2004, 34(7): 97-101.
- [5] Yiming Huang. Optimal design of the central heat supply network [J]. Master Degree Thesis. Xi'an University of Technology. 2007.
- [6] Xuzhong Qin, Yi Jing. Accessibility analysis of district heating loop-networks based on genetic algorithms. [J].

- Qinghua University(Science & Technology)*. 1999, 39(6):90-94.
- [7] Saolin Xi, Fengzhi Zhao. Optimum calculation method [M]. Shanghai: the Science & Technology Press in Shanghai, 1983.
  - [8] Zhen Li. *Two penalty functions of nonlinear programming* [D]. Shanghai: College of Sciences, Shanghai University, 2007: 29-32.
  - [9] Suwen Li. *The research of nonlinear conjugate gradient method* [D]. Nanjing: College of Sciences, Nanjing University of Science and Technology. 2008: 3-6.
  - [10] Shanhua Li, Hui Kang, etc. *The Design Manual for Thermal Pipeline* [M]. Beijing: China Electric Power Press, 1995.
  - [11] National Municipal Engineering Investment Estimation Index. [M]. China Plan Press, 23-70.
  - [12] Jinming Shu. *MATLAB Practical Guideline Pandect* [M]. Beijing: Electronic Industry Press, 2001.
  - [13] Zheng Xie. *Nonlinear Optimization* [M]. Changsha: National University of Defense Technology Press, 2003: 273-281.
  - [14] Zhiyong Zhang. *Proficiency of MATLAB 6.5*. Beijing: Beijing University of Aeronautics and Astronautics Press, 2003.
  - [15] Wei Chang. *MATLAB R2007* [M]. Beijing: Electronic Industry Press, 2007.
  - [16] Shoujun Zhou, Jihong Pan, Qingfeng Wang, etc. Primary network operational optimization and algorithm of a district heating system [J]. *Journal of Beijing University of Technology*. 2012(4): 629-635.
  - [17] Meijie Wang, Di Weimin. Study on new optimal design method for pipeline diameter of district tree path heating network. [J]. *Building Science*. 2012(10): 94-97.

**Xianling Yang** was born in 1975, senior engineer in North China Electric Power University. He is the director of the experimental center of power engineering department, engaged in the research of energy saving of heating. This work was financially supported by the Fundamental Research Funds for the Central Universities (13MS99).

**Cuicui Huang** was born in ShanDong (China) on December 1988, received the Bachelor's degree in Science and Technology College, North China Electric Power University, Baoding, China, at 2008-2012, and is a graduate student in North China Electric Power University.

# The Development and Implementation of Lathe Simulator

Hongge Fu; XiaoGuang Wang

North China Institute of Aerospace Engineering/Department of Mechanical Engineering, LangFang, China

**Abstract**—A lathe simulator has been developed and tested. It includes two parts: the physical and virtual part. The physical part is constructed based on Lathe motor system of an actual lathe. With the virtual part, the computer can display the work-piece rotation, the chips, the sound and the translation of the cutter on the screen in real time. In addition, there are machines introduction and the internal structure of lathe. The simulator provides a good platform for lathe learning beginners and students to learn and practice.

**Index Terms**—lathe; simulator; virtual reality; machining operations

## I. INTRODUCTION

Virtual reality is a high and new technology in recent years, which using computer simulation to create a 3D virtual world, to provide users simulation about senses such as vision, hearing, touch, let users be personally on the scene. It is becoming increasingly popular for a wide range of applications, such as education and training for areas including automobile, machine and engineering.

A typical application example is used for engineering education and training, Simulation can help beginners to acquire some basic operating skills safely and effectively, especially when there is a danger or high cost in training with an actual machine. For example, It is necessary for the trainee to train with a flight simulator before he or she obtain the pilot qualification.

In the process of learning machine operation, it is known that a wrong operation may damage to the operator or the machine. So, it is important to make a equipment which provided with a warning message and operational safety information when a dangerous action is appeared during a beginner's training stage.

As a result, a lathe simulator was developed and implemented. Lathe simulator is a system for Machine operators and students to learn the basic knowledge of metal cutting and operating skills. It have virtual functions such as a feeling of force, sense of sight, hearing and touch and provides the operator, in real-time, with some real feeling, as if he or she were operating an actual lathe.

## II. THE WORKING PRINCIPLE OF THE LATHE SIMULATOR

Lathe simulator is a simulation system integrated of technology such as machinery, electronics, computer, simulation of the simulation equipment. The main purpose of designing the simulator is to simulate the basic function of the CA6140 lathe. As shown in figure1,

lathe simulator is mainly composed of lathe model, sensor, A/D converter, single-chip microcomputer, computer, etc equipment.

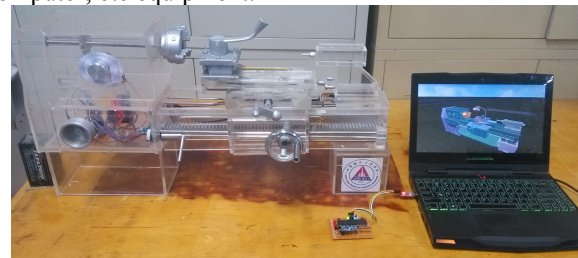


Figure 1. The Lathe Simulator

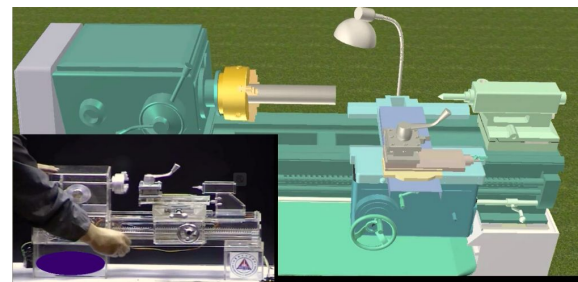


Figure 2. The Working Figure of The Lathe Simulator

As shown in figure 1, the lathe simulator is composed of two parts. The first part is the lathe model on the left; its appearance is designed according to the lathe CA6140 and is mainly used in signal perception, acquisition signal, the signal processing. There are spindle, apron, tailstock, small plate box and all fitted with sensors in the movement direction. There are also D/A converters, the Single chip microcomputer and Wireless transmission module in the model.

The second part is a 3D model on the right. It is build according to the proportion of 1:1 based on CA6140 lathe by computer, which can reflect the action of lathe model in real-time and there also add the internal structure of CA6140 video in the virtual reality software, which help beginners to study.

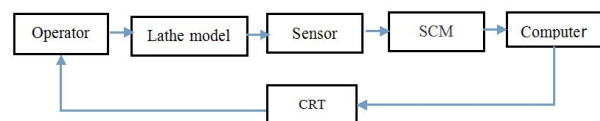


Figure 3. The Working Principle Diagram of the Lathe Simulator

As shown in figure 2, when the operator operate the lathe model with the joystick and buttons, the spindle rotate and tool feed. As is shown in figure 3, the sensor

collection the movement information of the lathe model, and sent into the Single chip microcomputer through a D/A converter, the Single chip microcomputer deal with the information and send it to the computer through Wireless transmission module or the Computer serial port. 3D model of lathe in the computer makes the corresponding action, send out the scene according to the variation of data. Meanwhile, the computer calls the visual processing module to Simulate of the chips and lights, which will be shown by the CRT. As a result, the simulation of cutting scene can be reached. Besides the cutting scene, the computer also calls the sound synthesis module to simulate the sound of the real cutting, which is broadcast by the sound box.

### III. FUNCTION OF SIMULATING THE CUTTING FORCE

In actual cutting process and a turning job with manual feed, the operator feeds the byte to cut into the work-piece, and then moves the byte along the feed direction to Cutting the work piece. In this case, the cutting force acting on the byte transmits to the cross slide and the carriage through the tool rest, and further to the feed handles. So, the operator feels the cutting resistance to the material while turning the feed handles.

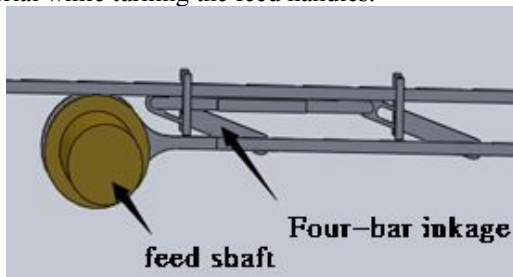


Figure 4. The Working Principle of the Four-Bar Linkage

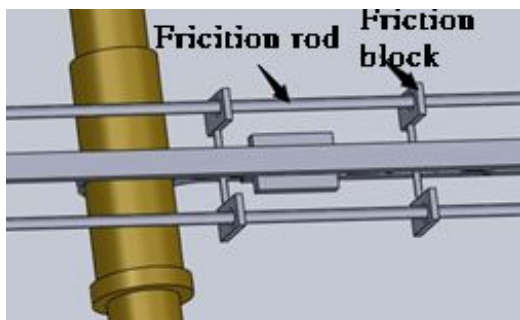


Figure 5. The Four-Bar Linkage to Simulate the Cutting Force

In this lathe model, As shown in figure 4, 5, A Four-bar linkage is used to simulate the cutting force. When the feed shaft moves to the left to Cut the work piece, the top of the four-bar linkage rod will touch the friction rod, which can make the friction block in a state of press, and there is a relative movement from of friction from the friction block and the friction rod, so as to simulate the cutting force. By contrast, when the feed shaft moves in the opposite direction, the top of the four-bar linkage rod will decline, so that the friction piece and friction rod is in a state of relaxation, then the cutting force can not be feel.

### IV. DISPLAY OF THE SENSE OF SIGHT

Quest3D VR Edition 4.3, the programming environment employed in the simulator's software, is an effective real-time 3D construction tools. Compared with other construction of visualization tools, such as web pages, animation, graphics editing tool, Quest3D can interact with objects in real time editing environment. Figure 6 shows a schematic of the 3D model of the lathe in the CRT.

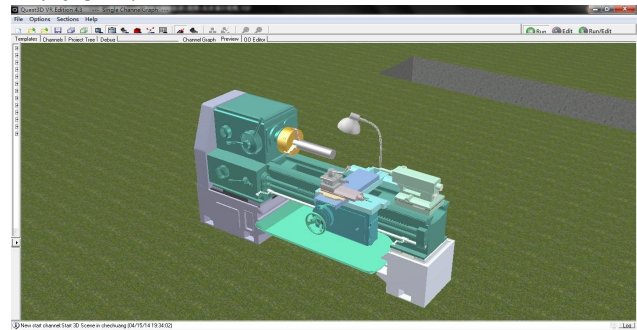


Figure 6. The 3D Model of the Lathe

There is a FM sound board in the simulator to produce working sound effects. Four sound source files, which correspond respectively to the sound of spindle rotation, the sound of a warning (e.g. emergency stop sound of lathe) and the sound of the spindle rotation and cutting the material have been implemented. The sound is automatically selected and executed based on operation status in progress so as to perform the sound effect.

There is also a collision module in the software. When the tool cut the work piece, the sensor detect the relative displacement of cutter and work piece, the software calls the collision module, and chips appear in the virtual environment. As a result, the actual cutting process is reflected in real-time.

### V.CONCLUSION

A lathe simulator has been developed to safely and efficiently enhance metal cutting skills for the beginners and students in industrial high schools and so on. The main functions and characteristics of the simulator are:

1. The lathe simulation can respond correctly and directly to the handles in the lathe model related to the operator's action and can display it on screen in real-time.
2. With the Four-bar linkage, the simulator can provide the operator with a sufficiently real feeling of force and touch as if he or she were operating an actual lathe.
3. With the three-dimensional model, the operator can know the external and internal structure of lathe more well.
4. The sounds of spindle rotation, cutting, and warnings, are designed to simulate real cutting environment.

### ACKNOWLEDGMENT

This work is supported by scientific research project of North China Institute of Aerospace Engineering (Project

Number: KY-2013-09). We thank Professor GuangHua Zheng and XiaoGuang Wang for enlightening discussions.

## REFERENCES

- [1] R.A. Hess,,T. Malsbury. "Closed Loop Assessment of Flight Simulator Fidelity". *Journal of Guidance Control and Dynamics* . 1991
- [2] Hess R A. "Pilot modeling with applications to the analytical assessment of flight simulator fidelity". *AIAA Modeling and Simulation Technologies Conference and Exhibit* . 2008
- [3] O. Stroosma,M. van Paassen,M. Mulder. "Using the SIMONA Research Simulator for Human-machine Interaction Research". *AIAA Modeling and Simulation Technologies Conference and Exhibit* . 2003
- [4] R. A. Hess,W. Siwakosit. "Assessment of Flight Simulator Fidelity in Multiaxis Tasks Including Visual Cue Quality". *Journal of Aircraft* . 2001
- [5] Eric N Johnson,,Amy R. Pritchett. "Generic pilot and flight control model for use in simulation studies". *AIAA 2002-4694* . 2002
- [6] Nahon M A,Reid L D,Kirdeikis J. "Adaptive simulator motion software with supervisory control". *Journal of Guidance Control and Dynamics* . 1992
- [7] H. Piet-lahanier,E. Walter. "Further results on recursive polyhedral description of parameter uncertainty in the bounded-error context". *Proc 28 th IEEE Conference on Decision and Control* . 1989
- [8] Hosman R,Advani S,Haeck N. "Integrated design of flight simulator motion cueing systems". *International Conference on Flight Simulation* . 2002
- [9] Schaut CL,Moffett DF,Moffett SB. *Human physiology foundation and frontiers* . 1990
- [10] Mark Karpenko,Nariman Sepehri. "Electrohydraulic force control design of a hardware-in-the-loop load emulator using a nonlinear QFT technique". *Control Engineering Practice* . 2012 (6)
- [11] Fu Jia Cai,Liu Xian Hua,Ma Tian Chu. "Experiment and Study of Electric Control Loading System". *Advanced Materials Research* . 2012 (462)
- [12] Yunjie WU,Xiaodong LIU,Dapeng TIAN. "Research of Compound Controller for Flight Simulator with Disturbance Observer". *Chinese Journal of Aeronautics* . 2011 (5)
- [13] Chifu Yang,Qitao Huang,Junwei Han. "Decoupling control for spatial six-degree-of-freedom electro-hydraulic parallel robot". *Robotics and Computer Integrated Manufacturing* . 2011 (1)
- [14] Zheng, Shupeng,Zheng, Shutao,Han, Junwei. "COTS and Design Pattern Based High Fidelity Flight Simulator Prototype System". *Journal of Computers* . 2011 (1)
- [15] Yao Jianyong,Jiao Zongxia, Shang Yaoxing,Huang Cheng. "Adaptive Nonlinear Optimal Compensation Control for Electro-hydraulic Load Simulator". *Chinese Journal of Aeronautics* . 2010 (6)
- [16] Brian P. Rigney, Lucy Y. Pao,Dale A. Lawrence. "Nonminimum phase adaptive inverse control for settle performance applications". *Mechatronics* . 2009 (1)
- [17] Kyoung Kwan Ahn, Quang Truong Dinh. "Self-tuning of quantitative feedback theory for force control of an electro-hydraulic test machine". *Control Engineering Practice* . 2009 (11)

**HongGe Fu** was born on September 22, 1980, in Hebei, China. She is a lecturer worked in North China Institute of Aerospace Engineering. Her research interests include machinery manufacturing and automation.

**XiaoGuang Wang** was born on May 05, 1964, male, Hebei province, North China Institute of Aerospace Engineering, professor, research field : Machinery and electronics engineering.

# Architectural CAD Course Construction in Higher Vocational Teaching

Chen Yu; Gao Haiying

Zhengzhou Vocational University of Information and Technology, Zhengzhou, China

**Abstract**—Aiming at the shortcomings in the past architectural CAD course teaching, the application of project teaching method in the CAD class studied the project teaching method. The project teaching method can cultivate students' good learning and innovation ability, realize the teaching objective.

**Index Terms**—CAD, project teaching method, teaching mode

## I. PROBLEMS EXISTING IN THE TRADITIONAL TEACHING OF ARCHITECTURE CAD

The construction of CAD teaching must be combined with construction application, if it is separated from the application architecture, CAD can not be called a building CAD. At present, many colleges and universities in the construction of CAD course as an independent course, students in the learning process to focus only on the software of learning and drawing skills training, they ignore the needs of practical CAD architecture. Architecture requirements of students learning CAD can draw construction plans, some temporary construction drawings and construction process.

In the 'Architectural CAD' construction of curriculum, teaching process is based on the traditional software

methods of operation and command line. The teacher explains how to use the command, and then the students practice own. Students complete a teaching content and then some exercises, so that the students often are in a passive position.<sup>[1]</sup>

The CAD command is various; the students in the "simple repetitive operation duck indoctrination" teaching mode face the various commands, and then lose patience soon, reduce the learning interest. When the students were asked to draw construction plans complete drawings, students often feel unable to start, the knowledge is scattered, difficult to digest, causing the disconnection between theory and practice, are not up to the good results of learning.

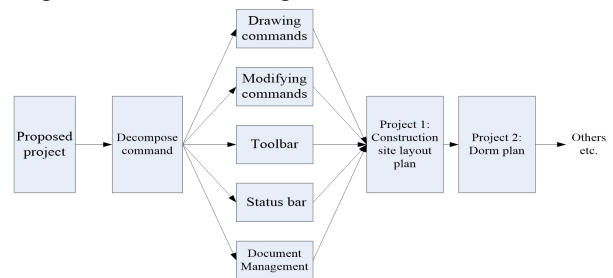


Fig 1. The main idea of the project teaching method

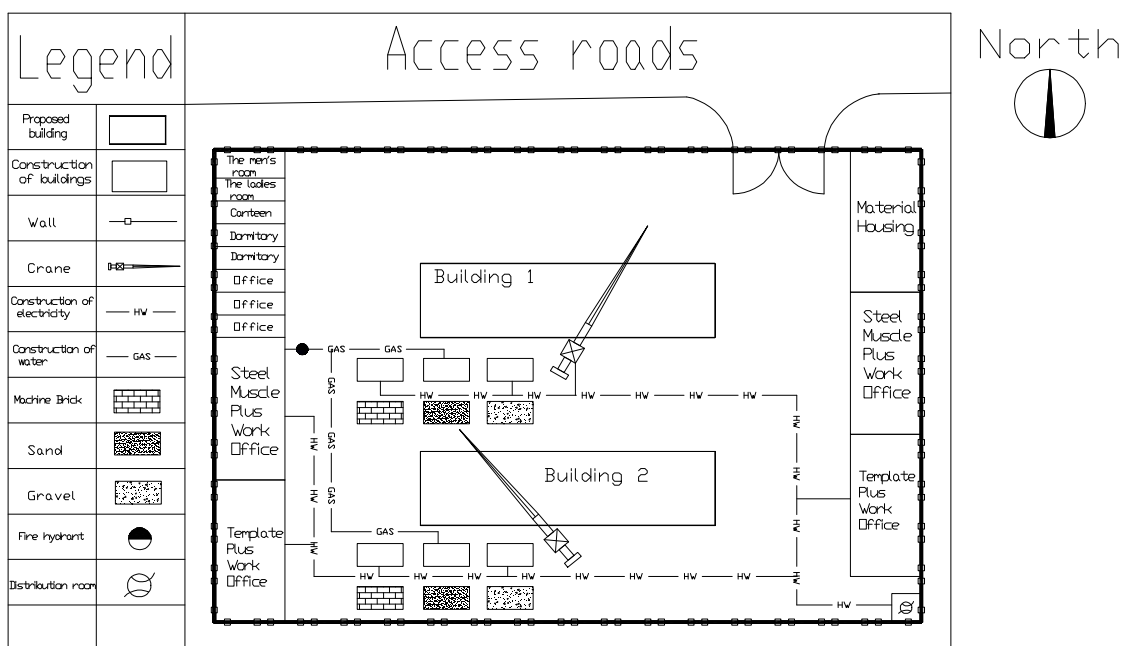


Fig 2. Construction site layout plan



process of teaching and learning tasks as the main line, teaching content implicit in it. Task-driven teaching method focuses on the cultivation of students' innovative thinking and self-learning ability.

'Case + Tasks' in teaching in the teaching mode is a combination of both, case teaching method used in teaching the theory, when using task-driven teaching skills practice, first developed in accordance with the actual situation of the task, then the task of situations, the actual construction applications drawings, for example, to enable students to apply the skills learned autonomously construct knowledge. By teaching practice in recent years found that 'Case + Task Method' in 'Architecture CAD' Teaching for solving the above problems with good results.

#### IV CONCLUSION

By building project teaching system, can both practice and theory, to make up for lack of appropriate, to achieve training objectives, a strong impetus to the reform of vocational teaching architectural CAD courses. Teaching system reform projects in line with the formation of the Professional Competence law, to explore ways of

professional and technical application of science ability. After intensive training and ethics of professional skills training and hands-on application capabilities can improve the comprehensive ability students, vocational training of qualified personnel.

#### ACKNOWLEDGMENT

The authors wish to thank Zhengzhou Vocational University of Information and Technology. This work was supported in part by a grant for the item number GZYB2014026.

#### REFERENCES

- [1] XIE Ying-Chuan, LIU Chang-Ling. "The Reform of Higher Vocational Architectural CAD Course Project Teaching", *Journal of Yueyang Vocational Technical College*, pp67-69, vol 27, No 4, Jul 2012
- [2] Zhu Linyuan, "Discussion on the Teaching Method of Architectural CAD software", *Journal of EDUCATION GUIDE*, pp56;78, April 2013
- [3] Huang Zhi, "Research on teaching reform of vocational architectural CAD", *Journal of Enterprise Science and Technology&Development*, pp84-85, No.16, 2013

# Adaptive Synchronization for Fractional-order Chaotic Systems Based on Observer

ZHANG Zhaohan<sup>1</sup>; ZHANG Yueping<sup>1</sup>; Zheng Wang<sup>2</sup>

1.Zhoukou Vocational and Technical College Zhoukou 466001, China

2.State Grid Zhengzhou Power Supply Company Information Communication Company

**Abstract**—Considering the adaptive synchronization of a class of fractional chaotic system in which the parameters are unknown and the state can not be all measured, the adaptive method combined with the observer are discussed, and moreover, by means of the theory of fractional-order calculus, the controller and adaptive law based on state observer are obtained. The theory of synchronization method is strict, easy to realize, and retains the nonlinear part, strong robustness, the synchronization of short time. The academic basis of the adaptive synchronization of a class of fractional chaotic system is provided. Finally, after the fractional-order Rossler System is discussed, the adaptive synchronization for fractional-order chaotic systems in which parameters are unknown and the state can not be all measured is realized. Theoretical analysis and computer simulation show the validity of the method.

**Index Terms**—fractional, synchronization, adaptive, observer

## I. INTRODUCTION

Although fractional calculation has nearly 300-year history, a high degree of attention of which has not been caused for a long time. However, with the further research of integer order chaotic system in the recent 10 years, scientists and engineers have gradually realized the many fine features of the fractional, and a crazy research of fractional order chaotic systems has been raised [2-3]

Owing to few studies of the fractional order system, the control method is also relatively simple [4-5], furthermore most of the control is achieved in the single condition of the system parameters are unknown or status can not be fully measured [6-8].However, to take general physical process into account, the parameters and state variables of the chaotic system can not be obtained. The synchronization control of fractional chaotic system in which the parameters are unknown and the state can not be fully measured has not been largely reported.

In order to consider fully the issue, the adaptive synchronization method and the nonlinear state observer are combined in this article, by means of the theory of fractional-order calculus, the estimated state of the observer instead of the state variables of the adaptive law and control law, and moreover, the control law and adaptive law based on a nonlinear state observer are given. The theoretical basis of the adaptive synchronization of a class of uncertain fractional chaotic system is provided. Theoretical analysis and computer simulation show that the strategy can realize the adaptive

synchronization of a class of fractional chaotic system in which the parameters are unknown and the state can not be fully measured.

## II. THE MATHEMATICAL MODEL AND PROBLEM DESCRIPTION OF SYSTEM

Fractional chaotic system is described as follows:

$$\frac{d^\alpha x}{dt^\alpha} = Ax + f(x), \tag{1}$$

$0 < \alpha < 1$ ,  $A \in \mathbf{R}^{n \times n}$ ,  $x \in \mathbf{R}^n$ ,  $f(x)$  as a nonlinear term, System (1) as the drive system, Response system as follows:

$$\frac{d^\alpha y}{dt^\alpha} = Ay + f(y) + u, \tag{2}$$

$0 < \alpha < 1$ ,  $A \in \mathbf{R}^{n \times n}$  Response system is unknown and the estimated parameter vector,  $y \in \mathbf{R}^n$ ,  $f(y)$  for a nonlinear term,  $u$  for the controller. If the state error  $e = y - x$  between the response system (2) with the drive system (1), and error vector  $e = (e_1, e_2, \dots, e_n)^T$ , to meet  $\lim_{t \rightarrow \infty} \|e(t)\| = 0$ , the appropriate controller  $u$  and the corresponding adaptive law are selected.

The typical fractional order chaotic systems and fractional order hyperchaotic systems such as Lorenz systems chen system and Rössler system are described in the system (1).

## III. THE DESIGN OF ADAPTIVE SYNCHRONIZATION FOR FRACTIONAL-ORDER CHAOTIC SYSTEMS TO DEFINE

$$Ax = F(x)a,$$

$$Ay = F(y)a',$$

$$e_a = a' - a,$$

$$\text{The } Ay - Ax = Ae + F(x)e_a \tag{3}$$

$F(x), F(y)$  are the matrix  $n \times m$  in which  $x, y$  are state parameters of the system.

The error system of the system (1) and (2) is as follows:

$$\frac{d^\alpha e}{dt^\alpha} = Ay - Ax + f(y) - f(x) + u$$

$$= Ae + F(x)e_a + f(y) - f(x) + u \tag{4}$$

Lemma 1 For the fractional-order chaotic system (4), if any eigenvalue  $\lambda$  of coefficient matrix  $A$  meet  $|\arg(\lambda)| \geq \frac{\alpha\pi}{2}$ , the fractional system is stable.

Theorem 1 If the selected controller

$$u = f(x) - f(y) - ke, \tag{5}$$

$$k = \text{diag}(k_1, k_2, \dots, k_n)$$

Parameter adaptive law is

$$\begin{aligned} \dot{k}_i &= \beta e_i^2 (\beta > 0) \\ \dot{e}_a &= \dot{a}' - \dot{a} = -[F(x)]^T e, \end{aligned} \tag{6}$$

So fractional error of system is asymptotically stable (4).

Proof: Taking the the controller and parameters adaptive law (5), (6) into the error system (4), we obtain:

$$\begin{aligned} \frac{d^\alpha e}{dt^\alpha} &= Ay - Ax + f(y) - f(x) + u \\ &= Ae + F(x)e_a - ke \\ &= (A - k)e + F(x)e_a \end{aligned}$$

Obviously, the  $e = 0$  is equilibrium point of the error system (5),  $A - k$  is Jacobi matrix of the System (4) at the equilibrium point, If the

$|\arg(\lambda_i(A - k))| > \frac{\alpha\pi}{2} (i = 1, 2, 3)$ , and by means of

Lemma 1, the  $e = 0$  is asymptotically stable equilibrium point of system (4), therefore,  $\lim_{t \rightarrow \infty} \|e\| = 0$ , the response system (2) and the drive system (1) can achieve synchronization.

Considering the above-mentioned conclusion, if the appropriate matrix  $k$  is selected,  $|\arg(\lambda_i(A - k))| > \frac{\alpha\pi}{2} (i = 1, 2, 3)$ , fractional chaos synchronization of response system (2) and the drive system (1) can be achieved.

However, when the system state can not be fully measured, the controller (5) is invalid. In order to achieve synchronization, a nonlinear state observer to estimate the state of fractional order chaotic systems is needed.

#### IV. THE DESIGN OF NONLINEAR STATE OBSERVER

General fractional nonlinear system can be expressed as

$$\begin{aligned} \frac{d^\alpha x}{dt^\alpha} &= Ax + g(t, u, y) + f(t, u, x), \\ y &= Cx \end{aligned} \tag{7}$$

$x \in R^n$  is the status of the system,  $A \in R^{n \times n}, C \in R^{n \times n}$ ;

$y \in R^m, u \in R^p$  are the output and input of the system,  $g(t, u, y), f(t, u, x)$  are non-linear mapping, and  $f(t, u, x)$  satisfies the following Lipschitz condition:

$$\|f(t, u, x1) - f(t, u, x2)\| < r \|x1 - x2\|, \tag{8}$$

where  $r$  is the Lipschitz constant,  $\forall u \in R^p, t \in R^+$ ,

$[A, C]$  is considerable, For (7), the following observer can be established:

$$\begin{aligned} \frac{d^\alpha \tilde{x}}{dt^\alpha} &= A\tilde{x} + g(t, u, y) + f(t, u, \tilde{x}) \\ &\quad + L(y - C\tilde{x}) \end{aligned} \tag{9}$$

$\tilde{x} \in R^p$ , for observed variable;  $L \in R^{n \times m}$ , for the gain matrix.

Proof: To define  $w = x - \tilde{x}$

According to (7) and (9), the error system is:

$$\begin{aligned} \dot{w} &= (A - LC)w + f(t, u, x) \\ &\quad - f(t, u, \tilde{x}) \end{aligned} \tag{10}$$

Obviously,  $A - LC$  is Jacobi matrix of the system (10) in the equilibrium point. Selecting the appropriate feedback matrix  $L$  [9], and  $|\arg(\lambda_i(A - LC))| > \frac{\alpha\pi}{2} (i = 1, 2, 3)$ ,

in the light of Lemma 1,  $w = 0$  is an asymptotically stable equilibrium point of system (10), so  $\lim_{t \rightarrow \infty} \|w\| = 0$ ,

in other words, (10) is asymptotically stable.

#### V. NUMERICAL SIMULATION

In order to verify the validity of the before-mentioned strategy, the fractional-order *Rössler* system is chosen as the research object

$$\frac{d^\alpha x}{dt} = \begin{bmatrix} 0 & -1 & -1 \\ 1 & a & 0 \\ 0 & 0 & -b \end{bmatrix} x + \begin{bmatrix} 0 \\ 0 \\ x_1 x_3 + a \end{bmatrix} \tag{11}$$

Then discussing how to gain the synchronization, when the parameters of the system is unknown and the state can not be fully measured, Considering (11) as the drive system, the fractional response system is as follows:

$$\begin{aligned} \frac{d^\alpha y}{dt} &= \begin{bmatrix} 0 & -1 & -1 \\ 1 & a_1 & 0 \\ 0 & 0 & -b_1 \end{bmatrix} y \\ &\quad + \begin{bmatrix} 0 \\ 0 \\ y_1 y_3 + a_1 \end{bmatrix} + u \end{aligned} \tag{12}$$

$a_1, b_1$ , are the parameters that should be estimated of the response system,

$u = (u_1, u_2, u_3)^T$  is the controller, under the control of  $u$ , the drive system(11) and response system (12) can be achieve the synchronization.

Set up:

$$\begin{aligned} e_1 &= y_1 - x_1 \\ e_2 &= y_2 - x_2 \\ e_3 &= y_3 - x_3 \\ e_a &= a_1 - a \\ e_b &= b_1 - b \end{aligned}$$

Then the error system as follows:

$$\begin{aligned} \frac{d^\alpha e_1}{dt^\alpha} &= -e_2 - e_3 + u_1 \\ \frac{d^\alpha e_2}{dt^\alpha} &= e_1 + e_a x_2 + a_1 e_2 + u_2 \\ \frac{d^\alpha e_3}{dt^\alpha} &= y_1 e_3 + e_1 x_3 + e_a \\ &\quad - b_1 e_3 - x_3 e_b + u_3 \end{aligned} \tag{13}$$

According to (5), the controller is designed as follows:

$$\begin{aligned} u_1 &= -(k_1 e_1 + e_3 x_3) \\ u_2 &= -k_2 e_2 \\ u_3 &= -y_1 e_3 \end{aligned} \tag{14}$$

According to (6), parameters adaptive law is designed as follows:

$$\begin{aligned} \dot{k}_1 &= \beta e_1^2 (\beta > 0) \\ \dot{k}_2 &= \beta e_2 (\beta > 0) \\ \dot{e}_a &= -(x_2 e_2 + e_3) \\ \dot{e}_b &= x_3 e_3 \end{aligned} \tag{15}$$

To estimate the state of the fractional chaotic system, a nonlinear state observer is devised. If  $x_2, y_2$  are obtained in system (11) and (12), that is to say, the corresponding outputs of system (11) and (12) are  $x_2, y_2$ , then the observer of system (11):

$$\begin{aligned} \frac{d^\alpha \tilde{x}}{dt} &= \begin{bmatrix} 0 & -1 & -1 \\ 1 & a & 0 \\ 0 & 0 & -b \end{bmatrix} \tilde{x} + \begin{bmatrix} 0 \\ 0 \\ \tilde{x}_1 \tilde{x}_3 + a \end{bmatrix} \\ &\quad + L(x_2 - C\tilde{x}) \end{aligned} \tag{16}$$

The observer of system (12):

$$\begin{aligned} \frac{d^\alpha y}{dt} &= \begin{bmatrix} 0 & -1 & -1 \\ 1 & a_1 & 0 \\ 0 & 0 & -b_1 \end{bmatrix} y \\ &\quad + \begin{bmatrix} 0 \\ 0 \\ y_1 y_3 + a_1 \end{bmatrix} \\ &\quad + L(y_2 - C\tilde{y}) + u \end{aligned} \tag{17}$$

$L_1 = 27.0815, L_2 = 39.8847, L_3 = -138.7930$  are obtained. The observation status  $\tilde{x}, \tilde{y}, \tilde{x}_1, \tilde{z}, \tilde{e}_i$  ( $\tilde{e}_i = \tilde{y}_i - \tilde{x}_i, i = 1, 2, 3$ ) take the place of  $x, y, x_1, z, e_i$  ( $i = 1, 2, 3$ ) in (14) and (15), the control law and adaptive law based on state observers are gained.

The simulation results are shown in Figure 1, 2, 3, as is shown in the figures, because the system is controlled by the control strategy, the system shock is significantly reduced in the beginning, and after a very short time, the synchronization error of the fractional order systems  $e_i = 0 (i = 1, 2, 3)$  is finished. The parameter

errors in line with time quickly tends to zero and the parameters  $k_1, k_2$  on the basis of time quickly tend to a constant, which is shown in respective Figure 2 and 3.

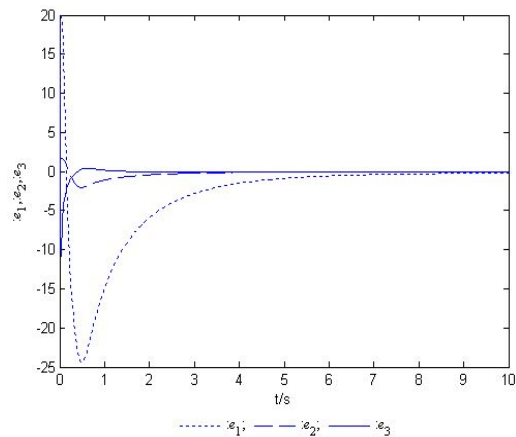


Figure 1. Evolution Curves of Error with time

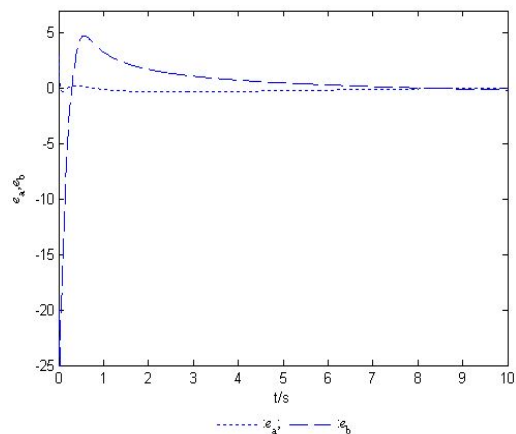


Figure 2. Evolution Curve of Parameter Error with the Time

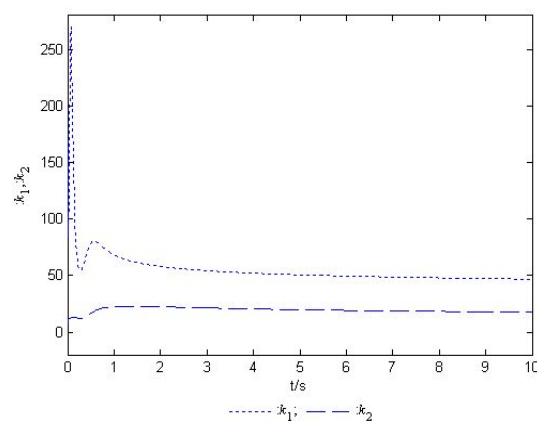


Figure 3. Evolution Curves of  $k_1, k_2$  with the Time

## VI. CONCLUSION

In this paper, considering the parameters and state variables of system are unknown, the control strategy of adaptive law combined with nonlinear state observer is put forward to .

1) Discussing a class of fractional chaotic systems in which parameters are unknown, the state can not be fully measured, the control law  $u$  and parameter adaptive laws that contain system state variables  $X$  are designed.

2) Considering the objective and the state of controlled system can not be fully measured, the state observer and the state estimation of which are respectively achieved.

3) Owing to the estimated state of the system instead of the state of control input  $u$  and parameter adaptive laws, the control law and adaptive law based on observer are gained.

The control strategy designed in the paper is simulate, and the simulation results can be seen, the shock is small in the beginning, the robustness is strong and synchronization speed is fast, when  $t = 0.8s$ , the synchronization can be achieved, therefore, the synchronous strategy is feasible.

#### REFERENCES

- [1] Butzer P L, Westpha I U "Formulation of Euler-Lagrange equations for fractional Variational problems," *An Introduction to Fractional Calculus*,2000
- [2] Podlubny I, "Using fractional order adjustment rules and fractional order reference models in model-reference adaptive control," *Fractional Differential Equations*, 1999.
- [3] Koeller R C, "Generalized synchronization in fractional order systems," *Appl.Mech*51 229,1984.
- [4] Matignon D. "Stability Results of Fractional Differential Equations with Applications to Control Processing,"*IMACS,IEEE-SMC*,Lille,France, 1996,11, pp. 963-968.
- [5] Zhang Chengfen, Gao Jinfeng Xu Lei. "Liu system of Fractional Order and Chaos in the fractional order unified system and the two different structures sync," *Physics*,2007,56(9),pp.5124-5131
- [6] Zhang ruoxun,Tian Gang,"Adaptive Control of Chaotic Systems with Parameter Uncertainty," *Physics*, 2008, 57(4),pp.2073-2081.
- [7] Wu Xiangjun, Lu Hongtao, "Generalized synchronization of a new Fractional-Order Hyperchaotic System Based on Observer," *Scientific and technological papers online china*,2009, 4(2),pp.135-140.
- [8] Vidyasagar, *Nonlinear Systems Analysis*,1978.
- [9] Yao Lina, Gao Jinfeng, "Based on the State Observer of the Control Chaos System," *Physics*,2002,51(03),pp.487-492.

**ZhaoHan Zhang** (1975-), Female, Han,China ,Lecturer, Master, Research area: Nonlinear Control of Engineering Systems, She is currently working in Zhoukou Vocational and Technical College as a teacher.

**YuePing Zhang** (1982-),. A master's degree in engineering of Zhengzhou University was earned in 2010. The nonlinear control and power system simulation are her major research field. She is currently working in Zhoukou Vocational and Technical College as a teacher.

# Separate-frequency Inversion of The Organic Carbon Content in Source Rock

Wei Yang<sup>1,2</sup>; Mingyi Hu<sup>1,2</sup>

1. Key Laboratory of Exploration Technologies for Oil and Gas Resources of Ministry of Education, Yangtze University, Wuhan, China;

2. Faculty of Earth Science, Yangtze University, Wuhan, China

**Abstract**—In this study, we combined with source rock geology characteristic logging and seismic response, we build the mathematical relation between quasi TOC curve and seismic data based on the single well TOC logging data and seismic internal attribute, it shown that it is not a single linear relationship that adhered by predecessors, while it had a complicated nonlinearity relationship. We used neural network algorithm and SVM to obtain the optimization relationship between quasi TOC curve and seismic attribute. We can achieve the goals of TOC prediction by the method of seismic inversion, Therefore, frequency division inversion method is introduced. The first of all, by using the neural network algorithm, optimal combinations of seismic attributes are identified; the second of all, spectrum analysis determining the effective frequency band range of data, and the original seismic data are divided into low, medium, high frequency data by using wavelet frequency division technology; the third of all, by using SVM, calculate the relationship between amplitude and frequency (AVF) under different thickness, introducing AVF relationship into the inversion, thus, the nonlinear mapping relation between TOC curve and seismic waveform is established. Finally, the inversion results is obtained.

**Index Terms**—TOC; Separate-frequency inversion; SVM; AVF; Spectral Decomposition

## I. INTRODUCTION

Since drilling cost too much in offshore basin, and the most of prospect wells lie in the high position of structure where usually lack of source rock, the wells which encounter source rock and the proper source rock samples are limited. Meanwhile the source limitedly distribute in region. It costs much to analysis the TOC of source rock in geochemical methods. The traditional geologic research methods cannot obtain continuous TOC in region, and it is difficult to predict regional source rock. How to economically、efficiently and accurately predict source rock by limited data becomes difficulty in offshore basin research. The results of research show a mathematical relationship between the various logging parameters and TOC,(Meyer B L *et al.* 1984) according to this relationship, an appropriate quantitative prediction model, can be established quantitatively to predict single well TOC of source rock. (Fertl W H *et al.* 1988)The advantage of source rock logging evaluation is the definition in “point”. The regional source rock prediction usually stresses on the seismic facies recognition of sedimentary facies which is

dark mudstone and shale, while not all dark mudstone and shale are rich of organic carbon, part of them can become effective source rock which contribute to hydrocarbon reservoir. The advantage of source rock prediction in seismic facies is that it can roughly confirm the beneficial area of source rock plane distribution, but it cannot quantitatively predict regional TOC. The geophysical inversion method combined with logging-seismic data is relatively seldom used in the regional quantitative prediction of TOC at present.

In this article, we firstly quantify the geophysical responses characteristic of source rock, based on the advantage of logs’ longitudinal magnification in “point”,(Herrson S L 1988)building the relationship between the TOC of testing samples and logs. (Mann U P *et al.* 1988)At the same time, using the relationship of well and seismic, we can transform the seismic data which is in “point” into “line”, as a result, the regional TOC can be predicted.

## II. PREDICTION METHODS OF SOURCE ROCK

### A. Technical Ideas

The organic carbon content geophysical prediction method is mainly based on organic carbon content (TOC) value tested by a few single well in source rock, using mathematical algorithms to establish the measured organic carbon content value and the mathematical relationship between different logging data, applying the mathematical relationship to value and predict organic carbon content of source rock in the other no single well.(Herron S L 1987)The advantages of single well logging evaluation method of organic carbon content source rock is TOC values accurately, but is limited to well point, difficult to predict source rock in regional area.

In the organic carbon content of seismic prediction, the commonly used method is to directly establish the measured linear relationship between TOC value and GR value, Then though the acoustic curve fitting by GR curve, establishing the relationship of pseudo wave impedance and TOC value, finally inverse source rocks TOC profile. The advantage of this method is rapid and direct, but the drawback is obvious. Firstly, it often does not exist linear relationship between the measured TOC value and GR, which will cause based value low accuracy in the TOC before inversion extrapolation, the inversion results not accurate. Secondly, the method of



Passey proposed a logging evaluation method of source rock, can calculate TOC value of different mature conditions.(Mohammad Reza Kamalia *et al.* 2004)This method is overlapping arithmetic coordinates of the acoustic logging curve and logarithmic coordinate of resistivity curve, when two curves in a certain depth "consistent" as the baseline, the baseline is determined, then distance of the reading between two curves in coordinate of resistivity log is  $\Delta\log R$ , the key point of  $\Delta\log R$  technique application to identify effective source rock, the characteristics of logging response: difference time between interval transit time and resistivity do not overlap, shaped like a discontinuous triangular unit in the vertical direction . (Passey Q R 1990)

The method that calculate organic carbon of source rock based on overlapping log curve of resistivity and interval transit time , which applying the following formula to calculate  $\Delta\log R$  :

$$\Delta\log R = \lg(R / R_{\text{baseline}}) + 0.02(\Delta t - \Delta t_{\text{baseline}})$$

In the formula;

$\Delta\log R$  : Space of the reading log in coordinate of resistivity;

R : Resistivity,  $\Omega \cdot m$ ;

$\Delta t$  : Value of acoustic travel time,  $\mu s / ft$ ;

$R_{\text{baseline}}$  : Resistivity value of non source rock baseline

corresponded to the  $\Delta t_{\text{baseline}}$

Overlapping curve of LF-A well shown (Figure 3), in the non source rock section, neutron and sonic curve coincides well, overlapping section of two well logging curves as a baseline in 3110m-3140m section of LF - A well. Used the above formula to calculate  $\Delta\log R$  and TOC value, fitted the relationship of LF-X well between the measured TOC and  $\Delta\log R$

$$TOC = \Delta \log R \times 10^{2.298 - 0.1665 Ro} \text{ (Ro: maturity of organic matter)}$$

The calculated error analysis of between the organic carbon content of measured samples core values shown that, calculated values agree well with the measured values of LF-X well, the error ranged from 2.23% to 11.22%, calculation value has High credibility. When  $TOC \geq 3$ , curve of interval transit time and resistivity do not overlap, shaped like a discontinuous triangular unit in the vertical direction, with response character of a high organic carbon content value. Shown, with the content of organic carbon increased the response of logging data of logging source rock become significantly, which has a better response of good quality source rocks (effective source rocks). Evaluated high quality source by the calculated TOC value, high quality source rocks thickness of LF-X is up to 26m.

3) Solving the multiple regression formula of TOC value

Organic carbon contains in source rock and various parameters of logging have a Mathematical mapping relationship, for more precise quantitative prediction of organic carbon from single logging data. People have put

forward ovarious simple equation, bivariate equation or variable multiple regression equation empirical quantitative mode which used total organic carbon content as dependent variables, single or multiple logging parameters of U and U / K ratio, density, neutron porosity, interval transit time, resistivity as independent variables. This method overcomes the shortcomings of a single response to physical properties in the source rock and consideres more comprehensive physical properties of rocks. In the practical research, through analyzing cross correlation of logging parameters and the TOC value of measured sample, taking into account the influence of weight index each logging curve and TOC value, integrating natural energy spectrum method and log R method. Establishing single well multiple regression equation of the organic carbon content and interval transit time (AC), density (DEN),  $\Delta GR / SGR$  and  $\Delta\log R$ , getting the TOC value as the dependent variable, four logging as independent variable, solving multiple regression equations of TOC value:

$$TOC = 0.452 \times (\Delta GR / SGR \times R^7 + 0.146) + 0.386 \times (\Delta\log R \times 10^{(2.297 - 0.1665 Ro)}) + 0.213 \times AC + 0.159 \times DEN + 0.323$$

Through solving the multiple regression, can avoid the uncertainty TOC value of single logging curve, improved correlation between logging curve and forecast of TOC value and the prediction accuracy of TOC curve.

In practical application, we used 113 samples that measured organic carbon content value and interval transit time (AC), the density of DEN,  $\Delta GR / SGR$  and  $\Delta\log R$  in the same depth, made multiple regression analysis from the single parameter to the multi parameters and multi composition, Compared with using single parameter, applying above four fitting parameters to predict organic carbon content will be more accurately, the correlation coefficient of the predicted organic carbon content and the measured values of single parameter is increased from 0.72 to 0.78, the standard error reduced from 1.72 down to 1.52, the method for prediction organic carbon content value of single well is best.

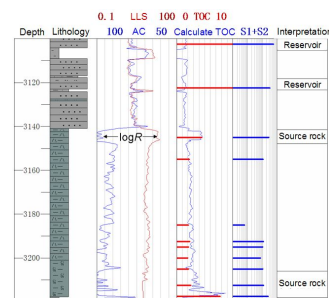


Figure 3.  $\Delta GR/SGR$  Evaluated Method of Source Rock for HZ-A well

### III. SEPARATE-FREQUENCY INVERSION

#### A. Seismic attribute optimization

The previous seismic prediction of TOC value, considered there is a direct linear relationship between TOC value and acoustic curves, mostly, directly transformed the TOC curve into pseudo acoustic curve,

and then through the original seismic data inversion into pseudo wave impedance profile to predict TOC value. (Russell B H 2004)Using quasi TOC curve obtained from single well and impedance crossplot (Figure 4), in the actual can be found TOC value and wave impedance linear correlation is low, the former method could cause the large prediction error. (Fu L Y 2004)

During this research, we selected method of seismic multi-attributes inversion to predict TOC value. Seismic multi-attribute inversion is process that change seismic internal attributes into lithologic character curve. Seismic internal attributes included instantaneous attributes, time-frequency attributes, filter sections, derivative, integral property attribute, time (linear gradient) and other types. (Robinson E A 1957; Robinson E A 1980) Firstly, we selected seismic attributes that have best fitting advantage degree with the quasi TOC curve, then, used neural network algorithm to establish the nonlinear relationship the various attributes that have selected and quasi TOC curve, applied this relationship to extrapolate seismic attribute, finally, we got the prediction of TOC profile.

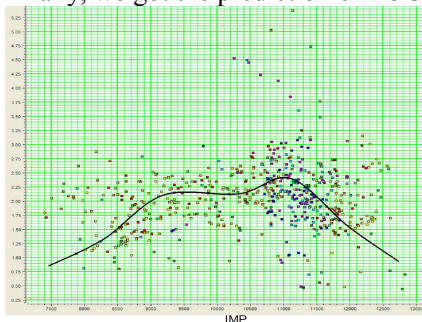


Figure 4. Crossplot of Quasi TOC Curve And Wave Impedance Value

In the seismic attribute optimization, must be crossplotted and correlation recognition between quasi TOC curve and multiple attributes generated from seismic near well, seismic attributes have different physical significance, the response that predicted characteristic curve of degree is also different, therefore it has to repeatedly extract and relates system error calibration of seismic attributes, to screen the optimum properties. Single attribute for response of characteristic curve is relatively single, multiple attributes combination can improve the correlation of quasi TOC curve, determined the optimal combination of multiple attributes in the optimization of the training process (Figure 5), the optimal combination of seismic attributes are amplitude envelope, 25/30 - 35/40 filter section, average frequency, trace integration.

When we established combination of seismic multi-attribute and quasi TOC curve, used the algorithm of multivariate regression algorithm and neural network. (Simon Haykin 1999; Lim J S 2005) Multiple regression algorithm is directly applying the linear weighted, got linear relationship of the predicted characteristic curve and multi-attribute of seismic, but between the seismic attributes combination and the predicted characteristic curve is not simple linear relationship, its exists a complex nonlinear relationship. In the course of practical research, we used of neural

network algorithm, through its independent learning established the nonlinear mapping relationship between seismic attributes and quasi TOC curve. Then, used neural network algorithm to fit, that between borehole side seismic attributes and quasi TOC curve correlation degree is 0.87, the average error is 0.59%, with such obvious effect, shown that this method is effective.

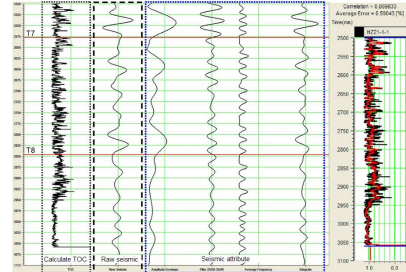


Figure 5. Seismic Multi-Attribute Selection and Fitting Results

B. Prediction method of TOC inversion

1) Method and principle

Seismic data has frequency bandwidth, and trace gathering of seismic contains high, medium, low, different frequency components. For a wedge model, with different frequency and Rick wavelet deconvolution, get a series of synthetic seismic profile, so as to obtain curve of amplitude and thickness at different frequencies, as shown in figure 10-left. Transformed 6-left, you can get varies relationship of frequency and amplitude in different time thickness (AVF) shown in figure 6-right.

Though studying the relationship between the amplitude and frequency of different thickness (AVF), putting AVF as an independent information into the inversion, rational used seismic information of high, medium, low frequency band, could reduce the uncertainty of thin layer inversion, and get a high resolution of the inversion result. Frequency-divided inversion form frequency body, then applied SVM technology to establish mapping relationship of division and the target well curve, changed the frequency inversion into characteristic curve. Frequency- divided inversion advantage lies in the relationship between amplitude and frequency of different thickness strata, without extracting wavelet, does not depend on the initial model and nonlinear inversion with high resolution (Zeng Hongliu et al.2000).

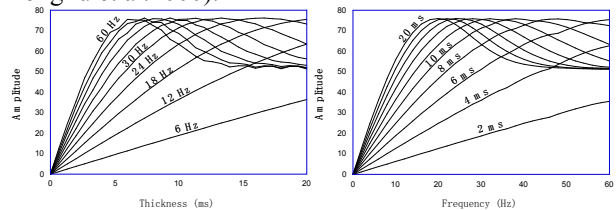


Figure 6.-above Tuning Curve of Relationship Between the Amplitude and Time Thickness at Different Frequencies. -Below Amplitude and Time Thickness At Different Frequencies

2) The principle of wavelet frequency division

$s(t) \in L^2(R)$  is Seismic record,  $L^2(R)$  represent energy limited function space,  $g(t)$  represent the basic wavelet,  $s(t)$  is defined as below:

$$S(b, a) = \frac{1}{a} \int_{-\infty}^{\infty} s(t) \overline{g\left(\frac{t-b}{a}\right)} dt \tag{1}$$

$a$  represent non-zero real number (called the scale factor) in the equation,  $b$  is a real number (called the translation factor),  $\overline{g(t)}$  represent complex conjugate of  $g(t)$ , the inverse wavelet transform for:

$$S(b) = \frac{1}{C_g} \int_{-\infty}^{\infty} \frac{1}{a^2} \int_{-\infty}^{\infty} s(t) g_R\left(\frac{t-b}{a}\right) dt da$$

$$C_g = \int_0^{\infty} \frac{\hat{g}_R(\omega)}{\omega} d\omega < \infty, C_g \neq 0 \tag{2}$$

$C_g$  is a real number in the equation,  $g_R(t)$  is real part of  $g(t)$ ,  $\hat{g}_R(\omega)$  represent Fourier transform of  $g_R(t)$ , The discretization of integral interval of  $da$ , equation(2) can be written as:

$$S(b) = \frac{1}{C_g} \sum_{i=1}^N \int_{a_{i-1}}^{a_i} \frac{1}{a^2} \int_{-\infty}^{\infty} s(t) g_R\left(\frac{t-b}{a}\right) dt da \tag{3}$$

Frequency division processing of seismic signal integration interval factor of different scales  $\{(a_{i-1}, a_i), i = 1, 2, \dots, N\}$  is expressed as:

$$S_i(b) = \frac{1}{C_g} \int_{a_{i-1}}^{a_i} \frac{1}{a^2} \int_{-\infty}^{\infty} s(t) g_R\left(\frac{t-b}{a}\right) dt da \tag{4}$$

Reconfiguration use time-varying linear combination:

$$s(b)^+ = \frac{1}{C_g} \sum_{i=1}^N C_i(b) \int_{a_{i-1}}^{a_i} \frac{1}{a^2} \int_{-\infty}^{\infty} s(t) g_R\left(\frac{t-b}{a}\right) dt da$$

$$= \sum_{i=1}^N C_i(b) S_i(b) \tag{5}$$

$C_i(b)$  represent time-varying coefficient, called reconstruction coefficient reconstruction;  $s(b)^+$  represent Seismic reconstruction signal

Using Marr wavelet processed frequency division, if the frequency in strict accordance with the doubling relation, it is reversible strictly, and each frequency signals are added can restore the original signal, calculate with minimum error.

Marr wavelet is a real number wavelet, simple calculation, fast speed, Marr wavelet not only satisfy the admissible condition of wavelet transform, and has good local performance, especially in frequency domain and time domain, morphology of the Marr wavelet consistent with Ricker wavelet, so it has strong physical meaning. Marr wavelet is two order derivative of Gauss function, generating function formula of Marr wavelet is as follows:

Time domain:

$$\Phi(t) = (1-t^2)e^{-\frac{t^2}{2}} = -\frac{d}{dt^2}\left(e^{-\frac{t^2}{2}}\right) \tag{6}$$

Frequency domain:

$$\Psi(\omega) = \sqrt{2\pi}\omega^2 e^{-\frac{\omega^2}{2}}, \Psi(\omega = 0) = 0 \tag{7}$$

$\sqrt{2\pi}f_m t$  replace  $t$  in The time domain expression of Marr wavelet. Which is the expression of the Ricker wavelet. in frequency domain and time domain, morphology of the Marr wavelet and Ricker wavelet is consistent, therefore, can be used Marr wavelet simulation Ricker wavelet to seismic frequency.

3) Application

1. Through the analysis of the frequency of seismic profile acrossing the LF-A well, to determine the effective frequency range (Figure 7-left), shows that the seismic gathers with 20HZ, 30HZ, 50HZ, three main frequency components.

2. Using the Wavelet Division Frequency Technology process original seismic data, Obtain three bands of divided body, extracted its instantaneous attributes

3. Quasi TOC curve processed by median filtering. This method is a kind of noise in nonlinear signal processing technology, the TOC curve is protection of the edge signal, eliminate the sharp noise, effective smoothing processing at the same time, also can make the seismic response characteristics of the vertical resolution filter and quasi TOC curve basically unchanged.

4. Main stages of source rock with low frequency continuous high amplitude reflection, analysis frequency with the reflection characteristics of seismic profile of deep lacustrine facies, frequency of source rock is 20HZ (Figure 7-right). When establish relationship of spectrum attributes and quasi TOC value curve, outstanced TOC value response character, increase the weight of influence coefficient of 20HZ frequency attributes, in order to enhance the accuracy of prediction of TOC.

5. Using SVM algorithm to calculate the amplitude and frequency of the different thickness for the seismic attributes of divided by frequency, put the relationship into the inversion, established a nonlinear mapping relationship between pseudo TOC curves and seismic waveform; eventually, input each frequency attributes, using having been learning the mapping relation between the body and the TOC frequency attributes that processed by SVM to predict the body good, finally, synthesized TOC value inversion body.

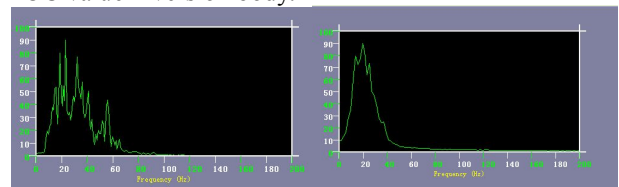


Figure 7. Analysis Seismic Profile and Dominant Frequency Of Semi-Deep Lacustrine Facies Arcrossing LF- A well

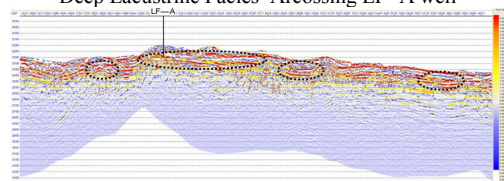


Figure 8. TOC Frequency Inversion Profile Arcrossing LF- A Well

As shown in the figure8, the LF - A well TOC frequency inversion profile can reflect the deep lacustrine facies, Wenchang formation of organic

carbon content is higher, the overall in the sets of effective Source Rocks continuous distributed in the region, TOC value increases on seismic section in deep subsag, which is more than 2. It reflected hydrocarbon generation center of the depression, area of TOC value with high value.

#### IV. CONCLUSION

During the evaluation process of source rock in the offshore basin of Huizhou depression, we established an organic carbon content of geophysical predicted method, from the measured TOC value and obtained quasi TOC value curve, to seismic inversion, achieved the TOC value "kind", "point", "line" stepwise prediction

1) During obtaining Quasi TOC value curve, established the multiple regression relationship with many well logging curve, can be more accurate when evaluate single well TOC value, and in accordance with a higher degree.

2) During seismic inversion of quasi TOC curve, considered a complicated nonlinear relationship between the TOC value and seismic attributes, the algorithm of neural network and SVM algorithm has a better relationship, in the inversion are respectively introduced multi attribute inversion of seismic inversion and frequency inversion method to TOC value inversion.

3) Through geophysical prediction method, to make up for the quantity of sample limited, Under the premise of ensuring economic and rapid prediction of TOC, compared previous seismic methods is more accurate and quantitative, can evaluate potential hydrocarbon of Huizhou depression in the region, provide basis for exploration.

#### REFERENCES

- [1] Meyer B L, Nederlof M H. Identification of source rocks on wireline logs by density/resistivity and sonic transit time/resistivity crossplots[J]. AAPG Bulletin, 1984, 68: 121-129.
- [2] Fertl W H, Chillinger G V. Total organic carbon content determined from well logs[J]. SPE Formation Evaluation, 1988, 3(2): 407-419.
- [3] Hester T C, Schmoker J W, Sahl H. Log-derived regional source-rock characteristics of the Woodford shale, Anadarko Basin, Oklahoma [J]. U S Geological Survey, Bulletin 1866D, 1990: 1-38.
- [4] Herron S L, Letendre I, Dufour M. Source rock evaluation using geochemical information from wireline logs and cores[J]. AAPG Bulletin, 1988, 72: 1007.
- [5] Mann U P, Muller J. Source rock evaluation by well log analysis (Lower Toarcian, Hils Syncline): Advances in organic geochemistry 1987 [J]. Organic Geochemistry, 1988, 13: 109-129.
- [6] BEERS R F. Radioactivity and organic content of some Paleozoic shales[J]. AAPG Bulletin, 1945, 29(1): 1-22.
- [7] Schmoker J W. Determination of organic content of appalachian devonian shales from formation-density logs[J]. AAPG Bulletin, 1979, 63: 1504-1537.
- [8] Schmoker J W. Determination of organic matter content of appalachian devonian shale from gamma ray logs[J]. AAPG Bulletin, 1981, 65: 1285-1298.
- [9] Schmoker J W, Hester T C. Organic carbon in bakken formation, united states portion of eilliston basin[J]. AAPG Bulletin, 1983, 67: 2165-2174.
- [10] Herron S L. A total organic carbon log for source rock evaluation[J]. The Log Analyst, 1987, 28(6): 520-527.
- [11] Passey Q R, Creaney S, Kulla J B, et al. A practical model for organic richness from porosity and resistivity logs[J]. AAPG Bulletin, 1990, 74(12): 1777-1794.
- [12] Mohammad Reza Kamalia, Ahad Allah Mirshady. Total organic carbon content determined from well logs using AlogR and Neuro Fuzzy techniques[J]. Journal of Petroleum Science and Engineering, 2004, 45: 141-148.
- [13] Lim J S. Reservoir properties determination using fuzzy logic and neural networks[J]. Journal of Petroleum Science and Engineering, 2005, 49: 182-192.
- [14] FERTL W H, RIEKE H H. Gammaray spectral evaluation techniques identify fractured shale reservoirs and source rock characteristics[J]. Journal of Petroleum Technology, 1980, 31(11): 2053-2062.
- [15] Gong Zai sheng, Li Si tian. Dynamic Research of Oil and Gas Accumulation in Northern Marginal Basins of South China a Sea[M]. Beijing: Science Press, 2004: 9-25.
- [16] Zeng Hongliu, Charise K. Amplitude versus frequency-application to seismic stratigraphy and reservoir characterization[A]. Society of Exploration Geophysicists, International Exposition and Seventieth Annual Meeting [C]. Calgary, 2000(8), 6-11.
- [17] Simon Haykin. Neural networks: a comprehensive Foundation. Second edition, 1999.
- [18] Zeng Hongliu, Charise Kerans. Amplitude versus frequency-applications to seismic stratigraphy and reservoir characterization. SEG, 2000.
- [19] Robinson E A. Predictive decomposition of time series with application to seismic exploration. Geophysics, 1954, 32: 418-484.
- [20] Robinson E A. Predictive decomposition of seismic traces. Geophysics, 1957, 22: 767-778.
- [21] Robinson E A, Treitel S. Geophysical Signal Analysis. Prentice-Hall, Inc, 1980.
- [22] Saggaf MM, Robinson E A. A unified framework for the deconvolution of traces of nonwhite reflectivity. Geophysics, 2000, 65: 1660-1676.
- [23] Fu L Y. Joint lithologic inversion. In: Wong P, Aminzadeh F, Nikravesh M eds. Soft Computing for Reservoir Characterization and Modeling. Springer-Verlag Publishers, 2002. 511-530.
- [24] Fu L Y. Joint inversions of seismic data for acoustic impedance. Geophysics, 2004, 69: 994-1004.
- [25] Russell B H. The application of multivariate statistics and neural networks to the prediction of reservoir parameters using seismic attributes[D]. Calgary: Department of Geology and Geophysics, Canada, 2004.
- [26] Chopra S, Blas E, Manerikar A, et al. Simultaneous acquisition of 3D VSP data-processing and integration[J]. SEG Technical Program Expanded Abstracts, Society of Exploration Geophysicists, 2002, 21: 2337-2340.

# The Design and Development of Basketball CAI Courseware

WEI Chunkui

Shandong Jiaotong University, Jinan Shandong China

**Abstract**—With the development and popularization of basketball in colleges and the further development of physical education reform at present, the quality of basketball teaching is paid more attention by people. With the rapid development of computers, basketball teaching with the use of multimedia has been realized. This paper discusses the necessity of basketball CAI courseware. It introduces the process of developing and realizing the CAI courseware by FLASH, DREAMWEAVER software and the impact on students, teaching and research.

**Index Terms**—basketball; CAI courseware; Multimedia material database

## I. INTRODUCTION

With the development of modern science and technology, computer technology has been developed rapidly in the field of education in our country. And as a result, a new study area called computer aided education (CBE), combined by comprehensive teaching and computer technology, has developed. Especially in recent years, with the maturity of computer multiply media, the search and spread of Computer Assisted Instruction gained a new success. However, in our country, the manufacture of computer media assisted software just at the very beginning and its applied range is also limited. In the 21st century, talents and science and technology compete sharply. The information characteristics of epoch will be more obvious. Media Assisted Instruction will be a crucial approach in stimulating integration of teaching steps. General basketball course aims at knowing well about basic basketball knowledge and tactical ability and developing teachers. When you go out to be a teacher, you will face all kinds of students in various school. Doing the subject well would be benefit of popularizing Multimedia Computer Assisted Instruction in sports teaching in every school. Thus, this subject has a very crucial theory and reality meaning. It will develop a new way in sports teaching, and also, it would awaken other teaching projects besides basketball.

## II. RESEARCH OBJECTS AND RESEARCH METHODS

### A. Research objects

This research puts the teaching content of general basketball course for the main content of the courseware, collecting a large number of relevant pictures and video, and make corresponding graphics, image and animation, and making a multimedia courseware used for classroom collective teaching. This research puts the teaching

content of general basketball course for the main content of the courseware, collecting a large number of relevant pictures and video, and make corresponding graphics, image and animation, and making a multimedia courseware used for classroom collective teaching.

### B. Research methods

The literature material method, expert interview method, questionnaire, software formation method and experts identified method, etc

## III. RESULTS AND ANALYSIS

### A. The types and modes of the courseware determine

Through the research at General basketball course teaching syllabus and teaching materials, and experts interview and questionnaire survey results, it is turn out that the courseware is a computer assisted teaching system, and it is mainly for the students to apply. Because it is flexible to use, we can utilize it to customised study progress and facilitate human-computer interaction. According to the multimedia course ware design principles and consider teaching truth as well proved that the mode of the courseware is collective teaching pattern.

### B. The selection of courseware content

Basketball CAI courseware's script was written in basic accordance with the People's Sports Publishing House of the Higher Education Sports Elective Course textbook series "Basketball" 's order, refer to the various versions of textbooks and related materials, the content is carefully conceived, well-produced video and pictures animation of nearly 200. The selection of courseware content to the material fully, Primary and secondary clear, and considers students how to do from simple to complex, from perceptual knowledge to rational knowledge of the learning process. The courseware services to the teaching material, and also can be separated from the teaching material to form a complete system.

### C. The design of overall courseware knowledge structure

By means of visited experienced teachers and professors who was engaged in long-period basketball major teaching, treat General basketball course teaching materials as a conception, based on General course teaching tasks, proceed with discuss and choose, finally locate the knowledge points of the basketball Theory courses. In the light of selected knowledge points to devise the structure. the result in figure 1

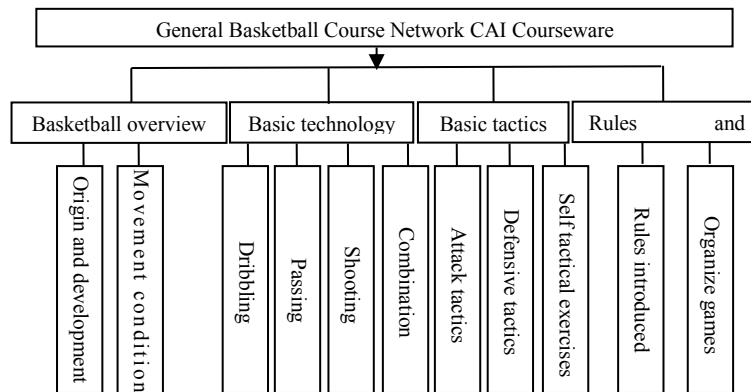


Figure 1. General basketball course CAI courseware structure

D. The establishment of Multimedia material database

Multimedia material database is the base of the software design in the multimedia courseware, and the main content of the courseware system design. Therefore, based on clearing the teaching task and content, collecting widely and downloading various related media material from network media, such as figures, pictures, music CD/VCD, videos and CD, etc.; meanwhile, with his own design and manufacture of graphics, image, animation, using the Windows enclosed recorder software to edit audio file, and provide commentary. background music and related media material. Finally establishing dubbing library, background library, pictures galleries, synchronous animation library and synchronous video library and so on, based on multimedia material database.

E. The design and fabrication for the courseware system

The courseware system mainly use FLASH MX 2004 and Dreamweaver multimedia development system, with picture disposed software Photoshop 6.0 was accomplished. The courseware system structure is shown in figure 2. By considering the need of collective classroom-teaching, courseware system structure shall prevail reticular formation, that is knowledge points as a unit, separately demo the unit. At the same time, among the unit, the unit between homepage both set up hyperlink. The animation effects of FLASH MX 2004 software can greatly provide the courseware animation effect, its unique video into further function can improve the courseware in the quality of the video action demonstration. After finishing the courseware, using development software DREAMWARE to change it into HTML document. Then put the HTML courseware on sever of school website. Students can study wherever through the Internet.

IV. CONCLUSION

With a platform of INTERNET, general basketball course network CAI broke through the restrictions on the time and the place for students' study. Adding auxiliary teaching to general basketball course network CAI is more advantageous to exert students' initiative and practice students' intelligence, which is quite helpful in strengthening students' subjective abilities. In teaching CAI courseware, the teacher puts forward some key

questions to guide the students to think and makes students focus on the key problems when studying, which can help students improve the ability of analyzing the questions and solving the problems. It is the basketball teachers' participation and design in the courseware that set up a new way to exploit the courseware of sports teaching.

Teachers should improve their own ability in developing and utilizing computer technology, design and make the suitable classroom-teaching software, do well in the teaching design, and applied in teaching. Pay more attention to the purpose of our multimedia CAI courseware teaching and understand the key meaning of computer assisted teaching is "assisted", the major of teaching still are teachers, we can not put the cart before the horse. Let student understand how to cooperate with teachers, change their educational concept, enjoy teaching process positively, think deeply, to catch the major content of the teaching.

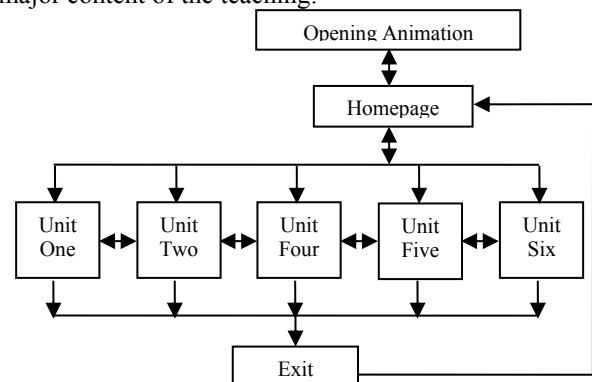


Figure 2. Courseware structure chart

REFERENCES

- [1] Zhongming Li, etc. "Multimedia teaching design and experiment in General swimming class", Journal of Beijing Sport University, 1999 (1) 3
- [2] Huaiyun Ruan. "Breaststroke technology development of MCAI courseware". Journal of Guangzhou Physical Education Institute 1999(1)4
- [3] Qingbo Li. "The high level of basketball game of weight function and the quantitative research", Journal of Tianjin Institute of Physical Education 2000, 15(2)
- [4] Jingsheng Zhao. "The volleyball "elective courses of CAI courseware development and application", Henan normal university (natural science edition) journal, 2000, 28(3): 111-114

# Reliability Analysis for the Metal Structure of Bridge Crane

Yanxu. Wei<sup>#1,2</sup>; Zhengmao. Yang<sup>#,2</sup>; Yugui. Li<sup>1,2</sup>; Feilong. Nie<sup>3</sup>

1. Shanxi Provincial Key Laboratory of Metallurgical Equipment Design and Technology State Key Laboratory Cultivation Base of Province-Ministry Co-Construct, Taiyuan 030026, China

2. School of Mechanical Engineering, Taiyuan University of Science and Technology, Taiyuan 030024, China

3. School of Mechanical Engineering, Tongji University, Shanghai 200092, China

<sup>#</sup>these authors contributed equally to this work.

**Abstract**—The bridge crane is the most widely used industrial and mining enterprises crane equipment, Its complex structure, size and huge, and which always works in complex and formidable environment. Reliability is an important problem needed to be considered in the course of their work, the reliability analysis of crane metal structure is currently pending in-depth study of the important issues. This paper try to develop a reliability analysis method for the metal structure of the bridge crane based on ANSYS software. Select 25t\_13.5m double girder bridge crane as object, its three-dimensional model is established in ANSYS. Probability finite element analysis and Monte Carlo numerical test and reliability analysis of the structure, proved the reliability of the structure under extreme loads. The results show that ANSYS provides a viable and strong method for the reliability analysis of the structure of the metal structural.

**Index Terms**—bridge crane, reliability analysis, Monte Carlo methods, sensitivity analysis, probability finite element

## I. INTRODUCTION

Currently, allowable stress method is mostly used in crane metal structure design, it generally regard relevant parameters as fixed values and select a safety factor by experience, then determine the final design results. In fact, there are a lot of uncertainty factors in the metal structures design, the safety factor cannot precisely measures the reliability of the metal structure, so certain risks inevitably exist in the designed metal structures and just have been limited to the extent human experience can accept<sup>[1-5]</sup>.

To clear the degree of this allowable risk, the paper uses probability finite element method combined ANSYS parametric design language (APDL) and Monte Carlo to bridge crane metal structure reliability. Select 25t\_13.5m double girder bridge crane as object, random variables are determined from a variety of design parameters, such as the actual size of the components, the material properties, the lifting load, and so on. The reliability analysis of crane metal structure, in the case of setting the statistical distribution, prove the reliability of the metal structure under extreme loads, and identify the factors affecting the reliability of the structure, and provide an effective and practical method and basis for cranes metal structural strength and reliability analysis<sup>[6-9]</sup>.

## II. THE THEORY OF STRUCTURAL RELIABILITY ANALYSIS

Structure function (limit state functions) as a function of the basic variables by  $X_1, X_2, \dots, X_n$ , can be expressed as:

$$Z = g(x_1, x_2, \dots, x_n) \quad (1)$$

The structural strength  $\sigma$  and the load effects  $S$  are main target of the reliability study of the mechanical structure. Functions between the two determine the reliability of the mechanical structure<sup>[10]</sup>. Such structure functions can be expressed as stress - strength interference model:

$$Z = \sigma - S \quad (2)$$

Therefore, the reliability of the mechanical structure is the probability of the limit state function  $g(x) \geq 0$ , to calculate the reliability of the structure is to calculate the probability  $g(x) \geq 0$  using ANSYS probability analysis function.

Set the  $f_x = \{x_1, x_2, \dots, x_n\}$  is the joint probability density function of the basic random variable  $x = \{x_1, x_2, \dots, x_n\}^T$ , then the failure probability of mechanical metal structure  $P_f$  can be expressed as:

$$P_f = \int \dots \int_{g(x) \leq 0} f_x(x_1, x_2, \dots, x_n) dx_1 dx_2 \dots dx_n \quad (3)$$

If the basic random variables are independent with each other, the probability density function of random variable  $x_i$  is  $f_{x_i}(x_i)$  ( $i=1, 2, \dots, n$ ), there are:

$$P_f = \int \dots \int_{g(x) \leq 0} f_{x_1}(x_1) f_{x_2}(x_2) \dots f_{x_n}(x_n) dx_1 dx_2 \dots dx_n \quad (4)$$

## III. APPLICATION OF MONTE CARLO FINITE ELEMENT METHOD IN STRUCTURAL RELIABILITY ANALYSIS

### A. Principle of Monte Carlo method

The basic theory of Monte Carlo method to solve the failure probability  $P_f$  is that the n basic random samples  $x_i$  ( $i=1, 2, \dots, n$ ) is generated by the joint density function of the basic random variables, which are taken into the function  $g(x)$ , and then count the sample points fallen into the failure area  $G = \{x: g(x) \leq 0\}$ . we can approximately obtain the failure probability estimate by the failure frequency  $N_f/n$ .

Here the equation (4) is written into the mathematical expectation form of the failure indicator function:

$$P_f = \int \cdots \int_{R^n} I[g(\hat{x}_i)] f_X(x_1, x_2, \dots, x_n) dx_1 dx_2 \cdots dx_n = E\{I[g(\hat{x}_i)]\} \tag{5}$$

Where  $R^n$ --n dimensional variable space;  
 $E\{ \cdot \}$ --mathematical expectation operator.

$$I[g(x_i)] = \begin{cases} 1, & g(x_i) \leq 0 \\ 0, & g(x_i) > 0 \end{cases} \text{ is the indicator function}$$

of the failure area.

The equation (5) shows that the failure probability  $P_f$  is the mathematical expectation of the failure area indicator function  $g(x_i)$ . According to the Law of large Numbers, the mathematical expectation of failure indicator function can be approximately replaced by the sample mean of failure area indicator function:

$$\hat{P}_f = \frac{\sum_{i=1}^n I[G(\hat{x}_i)]}{n} \tag{6}$$

Where:  $n$ -- the total number of sampling analog.

As shown in the expression, the results closely related to the sample size. It should be noted, in general mechanical structural reliability analysis, the structural failure probability is low, that the correctness of the Monte Carlo method is largely dependent on the size of the sample size, which is a limitation of the Monte Carlo method [11-13].

Reliability sensitivity is that the failure probability  $P_f$  is taken partial derivative of with respect to the distributed parameter  $\theta_{x_i}^{(k)}$  of the basic random variable  $x$ .

$$\frac{\partial P_f}{\partial \theta_{x_i}^{(k)}} = \int \cdots \int_F \frac{\partial f_X(x)}{\partial \theta_{x_i}^{(k)}} dx \tag{7}$$

The equation (7) makes the following transformations and the expression form of mathematical expectation of reliability sensitivity is obtained:

$$\begin{aligned} \frac{\partial P_f}{\partial \theta_{x_i}^{(k)}} &= \int \cdots \int_F \frac{\partial f_X(x)}{\partial \theta_{x_i}^{(k)}} \frac{1}{f_X(x)} f_X(x) dx \\ &= \int \cdots \int_{R^n} I_F(x) \frac{\partial f_X(x)}{\partial \theta_{x_i}^{(k)}} \frac{1}{f_X(x)} f_X(x) dx \\ &= E\left[\frac{I_F(x)}{f_X(x)} \frac{\partial f_X(x)}{\partial \theta_{x_i}^{(k)}}\right] \end{aligned} \tag{8}$$

Thus we can apply the Monte Carlo to calculate the reliability sensitivity(equation (7)) with the equation (8).

It is worth noting that in the process of digital simulation of the Monte Carlo we apply the mean of the sample to replace the ensemble average. The expression form of mathematical expectation of reliability sensitivity can be estimated by the followed average of the sample function.

$$\frac{\partial \hat{P}_f}{\partial \theta_{x_i}^{(k)}} = \frac{1}{N} \sum_{j=1}^N \frac{I_F(x_j) \partial f_X(x)}{f_X(x_j) \partial \theta_{x_i}^{(k)}} \Big|_{x=x_j} \tag{9}$$

Where  $x_j$ --the  $j$ th sample extracted from  $n$  samples according to the joint probability density function  $F_X(x)$ .

*B. Steps of ANSYS structural reliability analysis*

**Generate the analysis file:** Apply APDL and macro commands to build a bridge parameterized finite element model of bridge crane. Based on setting model size, material properties and unit type, the parameterized lifting load and constraint of the crane on actual operating conditions are applied to the finite element model for simulation of the forces under their work environment and finite element analysis. Then observe the model of the displacement, deformation and stress distribution, define result parameter, extract the results data that we are concerned about, such as the stress distribution on the upper and lower flange plate, the main and auxiliary web. Finally, form the analysis file (loop file) [14].

**Reliability analysis:** In the stage of reliability analysis, the various factors that affect the internal stress in the crane work process are extracted as random input variables, such as material elasticity modulus and density, flange plate thickness, lifting load and so on. The type of distribution of random variables is determined in accordance with the actual situation. On this basis, Monte Carlo simulation method is used for cycle simulation to determine the failure probability of the structural, that also says reliability of the structural, on the condition of lifting load and structural characteristics meeting certain distribution law.

**The results of the post-processing analysis:** In the post-processing stage, use simulation results as reference to examine the sampling process and random response to the situation in reliability analysis of the metal structure, to draw the failure probability distribution function, to complete sensitivity analysis, and finally to generate the analysis report.

IV. INSTANCE OF THE STRUCTURE RELIABILITY ANALYSIS

*A. Overview of analysis objects*

As shown in Figure 1, it is an entity photo of DQ25t\_13.5m double girder overhead crane. And in Figure 2, it is an ANSYS model of crane bridge structure.



Figure 1. Photo of Bridge Crane

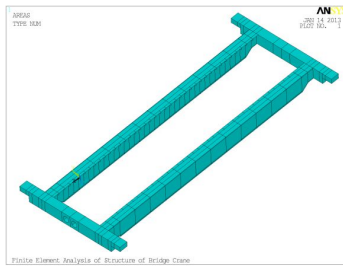


Figure 2. ANSYS Model of Bridge Crane

**B. Analysis of the factors affect the crane metal structure working**

**Technical parameters of crane metal structure:**

Span: 13.5m, upper and lower flange plates:  $0.69 \times 0.0014\text{mm}$ , main and auxiliary web:  $0.8 \times 0.006\text{mm}$ , diaphragm:  $0.6 \times 0.79 \times 0.006\text{mm}$ ;

**Lifting System: Lifting speed:** 1.2m/min, car running speed: 20m/min, carts running speed: 50m/min; Rated lifting weight:250kN;

**Material properties:** elastic modulus: 206GPa, density: 7852Kg/m<sup>3</sup>;

Set the contact between the car wheels and the main beam as point contact, and apply concentrated loads at the contact, the load capacity is rated lifting weight *W* and the assembly weight of the car is 26kN;

Selected random input variables include : material elastic modulus *YOUNG*, material density *DENSITY*, top flange thickness *E\_SYYB*, main web thickness *E\_FB*, main beam height *H1*, lifting load *W1* and the material yield limit *S*.

In reliability analysis process, input random variables distribution should be closely consistent with actual distribution of working conditions, so that obtained reliability analysis results is close to that of the actual situation. Thus in simulated condition, the lifting load is set for normally distributed variables, and the other material properties are correspondingly set to reasonable random distributed variables, as shown in table1.

TABLE I. TYPE OF DISTRIBUTION OF THE VARIABLES

Input random variables	Variables symbol	Distribution type	Parameters A	Parameters B
Elastic modulus	YOUNG	GAUSS	206GPa	10GPa
Materials density	DENSITY	UNIF	7065kg/m <sup>3</sup>	8625 kg/m <sup>3</sup>
Thickness of top flange plate	E_SYYB	UNIF	0.0134	0.0146
Thickness of main webs	E_FB	UNIF	0.0054	0.0056
Height of main beam	H1	UNIF	0.795	0.805
Lifting load	W1	GAUSS	W1	0.15 × W1
Yield linit	S	GAUSS	235MPa	11.75MPa

**C. Reliability analysis of crane metal structure**

Based on probability finite element ideological, Monte Carlo loop simulation is performed 200 times with computation time of 72min for the reliability analysis of the metal structure of the bridge crane. First observe the displacement deformation diagram, as shown in Figure 3, and the equivalent stress distribution nephogram, as shown in Figure 4. It can be seen that the maximum deformation is at the mid-span of the top flange plate, while the greatest stress exist at the intersection part between the top flange plate and the lower flange plate, the main web, the diaphragms of the box structure. The intersection part also is prone to appear the fracture and failure. Extract the maximum stress *MAXVON* in each loop experiment and draw diagrams showing the stress distribution law of the crane metal structure of simulation conditions.

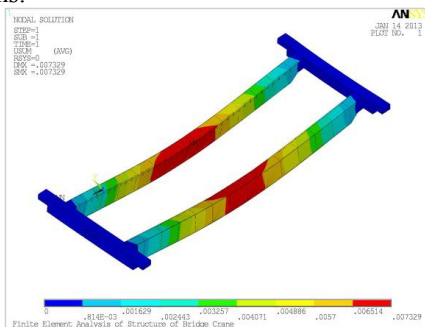


Figure 3. Stress of flange

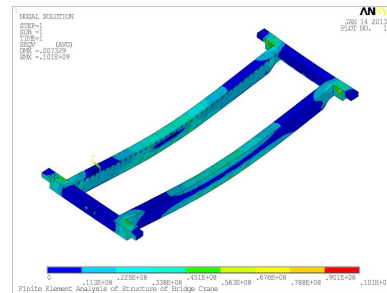


Figure 4. Distortion of flange

As shown in Figure 5, it is mean value history for *MAXVON* the maximum stress value in response to the random variable. Figure 6 is standard deviation history for *MAXVON*. The most effective way to determine whether the simulation cycles of Monte Carlo technology are enough is to view the mean and standard deviation history [15]. Because when the cycles are enough, the mean and standard deviation are gradually convergent, and the curve will tend to level. If the curves still show significant fluctuation with the cycles increase, it indicates cycles are insufficient and should be appropriately increased. The historical curve confidence boundary can be interpreted as the change accuracy of the sample statistical parameters. The more cycles the smaller range of the confidence boundary. As can be seen from the figure that the *MAXVON* curves in late have been approaching the gentle, showing the gradual convergence of the mean and standard deviation,

indicating the experimental sample size is sufficient for the calculation of the crane metal structure reliability.

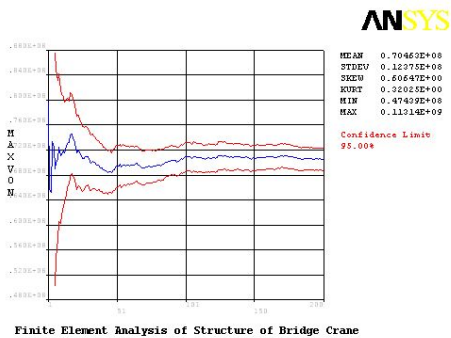


Figure 5. Mean Value History for MAXVON

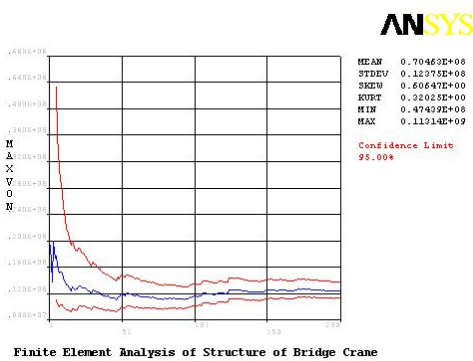


Figure 6. Standard Deviation History for MAXVON

In addition, the average maximum stress of the crane metal structure is shown close to 113MPa which is the center value of stress distribution. Figure 7 has shown that the contour of lifting load distribution histogram conforms to normal distribution curve. That means, in the sampling process, load data meets normal distribution requirements. When collated to Figure 5 and Figure 6, it can be explained that the applied simulation load in analysis process has well reflected the actual working conditions, thus the reliability analysis result has higher credibility.

According to stress-strength interference theory, the incident that stress exceeds the yield strength is not allowed during crane operation, so the failure criteria as follow:

$$MAXVON \geq \sigma_s \tag{10}$$

Where, MAXVON-- the maximum stress in the lifting work;

$\sigma_s$  -- yield strength of material;

Values of the cumulative distribution function at any point represent the probability of data appearing under that point<sup>[16-17]</sup>. It can be observed from Figure 8, maximum stress distribution interval is [74MPa, 113MPa], and it still has a large safety margin to the material yield strength of 235MPa, no failure risk and the reliability is one. So the reliability of bridge crane structure under extreme loads is proved.

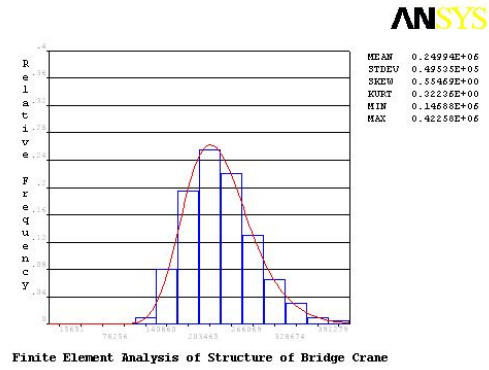


Figure 7. Histogram of Input Variable

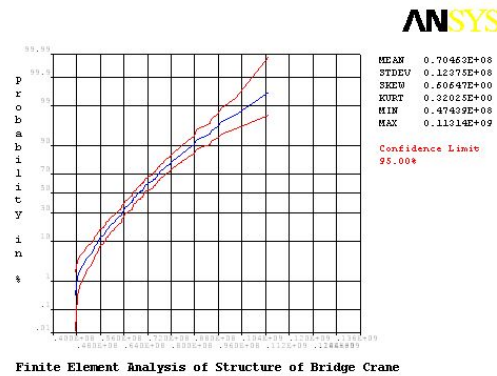


Figure 8. CDF of Output Parameter MAXVON(CDF--cumulative distribution function)

In the analysis of the reliability of the bridge crane metal structure, extract the maximum deflection of each experiment, and examine the impact of the variability of the input variables on the structural failure probability. If the influence level of the input parameters for the output parameter is in the 2.5% or less, the input parameters has classified to be little effective factors; else, the input parameters has classified to have a significant effect<sup>[18]</sup>.

As showed in Figure 9 and 10: the lifting load, the materials elastic modulus YOUNG and material density DENSITY have a significant impact on the probability of the structure failure. The impact of the three variables, variability has been descending ordered as: lifting load> material density DENSITY> elastic modulus YOUNG. So using ANSYS for structural reliability analysis, the main factors affecting the structure reliability can be obtained according to the parameter sensitivity analysis results, which help take measures to improve the structural reliability based on the main factors.

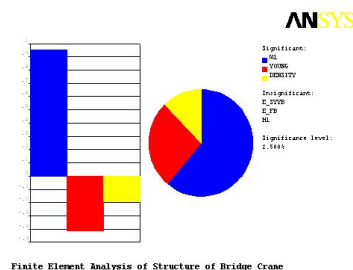


Figure 9. Sensitivity Plot for MAXVON

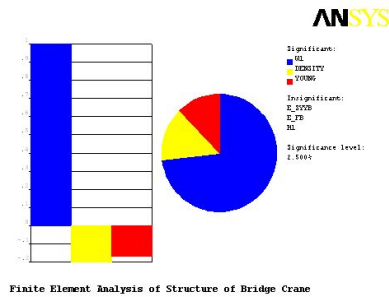


Figure 10. Sensitivity Plot for *MAXSUM*

V. CONCLUSIONS

This paper complete the reliability analysis of typical off-track box structure of bridge crane using ANSYS finite element analysis software, and prove the structure meets the strength requirements in the actual operation. Introduce a general method to analyze the mechanical structure reliability in detail, a combination of the probability finite element analysis and structural reliability theory. It provides a reference for reliability analysis for hoisting and conveying machinery metal structure, also has great significance for the safety analysis of other special equipment.

ACKNOWLEDGMENT

The project is subsidized by The National Natural Science Foundation of China 51075289, The National Natural Science Foundation International (Areas) Cooperation and Exchanges Project 51110105011. We thank Professor Liu, Jun S for a preprint of Ref. 7, and Professor Sara Ibrahim for enlightening discussions.

REFERENCES

[1] Pellissetti, M. F., and G. I. Schuëller. "On general purpose software in structural reliability—An overview." *Structural Safety* 28.1 (2006): 3-16.

[2] Choi, Kyung K., and Nam-Ho Kim. *Structural sensitivity analysis and optimization 1: linear systems*. Vol. 1. Springer, 2006.

[3] Hohenbichler, M., and R. Rackwitz. "Sensitivity and importance measures in structural reliability." *Civil Engineering Systems* 3.4 (1986): 203-209.

[4] Meng, Wen J, and Yang Zheng M et al. "Reliability Analysis-Based Numerical Calculation of Metal Structure of Bridge Crane." *Mathematical Problems in Engineering* 2013 (2013).

[5] Jiang, Chao, et al. "Structural reliability analysis based on random distributions with interval parameters." *Computers & Structures* 89.23 (2011): 2292-2302.

[6] Yanmei, Li, and Z. I. Chen. "Analysis of Load Factors Based on Interpretive Structural Model." *Journal of Computers* 7.7 (2012).

[7] Wan, Yi, and ChengWen Wu. "A New Intelligent Model for Structural Reliability Identification Based on Optimal Machine Learning." *Journal of Computers* 7.2 (2012).

[8] Chen, Aijiu, et al. "The Meso-level Numerical Experiment Research of the Mechanics Properties of Recycled Concrete." *Journal of Software* (1796217X) 7.9 (2012).

[9] Jin, Zhaoyan, et al. "MCHITS: Monte Carlo based Method for Hyperlink Induced Topic Search on Networks." *Journal of Networks* 8.10 (2013).

[10] Meng, Wen J, and Yang Zheng M. "Non-probabilistic Reliability Analysis of Bridge Crane Metal Structure Based on Support Vector Machine." *Mechanical Science and Technology for Aerospace Engineering*, 2014, 5:39-43.

[11] Liu, Jun S. *Monte Carlo strategies in scientific computing*. Springer, 2008.

[12] Meng, Wen J, and Yang Zheng M et al. "Optimization Design in Metal Structure of Bridge Crane with Reliability Requirement." *Hoisting and Conveying Machinery*, 2013, 12: 39-43.

[13] Melchers, R. E. "Search-based importance sampling." *Structural Safety* 9.2 (1990): 117-128.

[14] Reh, Stefan, et al. "Probabilistic finite element analysis using ANSYS." *Structural Safety* 28.1 (2006): 17-43.

[15] Schueller, G. I. "On the treatment of uncertainties in structural mechanics and analysis." *Computers & Structures* 85.5 (2007): 235-243.

[16] Der Kiureghian, Armen, and Pei-Ling Liu. "Structural reliability under incomplete probability information." *Journal of Engineering Mechanics* 112.1 (1986): 85-104.

[17] Gavin, Henri P., and Siu Chung Yau. "High-order limit state functions in the response surface method for structural reliability analysis." *Structural Safety* 30.2 (2008): 162-179.

[18] Adelman, Howard M., and Raphael T. Haftka. "Sensitivity analysis of discrete structural systems." *AIAA journal* 24.5 (1986): 823-832.

**Yan-xu Wei**, born in Hebei in 1987, is a Master of Mechanical Engineering in the School of Mechanical Engineering at the Taiyuan University of Science and Technology. His current research interests include Fracture and Damage Mechanics, Computational Mechanics and Mechanical design. He has authored 2 publications.

**Zheng-mao Yang**, born in Shanxi in 1988, is a Master of Mechanical Engineering in the School of Mechanical Engineering at the Taiyuan University of Science and Technology. His current research interests include Fracture and Damage Mechanics, Computational Mechanics (finite elements), Constitutive Multi-scale Phenomena, Sensitivity Analysis and Optimization. He awarded China Youth Science and Technology Innovation Award and National Scholarship for Graduate Students in 2013. He Awarded Shan Xi Youth May 4th Medal in 2014. He has authored or co-authored more than 20 publications and holds 9 Chinese patents.

**Yu-gui Li**, born in Shanxi in 1967, is a professor of Taiyuan University of Science and Technology, and gained the doctor's degree at Beijing Institute of Technology in China, Beijing in 2007. He has authored or co-authored more than 20 publications collected by EI or SCI, and holds more 10 Chinese patents. His achievements Granted with National 2nd class Progress Awards. Mr. Li is the executive director and the Deputy secretary general of Shanxi Mechanical Engineering Society. He is also a leader of Shanxi Province young academic and the leader of Engineering Research Center for Department of Heavy Machinery Education, Taiyuan University of Science and Technology.

**Feilong Nie** is a Doctor of School of Mechanical Engineering in Tong-ji University, His current research interests include Fracture and Damage Mechanics, Computational Mechanics. He has authored or co-authored more than 5 publications.

# Hybrid Ant Colony Algorithm for the Traveling Salesman Problem

Chuangdong Qin<sup>1</sup>; Huixia Zhao<sup>2</sup>

1. Institute of mathematics and information science, North National University, Yinchuan 750021, P.R. China

2. Business school, North National University, Yinchuan 750021, P.R. China

**Abstract**—Ant colony algorithm has strong ability to find a better solution, but there are also some disadvantages, such as prone to stagnation, the slow Convergence etc. But the ant colony algorithm can help the genetic algorithm to conquer the disadvantages. The ant colony algorithm can select the initial components in its each iteration, the solution based on the amount of information to select the initial components, and then the mutation operation is used to determine the value of the solution. Through the comparison of traveling salesman problem, the hybrid ant colony algorithm has better convergence speed and stability.

**Index Terms**—ant colony algorithm, genetic algorithm TSP.

## I. BACKGROUND

Ant colony algorithm (ACA) is a bionic optimization algorithm which is proposed by Italian scholar Marco Dorigo [1]. It is through the accumulation and the update of the pheromone to seek the optimal solution. The ants have the ability to find the shortest path without any cues from nest to food source. It can change with in the environment changes, adaptive search new paths and produce the new choice. The fundamental reason is that the ants can release a special kind of secretion pheromones in the process of the searching for food source. The probability of the ant chooses the path is directly proportional to the strength of the pheromones. When the ant pass a certain path more and more , the pheromone track which is left become more and more, then the probability which the ant chooses the path is the higher, at the same time ,it increases the intensity of the path pheromone[2]. The strength of the pheromone will attract more ants. Thus it forms a positive feedback mechanism. Through this kind of positive feedback mechanism, ants can find the shortest path in the end. When there is obstruction between the ant nest and food source, after a certain time of positive feedback, ants can not only bypass obstacles, but also seek the short path by the changes of ant pheromone track on different paths [3-5].

The main features of ant colony algorithm are distributed computing features, very strong robustness, easy to merge with other optimization algorithms. But when the algorithm was used to solve the large-scale optimization problems, the contradiction of the search space and time performance is present. It is easy to appear premature convergence to the global optimal solution and its calculating time is too long. In the

working process of the algorithm, the ants may be stagnated near a certain or some local optimal solution of the neighborhood. Genetic algorithm (GA) can remedy some of the shortage [6-7]. In this paper, we combine the ant colony algorithm and genetic algorithm to solve the traveling salesman problem (TSP), the experiment proved that the method is effective.

## II. THE TSP AND ACA MODEL

Ant colony algorithms are becoming popular approaches for solving all kind of optimization problems which were first introduced by Dorigo et al [1].The fundamental idea of ant heuristics is based on the behaviour of natural ants that succeed in finding the shortest paths from their nest to food sources by communicating via a collective memory that consists of pheromone trails. Due to ant's weak global perception of its environment, an ant moves essentially at random when no pheromone is available. However, it tends to follow a path with a high pheromone level when many

Ants move in a common area, which leads to an autocatalytic process. Finally, the ant does not choose its direction based on the level of pheromone exclusively, but also takes the proximity of the nest and of the food source, respectively, into account[8]. This allows the discovery of new and potentially shorter paths. Typical examples of ACO [9] are to solving the traveling salesman problem (TSP). The description of the TSP may be stated as follows: a salesman is required to visit the  $n$  given cities once and only once. He will start from any city and return to the original place of departure. In order to minimize the total distance traveled, what route should he choose? Based on the pheromone of ant colony algorithm to solve TSP problem calculation process is as follows:

Step 1: initiation. Allocate  $m$  ants were randomly put in  $n$  cities. The amount of the pheromone on each side is initiated into a tiny constant value  $\tau_{ij}(0)$ .

Step 2: Loop iteration. Ants  $k(k=1,2,\dots,m)$  determine the transfer direction according to the amount of information on each path. Ants prefer to move to cities which are connected by short edges with a high probability with which ant  $k$  in city  $i$  chooses to move to the city  $j$ .

$$P_{ij}^k(t) = \begin{cases} \frac{[\tau_{ij}(t)]^\alpha [\eta_{ij}(t)]^\beta}{\sum_{s \in allowed_k} [\tau_{ij}(t)]^\alpha [\eta_{ij}(t)]^\beta}, & j \in allowed_k \\ 0, & other \end{cases}$$

Here  $allowed_k = \{c - tabu_k\}, (k=1,2,\dots,m)$ ,  $\alpha$  and  $\beta$  are two parameters that control the relative weight of pheromone trail and heuristic value. The heuristic values used  $\eta_{ij}(t) = \frac{1}{d_{ij}}$ , where  $d_{ij}$  is the distance between cities  $i$  and  $j$ .

step 3: Update the pheromone, After pheromone updating has been performed by the ants, pheromone evaporation is triggered; the formula of the updating pheromone is  $\tau_{ij}(t+n) = (1-\rho) \cdot \tau_{ij}(t) + \Delta\tau_{ij}(t)$

with  $\Delta\tau_{ij}(t) = \sum_{k=1}^m \Delta\tau_{ij}^k$ , where  $m$  is the number of ants and

$\Delta\tau_{ij}^k$  is the amount of trail laid on edge  $(i,j)$ .

Step 4: the termination conditions, if meet the termination conditions, the loop ends. To compare the shortest path of each cycle and get the optimal solution; otherwise, empty tabu table, turn to step 2

### III. HYBRID ANT COLONY ALGORITHM FOR THE TSP.

Genetic algorithm (GA) can be understood as an “intelligent” probabilistic search algorithm which can be applied to a variety of combinatorial optimization [10]. The theoretical foundations of GAs were originally developed by Holland in 1975[11]. The basic idea is to simulate natural genetic mechanism and the evolution according to the principles of natural selection and “survival of the fittest”. The main features of genetic algorithm are: the global search ability, wide adaptability, stronger robustness, no special requirements to the search space, easily combined with other algorithm But there is premature and slow convergence speed and low accuracy of optimization obviously deficiencies. On the other hand, we found the ant colony algorithm can easily gain a relatively good solution set through a cycle of the ants. If we make the solution of the ACA to be the initial population of the GA, the GA can be reduced the number of the optimization and speeded up the convergence. The execution efficiency of the GA is improved. in this paper, the pheromone of ACA and GA will be combined to solve the TSP. the calculation flow chart can be find as follow.

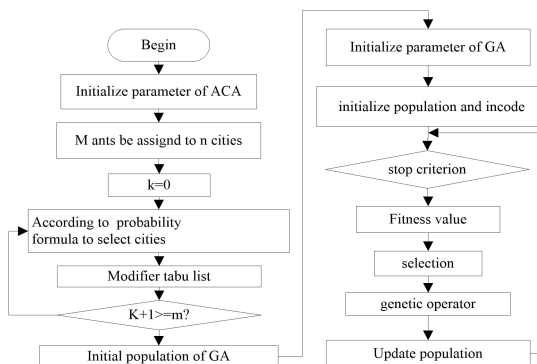


Figure 1. Flow Chart of Hybrid algorithm

### IV. EXPERIMENT

In this section, we present some computational results obtained by ant colony algorithm and genetic algorithm on some TSP instances. And at last, we will compare the results with the hybrid colony algorithm. As we know, the TSP is the problem of a salesman who wants to find, starting on his home town, a shortest possible trip through a given set of cities and to return to its home town. So in our experiment, we will use Euclidean TSP instances in which the cities are points in the Euclidean space and the inter-city distances are calculated using the Euclidean norm for the distance. All the TSP instances are taken from the TSPLIB Benchmark library which contains all kind of the instances. TSPLIB is found from the address <http://www.iwr.uni-heidelberg.de/iwr/comopt/soft/TSPLIB95/TSPLIB.html>.

We select the 50cities and 75 cities for the TSP instance respectively. The result can be found from the following list.

TABLE I. THE RESULT COMPARISON OF 50 CITIES FOR THE TSP INSTANCE IN THE DIFFERENT ALGORITHMS

	ACA	GA	HAG
50	460.483	453.547	446.862
100	458.624	452.457	441.284
1000	458.028	451.204	438.267

TABLE II. THE RESULT COMPARISON OF 75CITIES FOR THE TSP INSTANCE IN THE DIFFERENT ALGORITHMS

	ACA	GA	HAG
50	548.640	542.506	538.571
100	541.805	536.032	527.096
1000	540.061	535.105	525.584

To compare the HGA with other heuristics algorithm, we consider two sets of TSP problems.

The first set comprises three randomly generated 50-city problems, and the second set is composed three geometric problems of 75 cities. It is important to test those heuristics algorithm on both random and geometric instances of the TSP, because these two classes of problems have structural differences that can make them difficult for a particular algorithm and at the same time easy for another one. The heuristics algorithm with which we compare the HGA in this case are a genetic algorithm(GA), ant colony algorithm (ACA). Table I and Table II report the results on the randomly instances and the geometric instance. The distance of HGA is shortest than the other two. It is because the ant colony algorithm is compounded to the genetic algorithm.

### V. CONCLUSION

In conclusion, in this paper we have shown that the HGA is an interesting novel approach to parallel stochastic optimization of the TSP. The HGA has been shown to compare favorably with previous attempts to apply other heuristic algorithms like genetic algorithms, ant colony algorithm. Nevertheless, competition on the TSP is very tough. A combination of a Hybrid ant colony algorithm which is generated by the ant colony algorithm and the genetic algorithm can gain the better execution efficiency.

## ACKNOWLEDGMENT

The project is subsidized by The Natural Science Ningxia Foundation(NZ13095).

## REFERENCES

- [1] Marco Dorigo, Luca Maria Gambardella, A Cooperative Learning Approach to the Traveling salesman Problem, IEE transactions on evolutionary computation, 1997,vol. 1(1)53-66
- [2] H. B. Duan, Ant Colony Algorithms: Theory and Applications. Beijing: Science Press, 2005.
- [3] W. W. Kok, S. O. Yew,Hybrid fuzzy modelling using memetic algorithm for hydrocyclone control. Proceedings of the 3rd International Conference on Machine Learning and Cybernetics, Shanghai, 2004,vol. 2,26-29.
- [4] Blum, C. Beam-ACO—Hybridizing ant colony optimization with beam search: An applica-tion to open shop scheduling.Comput.Oper.Res.2005,32(6),1565–1591.
- [5] Blum, C., Dorigo, M.: Search bias in ant colony optimization: on the role of competition-balanced systems. IEEE Trans. Evol. Comput,2005. 9(2), 159–174.
- [6] Blum, C., Yabar,M., Blesa, M.J.: An ant colony optimization algorithm for DNA sequencingby hybridization. Comput. Oper. Res.2008. 35(11), 3620–3635.
- [7] Cant u-Paz, E.: Efficient and Accurate Parallel Genetic Algorithms. Kluwer, Boston, MA(2000)
- [8] Rahul Putha, Luca Quadrioglio. Comparing Ant Colony Optimization and Genetic Algorithm Approaches for Solving Traffic Signal Coordination under Oversaturation Condition Computer-Aided Civil and Infrastructure Engineering 2012,27 ,14–28.
- [9] Angus, D., Woodward, C.: Multiple objective ant colony optimizations. Swarm Intell. 2009, 3(1),69–85.
- [10] Balaprakash, P., Birattari, M.,St utzle, T.. Estimation-based ant colony optimization algorithms for the probabilistic travelling salesman problem. Swarm Intell., 2009,3(3), 223–242.
- [11] Xiao-jun Liu, Hong Yi, Zhong-hua Ni.Application of ant colony optimization algorithm in process planning optimization. J Intell Manuf, 2013 24:1–13DOI 10.1007/s10845-010-0407-2

# An Empirical Study on Factors Affecting LBS Users' Adoption

Zhaoyu An; Luchuan Liu

Shandong University of Finance and Economics, School of Management Science and Engineering, Jinan, China

**Abstract**—Mobile Internet has the most developmental potential with mobility, sociability and location-based service. Based on literature review, this paper put forward an extended technology acceptance model (TAM), and verify the model by data collected from a survey of LBS users. The study proves that LBS users' adoption is significantly influenced by the following four factors: privacy, perceived playfulness, perceived ease of use, network externality. Finally discussion of this study is carried out, and the significance is pointed out along with limitations of the research.

**Index Terms**— Mobile Internet, LBS, TAM, Adoption, SEM

## I. INTRODUCTION

Mobile Internet has no unified definition, but the research has already begun from the mid-1990s [1]. The definition of mobile Internet has been divided into broad sense and narrow sense, on the basis of the differences between access network and display terminal [2]. In the broad sense of the concept of mobile Internet, network refers to all wireless networks, and the terminal includes mobile phone, PDA, tablet PC, laptop and other handheld devices. In the narrow sense of the concept of mobile Internet, network specifically refers to the mobile communication network, and the terminal is limited to mobile phone [3]. Narrow sense of the mobile Internet is the focus of this research.

Mobile communication and Internet developed rapidly in recent years, mobile Internet as a combination of them, its prospect is even more attractive. According to "2012 Mobile Internet Trend Forecast" from IT analysis firm in 2012, the number of China Mobile Internet users is expected to transcend the number of Internet users by the end of that year, which will reach 600 million. In the business system of mobile Internet, applications which hold the characteristics of SoLoMo (So (social), social networking; Lo (local), the local position; Mo (mobile), mobile network) will be one of the most promising. The mobile LBS business based on social network is the most typical, such as Foursquare, Facebook Places and JiePang, RenRen Check-In. Through the research on patterns of mobile LBS users' behavior, this paper analyzes the key factors affecting users' usage of mobile LBS, provides the basis and train of thought for the extension

mechanism of new technology and product innovation of the LBS service provider.

## II. RESEARCH THEORY AND MODEL CONSTRUCTION

LBS is a mobile Internet business, with the support of geographic information system (GIS) platform, which takes advantage of the mobile communication networks (such as 2G, 3G network) of telecom operators or GPS to get the location information (geographical coordinates or geodetic coordinates) of mobile terminal users, and provides related services to terminal users. From technical aspect, LBS business is one of the information system strategies. Therefore, when the terminal users adopt LBS business, they also accept the technology and innovation activities related to LBS.

### A. The Technology Acceptance Model

In order to explain and predict the final status of users' acceptance of information systems, Davis raised the "technology acceptance model" based on TRA (Theory of Reasoned Action) [4]. The technology acceptance model extends the behavior relationship "belief-attitude-intention", from the theory of reasoned action, and proposes two major determinants: PU (perceived usefulness), which reflects the degree that the user feel when information technology improving their performance; PEOU (perceived ease of use), which reflects the degree of information technology's easy operation that the user feel. [5]. As the technology acceptance model is rigorous, meanwhile, it has high effectiveness and reliability, this paper put forward the following hypotheses, on the basis of the behavior relationship "belief - attitude - intention":

H1: Perceived usefulness has positive association with the attitude to use mobile LBS.

H2: Perceived usefulness has positive association with the intention to use mobile LBS.

H3: Perceived ease of use has positive association with perceived usefulness.

H4: Perceived ease of use has positive association with the attitude to use mobile LBS.

H5: The attitude to use LBS has positive association with the intention to use mobile LBS.

### B. Perceived Playfulness

If using information technology itself is relatively difficult, users will not feel interesting; otherwise, the information technology itself is easy to use, users may

Corresponding author: Luchuan Liu, Male, ShanDong University of Finance and Economics, School of Management Science and Engineering, Professor.

feel interesting, which prompts the users' intention to use the information technology. Lots of research work has revealed the regular pattern that perceived ease of use indirectly affects the intention to use information technology through perceived playfulness. Perceived playfulness is a focus factor of users, as other external factors which can also improve the efficiency of work. Mobile LBS is a typical business of mobile Internet, and the entertainment function is an important factor to be considered when a terminal user uses the business. Therefore, we introduce perceived playfulness into this study. Perceived ease of use has a positive association with perceived playfulness, and the more the perceived playfulness is, the more positive the attitude will be and the higher the intention is, and vice versa. This paper puts forward the following hypotheses based on the feature that mobile LBS itself has entertainment functions:

H6: Perceived ease of use has positive association with perceived playfulness.

H7: Perceived playfulness has positive association with the attitude to use mobile LBS.

H8: Perceived playfulness has positive association with the behavioral intention to use mobile LBS.

C. Privacy

There is still no unified definition for privacy, but the fact that people are unwilling to disclose their information is one point which numerous definitions have in common. For specific mobile LBS, privacy not only contains personal information such as name, contact, browse frequency, residence time of browsed webs, which are traditional Internet privacy, but the information related to geographical location. On the basis of predecessors' research, we can conclude that privacy is an key factor which influence the attitude and intention to use information technology[6], and LBS users are becoming more privacy sensitive. This paper puts forward following hypotheses:

H9: Privacy has positive association with the attitude to use mobile LBS.

H10: privacy has positive association with the intention to use mobile LBS.

D. Network Externality

Network externality refers to the value of a product or service, and it increases with the scale of users. As mobile Internet has typical network externality itself [7], mobile LBS based on mobile Internet also has significant network externality as well. Similar to the previous scholars, when we proceeded research on network externality's degree of influence, we adopted perceived number of users instead of actual number of users, and we can get the result that the perceived number of users can influence perceived usefulness [8]. As there are more perceived LBS users, there will be more exchange between old and new users on using method and experience, at the same time new users will consider mobile LBS as something useful, which means new users can hold a positive attitude to learn its function. To sum up, we propose the following hypotheses:

H11: Network externality has positive association with perceived usefulness.

H12: Network externality has positive association with the attitude to use mobile LBS.

H13: Network externality has positive association with the intention to use mobile LBS.

Based on the above 13 hypotheses, we can get the model of mobile LBS users' adoption, as is shown in figure 1.

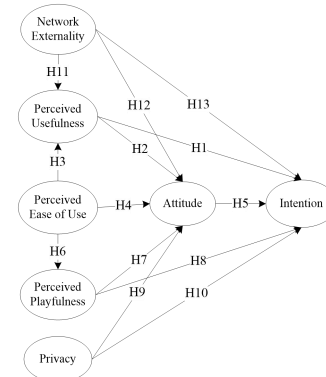


Figure 1. Mobile LBS Users' Adoption Model

III. DATA COLLECTION AND ANALYSIS

A. Definition of Variables

In the model, intention is the dependent variable, while attitude, perceived usefulness, perceived ease of use, perceived playfulness, privacy, and network externality are independent variables. As all the variable measurement items used in this study are derived from the literature that analyzed before, they have been verified through groups of data and methods. Validity can be guaranteed. In this paper, variables are shown in table 1.

TABLE I. DEFINITION AND SOURCE OF VARIABLES

Variables	Definition(Users deem that)	Items	Source
PU	Mobile LBS increases efficiency	3	Reference[4]
PEOU	Mobile LBS is easy to use	3	Reference[4]
ATT	Attitude to use Mobile LBS	2	Reference[4]
BI	Intention to use Mobile LBS	2	Reference[4]
PP	Having fun while using Mobile LBS	3	Reference[6]
PRI	Information that left unexposed	3	Reference[7]
NE	The scale of Mobile LBS users	3	Reference[8]

B. Data Acquisition

We collected research data through questionnaire survey, and 7 levels Likert scale was used to design the questionnaire, and 1 to 7 of each question corresponds to "totally disagree" to "totally agree". At the same time, in order to improve the validity of the questionnaire, we did pre-test to 12 teachers and students who were using mobile LBS or doing researches on mobile LBS, and then we revised questionnaire with the suggestion of them to eliminate the imperfection existed in the questionnaire. Questionnaires were distributed directly to undergraduates and postgraduates who had mobile LBS using experience among Shandong University, Shandong University of Finance and Economics, Shandong Normal University, University of Jinan and so on. 460 questionnaires were distributed and 434 valid

questionnaires were collected, the recovery rate was 94.3%. The age of research objects was ranging from 19 to 28 years old, and the major user group of mobile LBS gave priority to teenagers, so they were totally representative. Meanwhile, in regard to income, research objects whose monthly income were less than 1500 RMB accounted for 96.3% of the whole, fully went in line with the current situation that university students is the low income group.

C. Data Analysis

We carried out reliability analysis with SPSS through Cronbach's Alpha. The Cronbach's Alpha value of perceived usefulness, perceived ease of use, perceived playfulness, privacy, network externality, attitude, intention are separately 0.820, 0.731, 0.705, 0.763, 0.725, 0.807 and 0.78. (Cronbach's Alpha value greater than 0.7 means that the measured data are of high reliability)

KMO test was proceeded on the intermediate variables and independent variables, and, if KMO value is less than 0.5, the correlation among items is weak, which means they are not suitable for factor analysis. On the contrary, if KMO value is greater than 0.5 and close to 1, the items has strong correlation, and they are suitable for factor analysis [9]. Bartlett test of Sphericity on intermediate variables and independent variables can tell whether the correlation coefficients are different and positive. If the results are significant, the correlation coefficients can provide extraction factor for factor analysis. The results of KMO test and Sphericity test are shown in table 2.

D. Model Analysis

The hypotheses of the paths in the model were verified in LISERL with sample data, then we found that 10 of the 13 hypotheses were supported. The results are shown in figure 2.

TABLE II. KMO and Bartlett Test of Sphericity

Variables	KMO	Bartlett test of Sphericity		
		Chi-Square	DO F	Sig.
PU	0.740	230.435	3	0.000***
PEOU	0.711	55.568	3	0.000***
ATT	0.763	156.094	1	0.000***
BI	0.722	147.938	1	0.000***
PP	0.738	125.423	3	0.000***
PRI	0.606	149.698	3	0.000***
NE	0.588	230.011	3	0.000***

\*\*\* means difference is significant on the premise that significance level is 0.001.

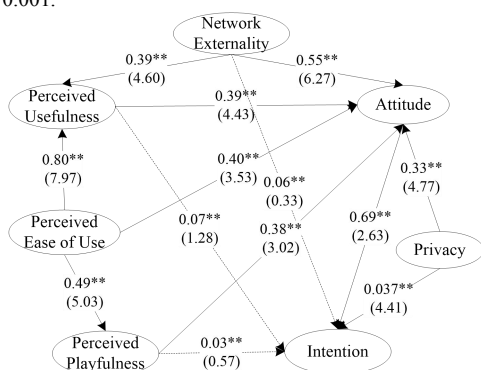


Figure 2. Result of Structural Equation Model Analysis

The fit indices of SEM after calculation through LISERL are as follows: Chi-Square is 376.88, DF (Degree of Freedom) is 153, P-Value is 0, RMSEA is 0.089, GFI is 0.77, AGFI is 0.82, CFI is 0.90, and NNFI is 0.88. The result shown above indicates that this model has good degree of fitting and is acceptable.

IV. DISCUSSION OF RESULTS

According to the analysis of the statistical results, the paper proposes the following results.

(1) Perceived usefulness and perceived playfulness of Mobile LBS are significantly influenced by perceived ease of use. If the users feel not easy in the use of mobile LBS, they may also deem that it is not useful, and then also feel boring, which will eventually lead to the fact that the users give up using.

(2) The attitude of using mobile LBS is significantly influenced by perceived playfulness. If the users feel that mobile LBS has entertainment function, they will have a strong positive attitude such as gratification, pleasure, and even excitement to it, and eventually promote the use of mobile LBS.

(3) The attitude and intention of using mobile LBS is significantly affected by privacy. If the users' privacy is properly protected, they will tend to continue using mobile LBS, and don't have to worry about exposure of their privacy.

(4) Perceived usefulness and attitude of using mobile LBS are strongly influenced by network externality, while perceived ease of use is not. Generally mobile LBS has social function, with the increase of mobile LBS users, the network effect of LBS will play a more important role, like new users want to use mobile LBS to pay attention to their friends or acquaintances. The increase of users makes mobile LBS more attractive, and it is more likely to be accepted by new users.

V. CONCLUSION

In this paper, after considering influence factors such as perceived playfulness, privacy and network externality, we conclude mobile LBS users' acceptance model through adjusting and expanding TAM, and we carry out empirical test for the model. The model has referential meaning to the further study of factors affecting users using mobile LBS. The user acceptance model is vital to mobile LBS developer and operators, it can help them with the quantitative analysis of the influencing factors of user behavior. At the same time, the service provider will focus on mobile LBS perceived playfulness, as well as the protection of user privacy and overall network externality of business, and then promote a better development of mobile LBS.

Although the results of this paper put forward a lot of meaningful suggestions on the factors which influence the use of mobile LBS, some deficiencies still exist, such as the concentration of places to distribute questionnaires and fewer measurement indicators of some factors. Future research will focus on the following two aspects: first, strengthen the optimization and control of the whole

investigation process; second, we need to research the other potential factors affecting the usage of mobile LBS, and introduce them to the model.

#### ACKNOWLEDGMENT

This research was funded by: National Natural Science Foundation of China (No.71373144), and Humanity & Social Science Fund of Ministry of Education (No. 12YJA860010).

#### REFERENCES

- [1] HaiYan Li, Yan Zhang. "Mobile Positioning Technology and Its Application in Mobile Communication Network," *Designing Techniques of Posts and Telecommunications*, Vol. 8, pp. 36-40, August 2006.
- [2] <http://www.199it.com/archives/62230.html>, August 2012.
- [3] Mokbel M F, Chow C Y and Aref W G. "The new Casper: query processing for location services without compromising privacy," *VLDB Endowment*, pp. 763-774, August 2006 [Proceedings of the 32nd international conference on Very large data bases]
- [4] Davis F D. "Perceived usefulness, perceived ease of use, and user acceptance of information technology," *MIS quarterly*, pp. 319-340, 1989.
- [5] Davis F D, Bagozzi R, Warshaw P. "User Acceptance of Computer Technology: A Comparison of two Theoretical Models," *Management Science*, Vol. 35, pp. 982-1003, 1989.
- [6] Tan M, Teo T S H. "Factors Influencing the Adoption of Internet Banking," *Journal of Association for Information System*, Vol. 1, pp. 21-44, 2000.
- [7] Kau F R J, Mcandrew S J, Wang Y M. "Opening the black box of Network Externalities in Network Adoption," *Information Systems Research*, Vol. 11, pp. 61-82, March 2000.
- [8] Wang Chih-Chien, Hsu Ya-Hui, Fang Wen-Chang. "Acceptance of Technology with Network Externalities: An Empirical Study of Internet Instant Messaging Services," *Journal of Information Technology Theory and Application*, Vol. 6, pp. 15-28, 2004.
- [9] Kaiser H F. "An Index of Factorial Simplicity," *Psychometrika*, Vol. 36, pp. 31-36, 1974.
- [10] May A, Bayer S H and Ross T. "A survey of 'young social' and 'professional' users of location-based services in the UK," *Journal of location based services*, Vol. 2, pp. 112-132, January 2007.
- [11] ErLing Zhou. "An Empirical Research on Motivation and Behavior of Mobile LBS Users Based on the Network Effect," *Beijing University of Posts and Telecommunications*, 2012.
- [12] "Data Analysis of University Students' Smart Phone Usage," <http://wenku.baidu.com/view/799819220722192e4536f690.html>, November 2012.
- [13] <http://www.199it.com/archives/24091.html>, May 2012.
- [14] Hongwei Liu, Peng Zhang and Jun Liu. "Public Data Integrity Verification for Secure Cloud Storage," *Journal of Networks*, Vol. 8, pp. 365-372, April 2013.
- [15] Dongbo Liu, Peng Xiao. "User-oriented Mobile Filesystem Middleware for Mobile Cloud Systems," *Journal of Computers*, Vol. 8, pp. 2209-2216, September 2013.
- [16] Weiwei Zhang, Yongyu Chang, Yitong Liu and Leilei Xiao. "A New Method of Objective Speech Quality Assessment in Communication System," *Journal of Multimedia*, Vol. 8, pp. 291-298, March 2013.

**Zhaoyu An** Male, postgraduate student from Shandong University of Finance and Economics, school of management science and engineering. Mainly do research on SNS users' behavior and privacy protection, management information system. Participate in National Natural Science Foundation of China since July, 2013, have published several papers majored in SNS users' sense of belonging, SNS users' privacy concern.

**Luchuan Liu** Male, Doctor's Degree, professor from School of Management Science and Engineering, Shandong University of Finance and Economics, Jinan, China. Supervisor of Graduate Students. Mainly responsible for two funds: National Natural Science Foundation of China (No.71373144), and Humanity & Social Science Fund of Ministry of Education (No. 12YJA860010).

# Flow Field Simulation and Structural Optimization of Air Baffle in the Passive Containment Cooling System

Chunlai Tian; Shan Zhou; Liyong Han

State Nuclear Power Technology Corporation Research & Development Center, Beijing, China

**Abstract**—Air baffle is a component in the passive containment cooling system. It is set in the annulus area and used to provide a pathway for natural circulation of cooling air outside the containment vessel. In order to optimize its design with lower pressure loss, the flow field model around the baffle is built in this paper. The problem is defined as a two dimensional steady incompressible problem and solved through computational fluid dynamics solver. The results demonstrate the inlet air flows at higher pressure than the outlet. The minimum pressure loss is 9.86 Pa. Lower pressure area appears near back of inclined plate. Inclined angle and width ratio are considered as key parameters following with discussions of affects on the pressure loss. As inclined angle increases, pressure loss increases, but the maximum velocity decreases. We chose optimization with the inclined angle 120 degree and the width ratio 0.550.

**Index Terms**—air baffle, flow field, structural optimization, passive containment cooling system, CFD

## I. INTRODUCTION

The AP series (AP-600 and AP-1000) pressurized water reactors are the advanced design with the third generation feature in the Westhouse nuclear power plant technology [1]. It applies a passive containment cooling system to remove heat released inside the containment vessel following postulated design basis accident [2-13]. During the accident, the interior of the steel containment vessel released lots of heat. Due to the evaporation of continuously flowing thin liquid film on the outside surface of the vessel, the containment wall temperature will decrease. Consequently, the inner pressure of the containment vessel is lowered as the same as temperature. The liquid film outside the vessel wall is formed by applying water at the containment dome from the water tank. There is an annular space or channel between the outside of the containment shell wall and the inside of a baffle suspended from the shield building wall. A schematic sketch of the AP series passive containment cooling system is shown in Figure. 1.

Moreover evaporation of the falling liquid film is enhanced by buoyancy driven flows in the annular space channel [6-9]. The air baffle of the passive containment cooling system is set in the upper annulus area as shown in Figure. 1. It is attached to the cylindrical section of the containment vessel. The function of the baffle is to provide a pathway for natural circulation of cooling air. The cooler air with higher density is drawn into the shield

building through the cooling air inlet at the top cylindrical portion of the shield building. The heat is transferred from the outer surface of the containment vessel to the air between the baffle and the containment shell [2-5]. This heated air with lower density flows up through the air baffle. It is discharged out from the air discharge port. It gives an enhanced heat transfer method to remove the heat from the containment vessel. The air baffle area in big scale is also shown in Figure. 1.

According with the basic function of the air baffle, the pressure loss of the pathway is important overall performance. The less loss of flow pressure could gives better buoyancy driven flow with enhanced heat remove [5, 12]. The structural design of the air baffle contributes the air flow cross pathway. As shown in Figure. 1, the air baffle plate is inclined with an inclined angle. In order to optimize the air baffle design, the flow field of the pathway is analyzed through the computational fluid dynamics method. The flow field model will be built and solved to obtain the pressure in this paper. Using this model, we can realize the flow characteristic around the air baffle. The affects of the structural parameters, such as the inclined angle, the inlet and outlet channel width ratio, will be discussed to utilize the structural optimization.

## II. MODELLING

### A. Mathematical mode

The simple steady incompressible Navier-Stokes equations are used to describe this two dimensions computational fluid dynamics (CFD) flow problem [14]. The governing equations include the mass continuity equation and the momentum equations. They are

$$\frac{\partial u}{\partial x} + \frac{\partial v}{\partial y} = 0, \quad (1)$$

$$\rho \left( u \frac{\partial u}{\partial x} + v \frac{\partial u}{\partial y} \right) = F_x - \frac{\partial p}{\partial x} + \mu \left( \frac{\partial^2 u}{\partial x^2} + \frac{\partial^2 u}{\partial y^2} \right), \quad (2)$$

$$\rho \left( u \frac{\partial v}{\partial x} + v \frac{\partial v}{\partial y} \right) = F_y - \frac{\partial p}{\partial y} + \mu \left( \frac{\partial^2 v}{\partial x^2} + \frac{\partial^2 v}{\partial y^2} \right), \quad (3)$$

where  $u$  is the velocity on  $x$  direction and  $v$  is the velocity on  $y$  direction,  $F_x$  is the force on  $x$  direction and  $F_y$  is the force on  $y$  direction,  $\rho$  is the density,  $p$  is the pressure,  $\mu$  is the kinematic viscosity.

The standard  $k-\varepsilon$  turbulent numerical model has been implemented for the investigated flow conditions. The model is

$$\rho \frac{\partial k}{\partial t} + \rho u_i \frac{\partial k}{\partial x_i} = \frac{\partial}{\partial x_j} \left[ \left( u + \frac{u_i}{\sigma_k} \right) \frac{\partial k}{\partial x_j} \right] + G - \rho \varepsilon, \quad (4)$$

$$\rho \frac{\partial \varepsilon}{\partial t} + \rho u_i \frac{\partial \varepsilon}{\partial x_i} = \frac{\partial}{\partial x_j} \left[ \left( u + \frac{u_i}{\sigma_\varepsilon} \right) \frac{\partial \varepsilon}{\partial x_j} \right] + c_1 \frac{\varepsilon}{k} G - c_2 \rho \frac{\varepsilon^2}{k}, \quad (5)$$

where  $\sigma_k$  and  $\sigma_\varepsilon$  are the turbulent Prandtl numbers of the  $k$  equation and  $\varepsilon$  equation,  $c_1$  and  $c_2$  are constant values and  $G$  is described as

$$G = \frac{\partial u_i}{\partial x_j} \left( \frac{\partial u_i}{\partial x_j} + \frac{\partial u_j}{\partial x_i} \right). \quad (6)$$

The above equations describe this problem. Finally, they will be solved to obtain the pressure fields through the semi-implicit method for pressure-linked equations.

**B. CFD mesh model**

The air flow field with the air baffle model is built. The air flows across the channel from inlet to outlet. The baffle plates and the domain sides are considered as wall. The air flow channel domain is established for the solution. The CFD simulation is performed in this domain. As shown in Figure. 2 (A), the model is built by the quadrilateral meshes with 8045 elements. The mesh near the baffle is refined with a growth ratio at 1.5.

**C. Boundary conditions**

According with the problem definition and modelling with configuration, boundary conditions are required with the inlet, the outlet and the wall conditions. The air velocity is set with constant values for the inlet condition. Wall boundary conditions with non-slip parameters are selected for the baffle surfaces and inclined plate. The pressure outlet boundary condition is selected for outlet.

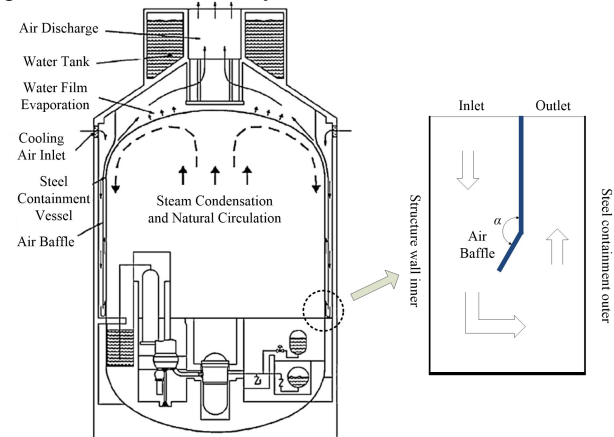


Figure 1. Passive containment cooling system and air baffle configuration [1-3]

**III. SOLVER**

The two dimensions incompressible flow problem is solved through the open source CFD solver software package OpenFOAM [15, 16]. Its steady-state solver ‘simpleFoam’ is used with the SIMPLE algorithm for turbulent flow. The solver parameters are configured by

‘fvSolution’ file, ‘fvSchemes’ file and ‘controlDict’ file in case system folder. The ‘relaxationFactors’ are defined in the ‘fvSolution’ file. The initial conditions with parameters definitions are stored in time 0 folder. The open source post-processing software ParaView is used for the results plotting [17].

**IV. RESULTS**

The problems with eight cases have been solved and the pressure results of the flow field are shown in Figure. 2 (B) to Figure. 2 (I). From the results, we can get a global view of the flow field. As shown with the pressure results, the air flows into from the inlet side domain at higher pressure than the outer side domain. There is pressure loss in the across domain near the baffle. The minimum pressure appears near the back of the baffle in each case. According with the different boundary conditions, the lower pressure area is significantly different. In all cases, the minimum pressure loss is 9.86 Pa. The more details will be discussed with followings.

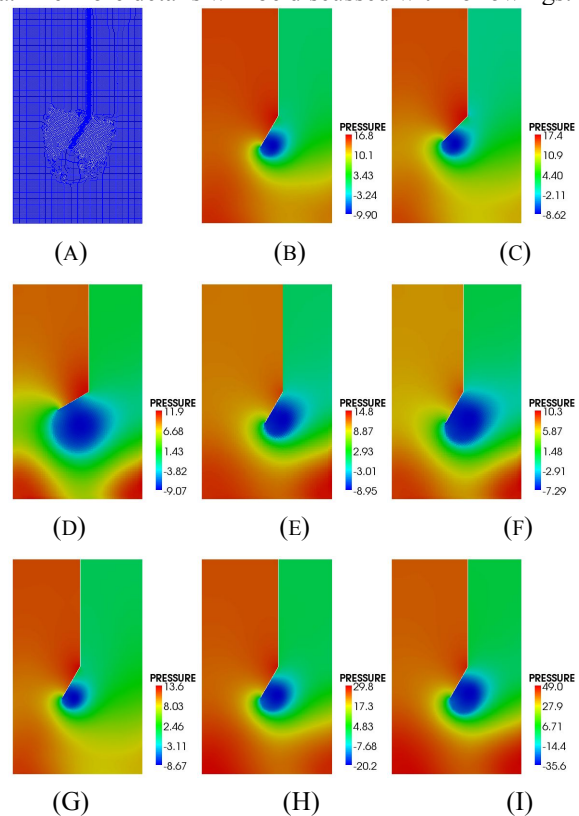


Figure 2. CFD mesh model and pressure field results

**V. DISCUSSIONS**

With aims of the design optimization, the affects of the structural parameters are discussed. These parameters include the inclined angle, the width ratio and the inlet wind velocity. The affects on the pressure loss and maximum velocity by the inclined angle are shown in Figure. 3. As shown in Figure. 3 (A), the pressure loss increases as the inclined angle increases. However the maximum velocity decreases as the inclined angle

increases as shown in Figure. 3 (B). The maximum pressure loss is 17.2 Pa. The minimum of the flow maximum velocity is 3.12 m/s under the inclined angle at 135 degree.

The affects on the pressure loss and maximum velocity by the width ratio are shown in Figure. 4. From Figure. 4 (A), the pressure loss is observed to fluctuate with increase of the width ratio. The maximum velocity trend is also similar to that of the pressure loss in Figure. 4 (B). The maximum pressure loss is 16.7 Pa on the width ratio 0.585. The maximum one of the maximum velocity is 4.82 m/s on the width ratio 0.625.

The affects on the pressure loss and maximum velocity by the inlet wind velocity are shown in Figure. 5. As shown in Figure. 5 (A) and Figure. 5 (B), the pressure loss increases similarly with the maximum velocity as the inlet wind velocity increases. The maximum pressure loss is 48.5 Pa. The maximum one of the maximum velocity is 7.92 m/s on the inlet wind velocity 4.00 m/s.

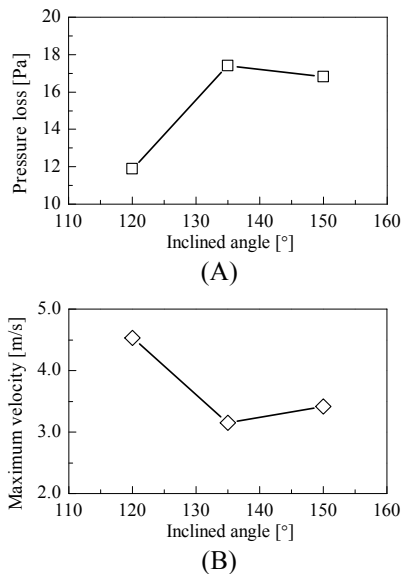


Figure 3. Inclined angle affects

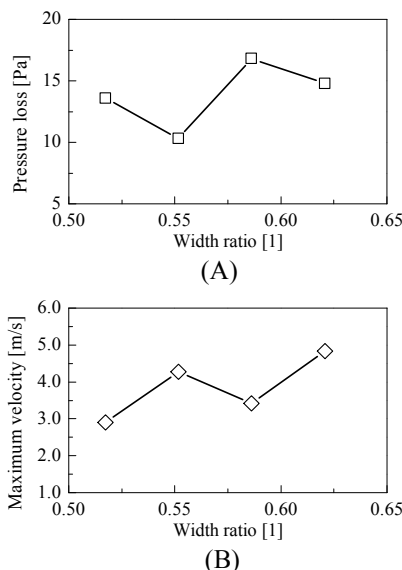


Figure 4. Width ratio affects

In order to optimise the structural design of the air baffle, the pressure loss and maximum velocity are considered as mainly optimization objective parameters. From the above discussions, we see the effects on the pressure loss and maximum velocity by the inclined angle, the width ratio and the inlet wind velocity. In this study, the inclined angle is chosen as optimization results with 120 degree and the width ratio is 0.550. For the investigation on details about more deeply research on the baffle optimization, more work will be done on transient CFD model with heat transfer in the future.

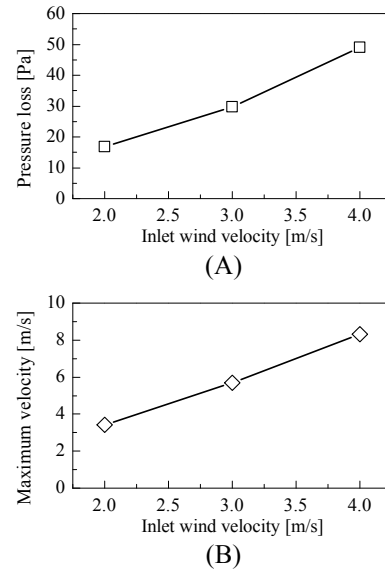


Figure 5. Inlet wind velocity affects

## VI. CONCLUSIONS

The computational fluid dynamics model of the flow field around the air baffle is established for the structural optimization analysis. The model is solved by open source software OpenFOAM. The pressure field results are obtained in different cases. There is a significant pressure loss while the air flows along the pathway around the air baffle. In all cases, the minimum pressure loss is 9.86 Pa. The lower pressure appears after the across domain in each case. The lowest pressure appears near the back of the baffle inclined plate.

In order to decrease the pressure loss from the baffle structural efforts, the affects by the inclined angle, the width ratio and the inlet wind velocity are discussed. While the inclined angle increases, the pressure loss increases. However the maximum velocity decreases as the inclined angle increases. The pressure loss fluctuates with increase of the width ratio and the maximum velocity trend is also similar to that of the pressure loss. Finally, the design parameters of the inclined angle and the width ratio are chosen as the structural optimization. This paper supports an optimization method through computational fluid dynamics simulation research on the flow field. It could be helpful for the air baffle design in the passive containment cooling system. The results could be used in the further research on the computational simulation for the passive containment cooling system.

## ACKNOWLEDGMENT

This work is supported by Staff Independent Innovation Fund of SNPTC (State Nuclear Power Technology Company, China) with Grant No. SNP-KJ-CX-2013-10 and National Science and Technology Major Project of the Ministry of Science and Technology of China with Grant No. 2011ZX06002-005.

## REFERENCES

- [1] Westinghouse Ltd. "AP1000 Design Control Document", Version 18, 2010.
- [2] X. W. Jiang, E. Studer and S. Kudriakov, "A simplified model of Passive Containment Cooling System in a CFD code," *Nuclear Engineering and Design*, vol. 262, pp. 579-588, 2013.
- [3] W. T. Sha, T. H. Chien, J. G. Sun, and B. T. Chao, "Analysis of large scale tests for AP-600 passive containment cooling system.," *Nuclear Engineering and Design*, vol. 16, pp. 197-216, 2004.
- [4] P. Broxtermann and H. J. Allelein, "Simulation of AP1000's passive containment cooling with the German Containment Code System COCOSYS," *Nuclear Engineering and Design*, vol. 261, pp. 326-32, 2013.
- [5] R. Viskanta and A. A. Mohamad, "Countercurrent natural circulation in an open, U-shaped thermosyphon," in *Proceedings of the ASME Winter Conference*, New Orleans, LA, USA: ASME, 1993, pp. 1-10.
- [6] Y. Kataoka, M. Murase, T. Fujii, and K. Tominaga, "Thermal hydraulics of an external water wall type passive containment cooling system," *Nuclear Technology*, vol. 111, pp. 241-50, 1995.
- [7] M. Aritomi, H. Kikura and M. Kawakubo, "Cooling characteristics of passive containment cooling system with vertical tube," *Bulletin of the Research Laboratory for Nuclear Reactors*, vol. 31, p. 15, 2007.
- [8] Y. Wang, "Analysis model for the passive containment cooling system," *Journal of Convergence Information Technology*, vol. 7, pp. 75-83, 2012.
- [9] M. Kawakubo, N. Inaba, H. Kikura, M. Aritomi, and T. Yamauchi, "Fundamental research on the cooling characteristic of Passive Containment Cooling System," *Proceedings of the International Conference on Nuclear Engineering*, Arlington, VA, USA: ASME, 2004, pp. 747-752.
- [10] X. Cheng, F. J. Erbacher and H. J. Neitzel, "Convection and radiation heat transfer in a passive containment cooling system," *Proceedings of the International Conference on Nuclear Engineering*, Nice, Fr: ASME, 1997, p. 36-40.
- [11] J. Yu and B. Jia, "PCCSAC: A three-dimensional code for AC600 passive containment cooling system analysis," *Nuclear Science and Engineering*, vol. 142, pp. 230-236, 2002.
- [12] Y. M. Kang and G. C. Park, "An experimental study on evaporative heat transfer coefficient and applications for passive cooling of AP600 steel containment," in *Ninth International Meeting on Nuclear Reactor Thermal Hydraulics*. vol. 204 Netherlands: Elsevier, 2001, pp. 347-59.
- [13] C. Li, H. Fan and R. Zhao, "The outside transport phenomena of the passive containment cooling system," in *ASME 2013 Heat Transfer Summer Conf.* vol. 4 Minneapolis, MN, USA: ASME, 2013, pp. 1-9.
- [14] Anderson J D. *Computational fluid dynamics*. New York: McGraw-Hill, 1995.
- [15] OpenCFD Ltd. *OpenFOAM User Guide documentation*. <http://www.openfoam.org/docs/user/>.
- [16] C. Tian, S. Zhou and L. Han, "Numerical simulation of plume motions for cooling tower in an inland nuclear power plant," *International Proceedings of Chemical, Biological & Environmental Engineering*, vol. 66, pp. 157-161, 2014.
- [17] Kitware Inc. *VTK / ParaView Tutorial and User Guide documentation*. <http://www.paraview.org/>.

**Chunlai Tian** was born in 1985. He is currently a senior researcher at State Nuclear Power Technology Research & Develop Center, State Nuclear Power Technology Ltd., Beijing, China. He received his Ph.D (2012) and B.Sc (2007) in Mechanical Engineering, Beijing Institute of Technology, Beijing, China. His research focuses on the theoretical and experimental research on general thermal engineering, measurement and control system in energy industry, especially in advanced nuclear power plant technology, power generator, internal combustion engine in automobile and measurement technology in energy industry. His research interests include CFD, FEA and others CAE solution, such as heat and mass transfer, multi-phase fluid, structural analysis and control system modeling. He has experience on complex thermal-hydraulic experiment research with measure instrument, control and theoretical analysis. He is investigating on the open source software applying on the CAE solution area. Moreover he has carried out some research on the quality management and control for energy industry engineering.

# Mildew Prediction Model for Warehousing Tobacco Based on QGA-BP

Zhang Lihua<sup>1</sup>; Le Guoqing<sup>2</sup>; Dai Xichang<sup>2</sup>

1.School of Software, East China Jiaotong University,Nanchang,China

2.School of Electrical and Electronic Engineering, East China Jiaotong University ,Nanchang,China

**Abstract**—Tobacco mildew forecasting has been one of the most important issues in the tobacco industry. Three tobacco mildew forecast models, using BP neural network, genetic optimization BP neural network and quantum genetic algorithm(QGA-BP), are proposed in this paper. 70 training samples are selected as training sample,14 prediction samples are used to test the proposed models. The results show that, QGA-BP model has higher prediction precision: the deviation of prediction and actually value is range from -0.00939 to 0.01496, and the absolute value of average relative error is 1.896%. Compared with BP model and GA-BP model , the prediction precision of QGA-BP model are increased by 88.182%, 18.696%. Moreover, QGA-BP model has better model stationarity, and provides an effective means for tobacco mildew forecast.

**Index Terms**—mildew prediction; BP neural network; GA-BP; QGA-BP

## I. INTRODUCTION

Anti-mildew of tobacco has important value on terms of economic and significance. There are many factors lead to tobacco mildew, such as geographical, tobacco types, bacterial category [1], and the tobacco mildew process is nonlinear and uncertainties. Tobacco mildew lies in the degree of prediction tobacco mildew, monitoring the change of tobacco storage environment in time, and build suitable environment for tobacco storage. In recent years, BP neural network has a simple structure and excellent nonlinear predictive capability, which is widely used in predicting[23].But the initial weights and thresholds of BP neural network are randomly selected, and if these parameters were not proper, it will slow the speed of convergence, meanwhile, it's easy to fall into local optimum value. Quantum genetic algorithm is a new genetic algorithm that combined classical genetic algorithm and quantum computing theory .It has a small population size, fast convergence and global optimization ability.In this paper,based on BP neural network tobacco mildew forecast model, genetic algorithm(GA-BP) and quantum genetic algorithm(QGA-BP) are used to avoid falling into local minimum of BP neural network training. To some extent,it optimize the BP neural network predictive performance .Eventually,an optimization BP neural network method based on quantum genetic algorithm(QGA-BP) of tobacco mildew forecasting model is proposed,and analysis of this model.GA-BP tobacco mildew forecast model and QGA-BP tobacco mildew forecast model are established.

## II. BP NEURAL NETWORKS TOBACCO MILDEW MODEL

Since the temperature and humidity of the storage environment directly influence tobacco mildew<sup>[4]</sup>, the water content of the tobacco directly related to the time and developing speed of the tobacco mildew<sup>[5]</sup>.Therefore, selecting temperature, humidity, and tobacco moisture as the input layer parameters of the BP neural network, that is, the number of nodes of the input layer is three. As the definition of mildew degrees<sup>[6]</sup>, that is after one cycle (30 days) in the case of a certain temperature, humidity and moisture, the proportion of mildew rate in total surface area of the tobacco mildew distribution ,so select the mildew degrees of the tobacco as the output layer parameter, the nodes of the output layer is one. Meanwhile, giving the mildew degree as following criteria: if moldy rate range from 0 to 0.01], then there is no mildew; if moldy rates range from 0.01 to 0.1, then mildew degree is slight ; if moldy rate in the range of (0.1, 0.2], then the moldy degrees of moderate mildew; if the moldy rate in the range from 0.2 to 1, it is severe mildew degrees. Therefore, BP neural network structure for the 3-x-1, as shown in Figure 1.

For training and testing has been established BP neural network model<sup>[7]</sup>, from the actual monitoring data collected from April 2004 to April 2011, 84 samples model, that is, monthly storage as a sample. These models are divided into two parts: the part of the 70 groups of training samples, another part of the group of 14 test samples. Variable is then laid one of the formula to the interval [0,1], a normalized as

$$R = \frac{x - X_{\min}}{X_{\max} - X_{\min}} \quad (1)$$

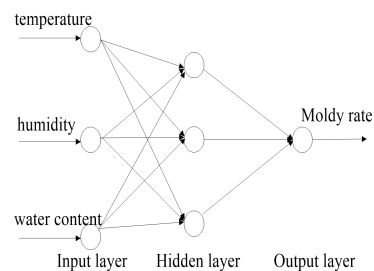


Figure 1. mildew forecasting model based on BP neural network of tobacco

Then,using BP neural network of MATLAB toolbox and standard BP neural network algorithm to train BP neural network .After simulation contrast, the network structure selected for 3-7-1.The set target error is

0.001, the maximum number of iterations to 1000. Select hidden layer neurons of the transfer function for S tangent function tansig, the transfer function of the output layer neurons selected type S logarithmic function logsig, select traingdx function for the training function.

By trained tobacco mildew prediction model of BP neural network, which is simulated in MATLAB7.0 software platform, obtained deviation of the predicted value and the actual value curve in Figure 2. The average absolute relative error is 16.044% and the prediction accuracy is 83.956%. Since the BP neural network based on gradient descent method, no global search ability, the training of paralyzed, slow network convergence and other shortcomings. As the weights and threshold of BP network training is given at random, the results is a certain randomness. To improve the prediction accuracy, it is necessary to optimize the BP neural network.

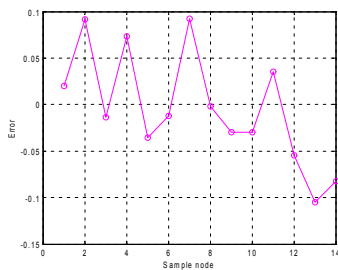


Figure 2. deviation of the predicted value and the actual value

### III. OPTIMIZE BP NEURAL NETWORK BY GENETIC ALGORITHM(GA-BP) TOBACCO MILDEW FORECAST MODEL

The purpose of the GA-BP model optimized is using global search of genetic algorithm<sup>[89]</sup> to overcome the defects of BP neural network gradient descent method. By calculating the fitness and genetic error norm, the neural network weights and threshold continuous adjustments. the error of the connection weights of the input layer and the hidden layer and the hidden layer and output layer by calculating ,and then obtain the best weights . Figure 3 is a flowchart of GA-BP.

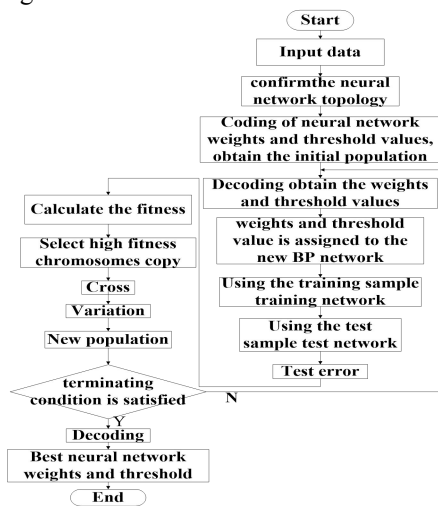


Figure 3. A Flowchart of GA-BP

In order to reduce the predictive value and the expected value when GA-BP model in predicting, we selected prediction samples of the predictive value and the

expected value of the norm of the error matrix as the output of the objective function. The fitness function adopts the sort of fitness distribution function.

$$f(x) = ranking(obj) \tag{2}$$

$$obj = \sum_{i=1}^l e(i)^2, e(i) = y(i) - y_m(i) \tag{3}$$

In the formula,  $obj$  is the objective function of the output,  $y(i)$  is the predicted value,  $y_m(i)$  is the expected value,  $e(i)$  are the error.

The population size of the GA-BP model is 40, the Maximum genetic algebra is 100, the number of binary bits of the variable is 10, the crossover probability is 0.7, the mutation probability is 0.01, the gap of generations are 0.95. BP neural network structure selected for 3-7-1, the set target error is 0.001, and the maximum number of cycles for 1000. we selected the transfer function of the hidden layer neurons is S-type tangent function tansig, and the transfer function of the output layer neurons is S-type logarithmic function logsig, and the function of trainlm for training function.

### IV. USING THE QUANTUM GENETIC ALGORITHM TO OPTIMIZE THE BP NEURAL NETWORK (QGA - BP) OF THE TOBACCO MILDEW PREDICTION MODEL

The Quantum genetic algorithm<sup>[10]</sup> is the product of the combination of quantum computation with genetic algorithms. Quantum genetic algorithm is to establish the basis of quantum state vector represented, representing the probability amplitude of quantum bits used in the encoding of the chromosome, such that a chromosome can express multiple superposition and quantum logic gates chromosome update operation, in order to achieve the target optimization solution.

The QGA - BP's <sup>[11]</sup>basic idea is: first, make the layers of BP network connection coefficient cascaded together to form quantum chromosome, and with the BP neural network output error norm minimum for target function, through the measurement, calculation fitness value, according to quantum revolving door to find the best value, if meet the requirements set algebra, the largest selected fitness value corresponding to the best weights and threshold value, then turned to the neural network BP algorithm, and then to carry on the forecast, to find the optimal solution. Quantum genetic algorithm ensures the hybrid algorithm is globally convergent, overcome the gradient descent method to the dependence of the initial weights and local convergence properties, and based on the gradient descent method of BP algorithm effectively avoid the quantum genetic algorithm the randomness and probabilistic problem. Figure 4 is QGA - BP algorithm flow chart.

In the QGA - BP model, quantum coding using paper [12] coding mode and quantum revolving door by paper [13] adjustment strategy. Adapted to the function choice, this article will predict the predicted sample expectations error matrix norm as the output of the objective function. Fitness function is the objective function of the opposite

number. So the greater the value of the objective function, the greater its fitness value.

$$f(x) = \max(obj) \tag{4}$$

$$obj = \sum_{i=1}^l e(i)^2, e(i) = y(i) - y_m(i) \tag{5}$$

In the formula,  $obj$  is the objective function of the output,  $y(i)$  is the predicted value,  $y_m(i)$  is the expected val The population size of the QGA-BP model is 40, the Maximum genetic algebra is 100, the number of binary bits of the variable is 10, the crossover probability is 0.7, the mutation probability is 0.01, the gap of generations are 0.95. BP neural network structure selected for 3-7-1, the set target error is 0.001, and the maximum number of cycles for 1000. we selected the transfer function of the hidden layer neurons is S-type tangent function tansig, and the transfer function of the output layer neurons is S-type logarithmic function logsig, and the function of trainlm for training function .ue,  $e(i)$  are the error.

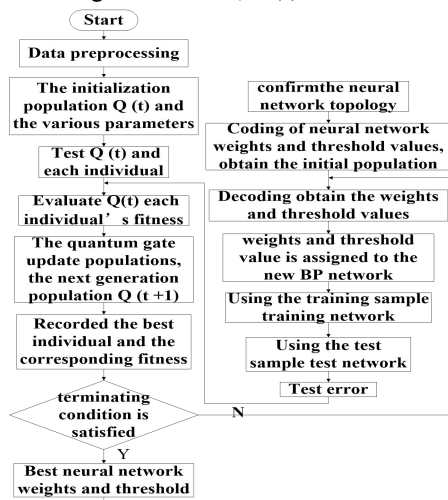


Figure 4. QGA - BP algorithm flow chart.

V. SIMULATION AND RESULTS ANALYSIS

In the Core i3 and 2G memory computer, use MATLAB7.0 software platform simulation training. Respectively with the BP neural network, GA - BP, QGA - BP on tobacco mildew respectively of prediction. First with 70 groups of samples to train the network, and then use the 14 sets of test sample to network model tests, and compared with the actual values, as shown in figure 5 shows. Figure 6 is a curve of error, the reaction of the deviation of each of the prediction value and the expected position. Figure 7 for GA - BP, QGA - BP error norm change curve, the error norm is smaller, the corresponding weights and threshold value are better. Form Table 1, it is known that the BP neural network model of the forecast value and the actual value deviation in [0.10478, 0.09216] between, the average relative error of the absolute value is 16.044%, GA - BP model predictive value and the actual value deviation in [0.01655, 0.01577] between, the average relative error of the absolute value is 2.332%, QGA - BP model predictive

value and the actual value deviation in [0.00939, 0.01496] between, the average relative error of the absolute value is 1.896%, then BP model, GA - BP model were increased by 88.182%, 18.696%, and the model of stability enhancements, provides an effective means for the tobacco mildew forecast. Form Table 2, it is known that QGA - BP model prediction error can be controlled within 2%, to meet the demand for engineering applications.

VI. CONCLUSION

According to the demand of tobacco mildew nonlinear prediction, the paper constructs the BP neural network prediction model. Due to the defects of BP neural network, in order to improve the prediction accuracy of tobacco mildew, and puts forward the tobacco mildew QGA - BP prediction model, the structure of the BP neural network for the 3-7-1, the network input for temperature humidity and their moisture content, the output for mildew rate. After the experimental results accuracy test, the model has better prediction effect. The final model based on embedded ARM + Linux + Web a tobacco warehouse intelligent monitoring system can be realized, and achieved good application effect, show that based on the QGA - BP tobacco mildew prediction model is of certain value for engineering application.

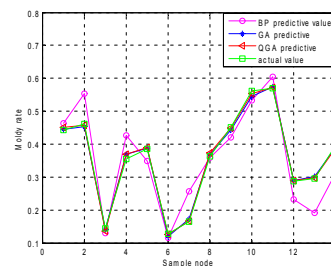


Figure 5. predictive value and the actual value curve

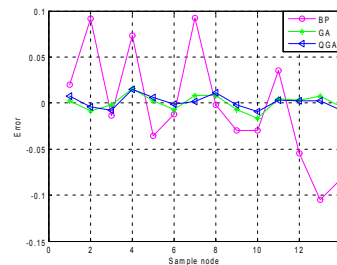


Figure 6. error curve

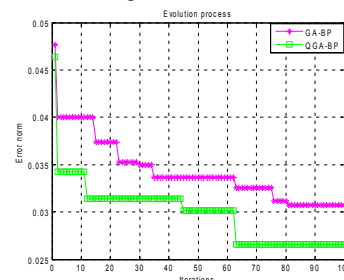


Figure 7. error norm curve

TABLE II. PREDICTIVE VALUE AND RELATIVE ERROR

Model	recision(100%)	average absolute relative error(100%)
BP model	83.956	16.044
GA-BP model	97.668	2.332
QGA-BP model	98.104	1.896

ACKNOWLEDGMENT

The author would like to thanks for the financial support by scientific research project fund of Jiangxi province(GJJ14371) and the aids from East China JiaoTong University. The authors would like to thanks the anonymous reviewers for their valuable comments and suggestions.

REFERENCES

[1] Kong Fan-yu, Lin Jian-sheng. Recent progress in research on mechanism and control of tobacco mildew during storage[J].Acta Tabacaria Sinica, 2009, 5(15): 78-81.  
 [2] Liu Hou-lin, Wu Xian-fang. Power predictcion for centrifugal pumps at shut off condition based on BP neural network[J].Transactions of the Chinese Society of Agricultural Engineering, 2012, 28(11): 45-49.  
 [3] Ren Guang-wei Wang Feng-long Gao Han-jie Wang Yong.Applying BP neural network to predict tobacco virus diseases transmitted by aphids[J]. Acta Tabacaria Sinica, 2004, 10(4): 23-26.  
 [4] Liu Qiang,Zhu Lie-shu.Influences of Different Temperatures and Humidities on Main Chemical Compositions of Tobacco Strips during Natural Alcoholization Process[J]. Hunan Agricultural Sciences, 2012, 1(15): 99-102.  
 [5] Zhang Cheng-sheng,Wang Hai-bin,Li Geng-xin,Sun Huili.Mildew Factor Analysis of Stored Flue-cured Tobacco Strips[J]. Acta Tabacaria Sinica, 2011, 32(3): 80-83.  
 [6] X.Wang, M.Zhang, etc.Spectral prediction of Phytophthora infestans infection on tomatoes using artificial neural

network(ANN)[J]. International Journal of Remote Sensing, 2008(2): 87-92.  
 [7] Zhang Lihua, Ma Junzhao, Le Guoqing, Mildew Prediction of Warehousing Tobacco Based on BP Neural Network. Journal of China Jiaotong University, 2013(03): p. 71-75.  
 [8] LI Song, LIU Li-jun, XIE Yong-le, Chaotic prediction for short-term traffic flow of optimized BP neural network based on genetic algorithm. Control and Decision,, 2011. 26(10): p. 1581-1585.  
 [9] Chen L H, Mei Y D, Dong Y J, et al . Improved genetic algorithm and its application in optimal dispatch of cascade reservoirs[J] . Journal of Hydraulic Engineering, 2008, 39(5): 550-556.  
 [10] G. X. Zhang, N. Li and W. D. Jin, "A Novel Quantum Genetic Algorithm and Its Application," Chinese Journal of Electronics, vol.32, pp. 476-479, March 2004.  
 [11] Yuli,Wangjiaquan,ApplicationResearchonComplexWaterQuality Prediction withImprovedQGA-BPMoel. Pattern Recognition and Artificial Intelligence, 2012. 25(4): p. 705-708.  
 [12] Yang Jun-an ,Zhuang Zhen-quan.Actuality of Research on Quantum Genetic Algorithm[J].Computer Science, 2003(11): 13-15,43  
 [13] Yang Shu-yuan ,Liu Fang,Jiao Li-cheng.The Quantum Evolutionary Strategies[J].Acta Electronica Sinica, 2001(12): 1874-1875

**Zhang Lihua** received the BS degree in Electrical Engineering from the East China Jiaotong University ,Nanchang, China in 1994,and the MS degrees from the school of Electrical and Electronic Engineering, East China Jiaotong University ,Nanchang, China in 2003.He received the PhD degree from the Beijing University of Aeronautics and Astronautics,Beijing,China in 2011. He is currently an postdoctoral researcher in the School of Electronic Information and Electrical Engineering at Shanghai Jiaotong University, Shanghai, china, and also an associate professor in the School of Software at East China Jiaotong University, Nanchang, China. His current research interests include information security, security protocol design in wireless mesh networks and wireless sensor networks. identity authentication and mobile communication. He is a member of the IEEE and ACM.

TABLE III. COMPARISON OF DIFFERENT MODELS

Number	Temperature	Humidity	Itself Water content	The actual value	BP Predictive value	GA-BP Predictive value	QGA-BP Predictive value	BP relative error	GA-BP relative error	QGA-BP relative error
1	0.5852	0.4182	0.3889	0.4424	0.4625	0.4448	0.4502	4.5547%	0.547%	1.761%
2	0.6370	0.5636	0.2778	0.4616	0.5533	0.4531	0.4572	19.859%	-1.843%	-0.942%
3	0.6815	0.1273	0.0556	0.1442	0.1306	0.1424	0.1366	-9.424%	-1.214%	-5.277%
4	0.4926	0.1455	0.5444	0.3539	0.4274	0.3697	0.3688	20.774%	4.456%	4.222%
5	0.4667	0.2727	0.5222	0.3846	0.3490	0.3868	0.3905	-9.246%	0.585%	1.526%
6	0.4481	0.1455	0.0182	0.1272	0.1153	0.1201	0.1257	-9.339%	-5.582%	-1.179%
7	0.4926	0.2222	0.3556	0.1644	0.2566	0.1727	0.1661	56.058%	5.073%	1.046%
8	0.5296	0.3818	0.3778	0.3620	0.3598	0.3700	0.3734	0.616%	2.196%	3.149%
9	0.5370	0.4545	0.4222	0.4502	0.4204	0.4433	0.4484	-6.615%	-1.539%	-0.391%
10	0.5444	0.4727	0.5333	0.5622	0.5326	0.5457	0.5528	-5.258%	-2.944%	-1.67%
11	0.5593	0.6364	0.4889	0.5689	0.6041	0.5738	0.5719	7.458%	2.056%	1.727%
12	0.5630	0.6545	0.1222	0.2869	0.2322	0.289	0.2891	-19.06%	1.042%	0.756%
13	0.5704	0.7636	0.0889	0.2952	0.1904	0.3024	0.2978	-35.49%	2.446%	0.877%
14	0.5667	0.7091	0.2222	0.3948	0.3124	0.3904	0.3868	-20.86%	-1.125%	-2.016%

# Reciprocal Effects of Occupational Conditions and Psychological Functioning: A Case Study

Qingbo Song

Research Center of Teenager Issues, Henan Normal University, Xinxiang, China

**Abstract**—The aim of this study is to demonstrate the existence of reciprocal effects between occupational conditions and psychological functioning and to consider the implications of the existence of such effect. The data used come from the Socio-environmental Studies' (SSES) longitudinal social survey on the psychological effects of occupational conditions. This paper begins by presenting definitions of some important concept and hypothesis. Second, we briefly describe the occupation and psychological functioning study in terms of study design and statistical analysis. Third, this paper presents findings and considers implications for psychology and sociology. Finally, we consider implications for cross-cultural studies.

**Index Terms**—Occupational Condition, Statistical Analysis, Improve Performance

## I. INTRODUCTION

The fact that cultural characteristics affected by occupational conditions centuries ago continue to affect psychological functioning across time and geography represents a striking example of "cultural lag" - the relative slowness of embodying something in a cultural corpus and the likelihood of its staying once embodied. Such cultural lag fits with the various theories of cultural psychologists reviewed by which postulate that a major differences among cultures result from differences in the nature of the human interactions involved in the central production processes (e.g., farming and herding) prevalent during their cultures' formative periods.

## II. METHODOLOGY

### A. Definition of Concepts and the Environmental Complexity Hypothesis

In this section, we present definitions of some important concepts. After that, I propose the "environmental complexity hypothesis." Definitions of status, social structure and culture are based on Robert Merton's general view.

"Psychological functioning" includes the mode and effectiveness with which individuals deal with whatever cognitive complexities their environments present, their orientations and attitudes towards themselves and others, the ways that they relate to others and their goals and their values.[1]

"Work" is physical or mental effort directed toward the production or accomplishment of something through which one earns one's living or which provides for one's sustenance.

"Status" is a position in a social system occupied by designated actors (i.e., individuals or social organizations) that consists of a set of roles that define the incumbents' expected patterns of interrelationships with incumbents of related statuses. Statuses may be ranked hierarchically in terms of the interrelated concepts of (1) prestige, (2) unequal distribution of relatively scarce social resources and unequal opportunity for acquiring them, (3) power-the ability to induce others to fulfill one's goals .

"Social Structure" is the patterned interrelationships among a set of individual and organizational statuses, as defined by the nature of their interacting roles.

"Culture" is a historically determined set of denotative (what is), normative (what should be), and stylistic (how done) beliefs, shared by a group of individuals who have undergone a common historical experience and participate in an interrelated set of social structures. -and or the products thereof.

Environmental Complexity Hypothesis: To the degree that complex environments reward cognitive effort, individuals should be motivated to develop their intellectual capacities and to generalize their use to other situations. On the other hand, continued exposure to relatively simple environments may result in a decrement in intellectual functioning in keeping with the low level of environmental demand.

According to the roughhewn theory on which it is based, the more diverse the stimuli, the greater the number of decisions required, the greater the number of considerations to be taken into account in making these decisions, and the more ill-defined and apparently contradictory the contingencies, the more complex the environment.

### B. Brief Overview of Occupation and Psychological Functioning Study

Data come from a three wave longitudinal study 1964-1974-1994/1995. The SSES planned the study, developed the questionnaire and analyzed the data. The National Opinion Research Center selected the representative sample and conducted the interviews.

The subjects of the 1964 survey were essentially representative of all men over 16 then in labor force (N=3101 men). In the 1974 survey, the men were a sub-sample 1/4 of 1964 respondents less than 65 years old in 1974. About 80% of those eligible were interviewed (687 men). Their wives were also interviewed (555 women). The total number of subjects was 1242 (N=1242). In the 1994 survey, 95% of 1974 sample were located, about

80% of those eligible were interviewed. The total sample was 635 (N=635, 315 men; 320 women). The working sample (working in both 1974 and 1994) was 233 (160 men; 73 women).

In the questionnaire, most items were closed-ended questions dealing with occupational conditions, work and personal history, life circumstance, values and orientations towards oneself and others. Semi-open ended questions were also used to query about the complexity of work with things, data and people. Each respondent's answers to these questions were coded using the US Department of Labor's Coding Manual for complexity of work with things, data and people. In the 1964 and 1974 waves there were four measures of intellectual flexibility; 1) Witkin Embedded 2) what to take into account in choosing a hamburger stand, 3) arguments for and against having cigarette commercials on TV, 4) the interviewer's rating of the respondent's intelligence. In 1994 a battery of standard psychometric tests of intellectual functioning was also included in the survey.

Almost all analyses used structural equation modeling (SEM). SEM provides several advantages. For example it: 1) essentially removes measurement error from latent factors, 2) it permits the estimation of causal models through regression analyses, 3) it statistically evaluates the degree to which its estimated model's fit the original input data, 4) it permits the evaluation of identified reciprocal effects models—a central concern of our analysis.

Identification of the reciprocal effects is achieved by estimating the reciprocal effects only "concurrently" and not by simultaneously testing for cross-lagged effects (shown in dashed lines). [2] The consequence of this modeling procedure is that for each pair of variables involved in a reciprocal relationship the observed "concurrent" effect of one variable on the other is the sum of the true contemporaneous effect and the omitted cross-lagged effect. Consequently we can say that such effects are real, although we cannot assess how much of the effect is actually lagged and how much is current.

To demonstrate environmental effects on psychological functioning one must go beyond mere correlation and deal with the possibility that any correlation found between an environmental condition and a psychological characteristic can come about either because of selective recruitment into the environment and/or because that environment causes that characteristic. For example, smart people can be selected into a complex environment because they can do complex things or because doing complex things makes them smarter, or both. Thus SEM is our key to establishing causal directionality between environmental conditions and psychological characteristics

In the following section, we more concretely describe specific analyses aimed at demonstrating the validity of the environmental complexity hypothesis, I then present the implications of these analyses for psychology and sociology.

These results have three important implications for psychology: (1) By showing that social-structurally influenced environmental circumstances can have notable effects on intellectual functioning, the findings provide striking evidence against socio-biological theories that posit strong forms of genetic determinism. (2) They provide an explanation of the Flynn Effect - the trend since IQ testing began for scores over a wide range of intelligence tests to rise by three IQ points per decade—given the increase in environmental complexity during this time period (Dickens & Flynn 2001). (3) The findings provide evidence for developing modes of intervention to improve intellectual functioning. As shown in Figure 1 we similarly examined the potential reciprocal effect between occupational self-direction and an individualistic, self-directed orientation.

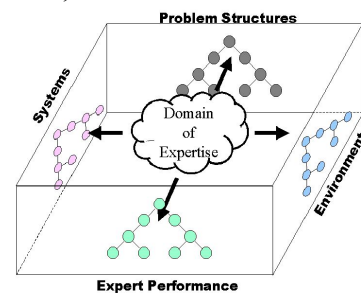


Figure 1. An Analysis Modeling Language providing multiple views into a body of expertise

Our finding of a reciprocal effect between occupational self-direction and self-directed orientation has several implications for psychologists: (1) It argues against those who believe that such orientations are set early in life by genetic (Rowe 1994) or early environmental influences (Kassler et al. 2002). (2) It provides further support for the hypothesis that dealing with complex environments increases, not only intellectual functioning, but also the value placed on self-direction and autonomy. (3) It provides further evidence that the degree to which people learn and generalize from their environments is not affected by age. (4) It provides evidence, not readily obtainable from cognitive experiments, of wide-spread learning generalization, especially involving far transfer in older individuals.

These findings also have important implications for sociologists. The existence of reciprocal effects between occupational self-direction and both intellectual functioning and self-directed orientations point to a "feedback loop" through which over time those who have gain and those who have not lose. An initial advantage in either or both, of these psychological characteristics is likely to multiply over time. [3] Thus, an individual with an initially high level of intellectual functioning is more likely than one with a lower level to get a self-directed job. The job, in turn, will increase his or her level of intellectual functioning. The reverse would be true for someone with an initially relatively low level of intellectual functioning. The same feedback loop would exist for self-directed orientations would have the same feedback loop.

Self-directed orientations and intellectual functioning tend to be highly correlated with each other, and self-

directed orientations and intellectual functioning tend to be highly correlated with social status, particularly in case of industrial and post-industrial societies. Consequently, those who start with relatively low social status start off with disadvantages in social orientations and intellectual functioning that may multiply over time and tend to lead to further decline in social status.

### III. CONCLUSIONS AND FURTHER EXPLANATIONS

The indication that occupational self-direction leads to self-directed orientations in a society raises the possibility that the level of occupational self-direction fostered by the modes of production within a society may come to affect the level of individualism in that society's norms.

Evidence for such a possibility comes from the 1974 occupational survey wave. In that survey wave, even when other relevant variables such as occupational self-direction were controlled, American men from ethnic groups with a recent and pervasive history of serfdom tended to show the non-individualistic, conformist orientation, as well as the lack of flexible, effective intellectual functioning of men working under the environmental conditions characteristic of serfdom. Thus these analyses indicated that:

Recent serf ethnic group men → non self-directed values

Recent serf ethnic group men → lower intellectual functioning

The pattern of these ethnic differences suggests that the restrictive, social and occupational conditions that prevailed within European societies affected those societies' cultures in a manner analogous to the way in which the lack of occupational-self direction affects an individual's orientations to self and others.

The fact that cultural characteristics affected by occupational conditions centuries ago continue to affect psychological functioning across time and geography represents a striking example of "cultural lag" - the relative slowness of embodying something in a cultural corpus and the likelihood of its staying once embodied. Such cultural lag fits with the various theories of cultural psychologists reviewed by (Stolurow 2001) which postulate that a major differences among cultures result from differences in the nature of the human interactions involved in the central production processes (e.g., farming and herding) prevalent during their cultures' formative periods.[4]

Among reasons why individualism may not lead to economic development: In some circumstances high

levels of individualism may create a chaotic no-rules-hold situation where individuals: (1) cannot plan ahead, (2) cannot interact with each other with a necessary modicum of trust, (3) cannot successfully accumulate and hold on to their gains.

Another possible difference between societies in which individualism leads to economic and technical progress is the degree to which individualism is institutionalized in a society. One of the great differences between 20th century China and 20th century England is the far greater level to which individualism was institutionalized in the latter. However, the existence of individualism in 16th century Japan, let alone its degree of institutionalization, is an historical question. It is worth noting that none of the cultural differences in modes of production listed in the slide is directly linked by the theorists to the complexity of the tasks done. If doing complex work leads to both higher levels of intellectual functioning and self-directed values, an argument can be made that these psychological characteristics can lead to technical development.

### ACKNOWLEDGMENT

This work is supported by Science and technology research projects of Educational Commission of Henan Province (No. 14A880019 ).

### REFERENCES

- [1] Marton, F. (1994). Knowledge objects: Understandings constituted through intensive academic study. *The British Journal of Educational Psychology*, 64(1), 161-178. Wood, D., Bruner, J. S., "The role of tutoring in problem solving", *Journal of Child Psychology and Psychiatry*, vol. 17, pp.89-100, 1976.
- [2] .Nielsen, J. (2000). *Designing web usability: The practice of simplicity*. Indianapolis, IN: New Riders Publishing.
- [3] J. Choi, K. Shim, S. Lee; K. Wu, "Handling Selfishness in Replica Allocation over a Mobile Ad Hoc Network", *IEEE Transaction on Mobile Computing*, Volume 11, Issue 2, Pages 278 – 191, Feb, 2012.
- [4] Stolurow, L. M. (2001). Some Factors in the Design of Systems for Computer-Assisted Instruction. In R. C. Atkinson & H. A. Wilson, *Computer-Assisted Instruction: A Book of Readings*. New York: Academic Press.

**Song Qingbo** born in 1971, he received his Ph.D. degree from the College of Philosophy, Wuhan University. His research interests include the Social Stratification and Social stratification and social mobility.

# Research on Curriculum Topic Map Based Domain Knowledge Management

Zhang Jin<sup>1</sup>; Wang Tianyi<sup>2\*</sup> (corresponding author)

1.Department of Educational Technology, Henan Normal University, Xinxiang, China

2.Library, Henan Normal University, Xinxiang, China

**Abstract**—In this paper, we put forward a domain knowledge management based on topic map, and build the model of the Topic Map-based Domain Knowledge Management (TMDKM). Then some studies have been done on the knowledge model and knowledge services in TMDKM with description logic. And finally we use TMAPI and Java to develop the prototype of TMDKM, which verifies the model we created. At the time of representing domain knowledge correctly and completely, TMDKM provides strong support in the knowledge communicating, sharing and creating, which can achieve the aim of domain knowledge management.

**Index Terms**—topic map, domain knowledge management, knowledge model

## I. INTRODUCTION

The traditional methods of domain knowledge management are usually based on case (Case-based) knowledge management [1], which managed through the fixed hierarchy relationship of a database or knowledge base, cannot meet the constantly changing needs of knowledge updated. With the development of information technology, the knowledge management system based on ontology [2] was emerged, but the knowledge acquisition, storage, and so on are carried out based on XML in these systems, it needs a transformation process from ontology to XML, but the ability to express the semantics of XML is weak, the ontology content cannot be completely converted, and easily distorted, so reduced the system's open and dynamic nature [3].

Topic Maps has been widely used in knowledge organization and knowledge management, such as to annotation distributed knowledge on digital libraries based on topic maps, use the topic maps to organize and manage the site knowledge, topic maps-based manage the virtual reference library of digital cultural heritage based on topic maps, and so on.

In the literature [4], established a formal model based on topic map courseware (TMC), established the mapping between topic maps and network courseware knowledge structure, and gives the mapping rules and nature, laid the foundation for the curriculum domain knowledge management. On the basis of the literature, this article proposed topic map-based domain knowledge management.

Topic maps-based knowledge management has a strong semantic skills, it could be able to establish a clear

architecture for knowledge and resources, not likely to cause distortion of information; it can be constantly updated with the changing knowledge, to solve an opening and dynamic problems in the traditional domain knowledge management, provides a strong support for the exchange of knowledge sharing and knowledge creation. The main work of this paper is to establish TMDKM knowledge management model, to research the structure of the knowledge model and knowledge services, and development the TMDKM prototype, then validated the model.

## II. METHODOLOGY

This chapter gives a brief introduction to TMC's related knowledge, the three main elements and the relevant language of topic map provides a theoretical basis for TMC.

### A. Topic map

Topic Maps was proposed by the International Standardization Organization ISO in 1999, began to build intelligent electronic index and can support mutual integration between these indexes at the beginning, then gradually developed into a set way to express knowledge and organization information, use of this method can provide the best information navigation. There are three basic elements in the topic map, namely: topic, association, and occurrence, the topic map was constituted of these major part.

Topic maps are a simple ontology language, and the different is that it provides a topic-oriented, standard-based knowledge encoding, with pre-defined semantics [5], but also has its own description language and query language. Topic Maps focus on the linkages which in the overall knowledge of its specific location in the environment and related topics to locate knowledge resources, emphasis meaning mining on resources individual in a specific environment, but also supports a variety of ways to organize the knowledge resources, these features specially fit for the requirements of knowledge management.

### B. TMC

The application of topic maps in the online teaching has become a hot topic, Dicheva (2005) proposed a network courseware based on topic maps (TMC), using topic maps to represent the network courseware

knowledge, abroad website has developed a topic map-based web courseware for the Java language learning.

On the basis of analysis the traditional network courseware structure, use topic maps to indicate domain knowledge, and TMC has established a formal model. In traditional network courseware, content structure model and the knowledge structure model is separated, and TMC can simultaneously represent the content structure and the knowledge structure of the network courseware, thus establishing the TMC model, you can easily use the model for domain knowledge management.

C. TMDKM

This paper argues that Topic Map-based Domain Knowledge Management (TMDKM) can be viewed as the synthesis of knowledge model and knowledge services. Based on the domain knowledge model built, defining its complete set of knowledge services. In this way, it can reflect the domain knowledge completely and accurately and support the communication, sharing and innovation of knowledge at the same time so as to achieve the goal of knowledge management.

This paper adopts description logic to formalize modeling of TMDKM. The description logic is a formalization of knowledge representation based on the objects, originating from semantic network and KL-ONE. It has a strong power of expression and it is suitable for the modeling of Topic Map-based Domain Knowledge.

Generally speaking, the teaching content of a course has a hierarchical structure, namely it can generate a tree structure according to decomposition relationship. Therefore, according to the chapters, this part classifies the domain knowledge of a course. It argues that a course is composed of different chapters, each chapter contains different sections and each section has multiple knowledge points. Correspond to topic map, viewing each chapter or knowledge point as a topic. There are different types of connection between topic and topic, and each topic can also be associated with the abundant teaching resources on the network.

Topic Map Data Model builds the domain knowledge model of TMDKM as shown in Figure 1.

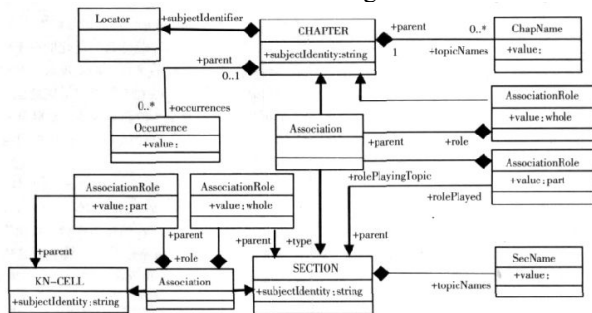


Figure 1. Domain knowledge model of TMDKM

Types of knowledge services

Domain knowledge services provides a variety of domain knowledge application, since the main object of TMDKM are learners, according to their required services in the learning process currently the type of domain knowledge services are divided into: knowledge navigation, knowledge positioning, knowledge

recommended, resource association and other diagnostic and counseling. As research continues in the future, its type will be further expanded and improved.

(1) Knowledge Navigation, (KN):

Knowledge Navigator is guide the students to view and learn the knowledge and resources are needed in the network courseware. TMDKM achieved the function of knowledge navigation, completely and accurately showing the content and structure of the course knowledge, help learners to grasp the structure of the curriculum.

(2) Knowledge Positioning, (KP):

Knowledge positioning means the process that through knowledge query language to quickly determine the exact location of a particular knowledge, then presenting knowledge to learners. TMDKM using Topic Maps Query Language (TMQL) to achieve search and find the knowledge in order to achieve accurate positioning of knowledge points.

(3) Knowledge Recommendation, (KR):

Knowledge recommendation has always been a hot research, such as the common recommendation algorithm used collaborative filtering recommendation, based on the interest model recommendation, based on domain knowledge personalized recommendations. The main idea of these algorithms is they recommend interest information and knowledge to the users.

The study is the knowledge that exists between a knowledge and other domain of the curriculum associated with different types of knowledge to fully understand a point must be master all the associated domain knowledge-based. Recommendation knowledge in the TMDKM recommended the types of these points and the associated recommendations to the learner, while learners are learning a knowledge can understand the associated when linked with this knowledge, and you can directly click on link knowledge of learning, help learners to grasp the overall course content.

(4) Resource Association (RA):

TMDKM put the massive teaching resources of the network and domain knowledge together, so that learners could take advantage of teaching resources on the network while learning programs, thus increasing the dynamics and openness of knowledge.

(5) Diagnosing and Tutoring, (DT):

Tracking learners' learning process, collecting their learning behavior, diagnosis the current problems of learners in the learning process and the reasons based on data collection, to give targeted learning guidance and advice.

This section using logic describe to formal description for domain knowledge services, thus established a more complete conceptual model, making the formal unity of knowledge services. With a clear model-theoretical mechanisms of the logic describe, and provide useful reasoning services, to facilitate future study of knowledge reasoning, query optimization, etc.

Knowledge Navigation (KN)

$$KN = \frac{T_c = \exists has - type .Chap}{\langle T_1, Root \rangle : sub - child} \cap \frac{T_s = \exists has - type .Sec \cap T_c = \exists contains .T_s}{\langle T_s, T_c \rangle : sub - child} \cap \frac{T_k = \exists has - type .K_n \cap T_s = \exists contains .T_k}{\langle T_k, T_s \rangle : sub - child}$$

Its meaning is: TMDKM constructed in accordance with the type hierarchy structure curriculum topics to present knowledge content. Where Root is the root, which means that a course, representing the course of a chapter, a lesson, a knowledge point.

Knowledge Positioning (KP)

$$KP = \frac{T_c = \exists R.T_r}{T_e} \cup \frac{T_s = \exists R.T_r}{T_s} \cup \frac{T_k = \exists R.T_r}{T_k}$$

Tr is the need queries knowledge of the learners, Tc,Ts,Tk respectively represent one curriculum chapter , a knowledge point, and R is any possible association between the two topic. TMDKM to accurately positioning a knowledge point by relevance type.

Knowledge Recommended(KR)

$$KR = \frac{T_c = \exists R.T}{\langle T_c, T \rangle : recommend} \cup \frac{T_s = \exists R.T}{\langle T_s, T \rangle : recommend} \cup \frac{T_k = \exists R.T}{\langle T_k, T \rangle : recommend}$$

T for a topic, R for recommended between this topic and other topics, Tc,Ts,Tk respectively represent one curriculum chapter ,one lesson, a knowledge point. TMDKM determined of knowledge with the recommended knowledge by the associated type.

Resources Association(RA)

$$RA = \frac{T_c = \exists R.O}{\langle T_c, O \rangle : relate} \cup \frac{T_s = \exists R.O}{\langle T_s, O \rangle : relate} \cup \frac{T_k = \exists R.O}{\langle T_k, O \rangle : relate}$$

O as teaching resources, R is associated with a topic and the resource, Tc,Ts,Tk respectively represent one curriculum chapter, one lesson, a knowledge points. TMDKM through link address of resource source integrate the resources and topics.

Diagnosis and Tutorship(DT)

$$DT = \frac{SM \cap LP}{SD} \cup \frac{S D}{S T}$$

Its meaning is through the student model (SM) and students' learning process (LP) to give a diagnosis to the student (SD), and then make the appropriate counseling (ST) to the students according to the diagnosis. Which track student learning process (LP) is based on the TMDKM to complete.

### III. CONCLUSIONS AND FURTHER EXPLANATIONS

Knowledge recommendation algorithm using TMAPI(Topic Map Application Programming Interface)

to recommended knowledge by searching the type associated with all the knowledge points to a knowledge associated recommend to the learner, also at the same time explains the reasons for recommendation, it is more favorable for learners to grasp the overall course content compared with the traditional recommendation knowledge. The recommendation algorithm only needs to traverse the topic map once, the time-consuming complexity is: T (Recommend\_KN) = O (n), where n is the number of topics.

Knowledge navigation interface through the left navigation bar and click interface, and can be observed in the right part of the contents of the corresponding knowledge points, the interface is recommended for learners lower right knowledge associated with the selected links to all the knowledge points by clicking on these links can go to the appropriate interface knowledge of learning.

### ACKNOWLEDGMENT

This work is supported by Science and technology research projects of Educational Commission of Henan Province (No. 14A880019 ).

### REFERENCES

- [1] E. Freese. Using Topic Maps for the representation, management and discovery of knowledge. In XML Europe2000 Proceedings.
- [2] <http://www.gca.org/papers/xml europe2000/papers/s22-01.html>, June 2000.
- [3] ISO/IEC 13250. Topic Maps, 2002. available at [http://www1.y12.doe.gov/capabilities /sgml/sc34/docume nt/0322 \\_files/iso13250-2nd-ed-v2.pdf](http://www1.y12.doe.gov/capabilities /sgml/sc34/docume nt/0322 _files/iso13250-2nd-ed-v2.pdf).
- [4] Lachica, R. & Karabeg, D. (2008). Metadata Creation in Socio-semantic Tagging Systems: Towards Holistic Knowledge Creation and Interchange. In Maicher, L. & Garshol, L.M. (eds.). Scaling Topic Maps. LNAI4999. Springer.
- [5] Choi, D. H., Kim, J., & Kim, "Training with a web-based electronic learning sys tem: The flow theory perspective", International Journal of Human-Computer Studies,vol.65, pp.223-243,2006.
- [6] G. R. Librelotto, J. C. Ramalho, and P. R. Henriques. Constraining topic maps: a TMCL declarativeimplementation. In Extreme Markup Languages 2005: Proceedings. IDEAlliance.

**Zhang Jin** born in 1983, she received her Master degree in educational technology from the Yunnan Normal University. Her research interests include Multicriteria Decision Analysis, Intelligent decision support systems.

**Wang tianyi** born in 1981, he received his Master degree in educational technology from the Henan Normal University. His research interests include Educational Technology.